FUNCTIONAL CHARACTERIZATION OF RICE β-GLUCOSIDASE Os1BGlu4

Chen Rouyi

A Thesis Submitted in Partial Fulfillment of the Requirements for the Degree of Doctor of Philosophy in Biotechnology

Suranaree University of Technology

Academic Year 2012

คุณสมบัติและหน้าที่ของ Os1BGlu4 เบต้ากลูโคสิเดสจากข้าว

นายเฉิน รองยี

วิทยานิพนธ์นี้เป็นส่วนหนึ่งของการศึกษาตามหลักสูตรปริญญาวิทยาศาสตรดุษฎีบัณฑิต
สาขาวิชาเทคโนโลยีชีวภาพ
มหาวิทยาลัยเทคโนโลยีสุรนารี
ปีการศึกษา 2555

FUNCTIONAL CHARACTERIZATION OF RICE β-GLUCOSIDASE Os1BGlu4

Suranaree University of Technology has approved this thesis submitted in fulfillment of the requirements for the Degree of Doctor of Philosophy.

Thesis Examining Committee

_____
(Asst. Prof. Dr. Panlada Tittabutr)
Chairperson

_____
(Assoc. Prof. Dr. Mariena Ketudat-Cairns)
Member (Thesis Advisor)

_____
(Prof. Dr. James R. Ketudat-Cairns)
Member

_____
(Prof. Dr. Zheng Changxiang)
Member

_____
(Asst. Prof. Dr. Nooduan Muangsan)
Member

_____
(Prof. Dr. Sukit Limpijumnong)
Vice Rector for Academic Affairs

_____
(Asst. Prof. Dr. Suwayd Ningsanond)
Dean of Institute of Agricultural Technology

เฉิน รองยี : คุณสมบัติและหน้าที่ของ Os1BGlu4 เบต้ากลูโคสิเดสจากข้าว
(FUNCTIONAL CHARACTERIZATION OF RICE β-GLUCOSIDASE Os1BGlu4)
อาจารย์ที่ปรึกษา : รองศาสตราจารย์ ดร.มารินา เกตุทัต-คาร์นส์, 194 หน้า

เบต้ากลูโคซิเดส (β-D-glucopyranosideglucohydrolases, E.C. 3.2.1.21) เป็นเอนไซม์ที่สามารถย่อยสลายพันธะไกลโคซิดิก และปลดปล่อยหมู่ไกลโคซิลออกจากไกลโคไซด์ และโอลิโกแซคคาไรด์ ในจีโนมของข้าวพบยีนเบต้ากลูโคซิเดสทั้งหมด 34 ยีน จากการวิเคราะห์ลำดับโปรตีนโดยอาศัยความสัมพันธ์เชิงวิวัฒนาการ พบว่า Os1BGlu4 จากข้าวจัดอยู่ในกลุ่มเดียวกันกับ BGLU42 จาก *Arabidopsis* และ latex cyanogenic β-glucosidase จาก *Heveabrasiliensis* และเป็นอิสระจากกลุ่มอื่น ๆ เพื่อให้เข้าใจถึงบทบาทหน้าที่ของเอนไซม์ Os1BGlu4 จึงทำการผลิตโปรตีนลูกผสม (recombinant Os1BGlu4; rOs1BGlu4) ใน *Escherichia coli* สายพันธุ์ Origami B(DE3) พบว่าเวลา 16 ชั่วโมง ที่อุณหภูมิ 20 องศาเซลเซียส เป็นสภาวะที่เหมาะสมในการผลิตโปรตีนลูกผสมนี้ โดยไม่จำเป็นต้องมีตัวกระตุ้น (isopropyl β-D-1-thiogalactopyranoside; IPTG) การวิเคราะห์ทางชีวเคมีพบว่าที่ค่าพีเอช 6.5 และอุณหภูมิ 45 องศาเซลเซียส เป็นสภาวะที่เหมาะสมสำหรับการทำงานของเอนไซม์ การวิเคราะห์ความจำเพาะของเอนไซม์ rOs1BGlu4 ต่อสารตั้งต้น พบว่าในระดับขั้นโพลีเมอไรเซชัน (degree of polymerization; DP) ของเอนไซม์ลูกผสมนี้มีความสามารถในการย่อยสลายพันธะ β-(1, 3)-linked oligosaccharides ที่ระดับ 2-3 และพันธะ β-(1, 4)-linked oligosaccharide ที่ระดับ 3-4 การศึกษาความสามารถในการย่อยสลายซับสเตรท โดยอาศัยพื้นฐานของตัวแปรทางจลนศาสตร์ พบว่าเอนไซม์นี้สามารถย่อยสลาย *p*NP-glucopyranoside (*p*NPG) และ *p*NP-fucopyranoside ได้อย่างมีประสิทธิภาพ นอกจากนี้การวิเคราะห์ด้วยโครมาโตกราฟีแบบแผ่นบาง (thin layer chromatography; TLC) ยังแสดงให้เห็นว่าเอนไซม์ชนิดนี้สามารถย่อยสลายสารตั้งต้นจากธรรมชาติ เช่น salicin esculin และ para-coumaryl alcohol glucoside ได้ ในการศึกษาลำดับการย่อยสลายของเอนไซม์โดยใช้ *p*NP-cellobiside เป็นสารตั้งต้น พบว่าเอนไซม์นี้สามารถทำงานได้เมื่อสารตั้งต้นประกอบไปด้วยกลูโคสตั้งแต่ 2 โมเลกุล ขึ้นไป การศึกษาทรานไกลโคซิเลชั่น พบว่าที่ความเข้มข้น *p*NPG ในระดับสูงเอนไซม์ rOs1BGlu4 มีความสามารถในการส่งต่อกลุ่มของกลูโคสจาก *p*NPG ไปสู่เอทานอลและ *p*NPG ได้ จากการศึกษาสารยับยั้งการทำงานของเอนไซม์นี้แสดงให้เห็นว่า $HgCl_2$ delta-glucono-lactone และ $FeCl_3$ มีอิทธิพลในการยับยั้งการทำงานของเอนไซม์ rOs1BGlu4

การศึกษารูปแบบการแสดงออกของยีน *Os1bglu4* พบว่ายีนนี้มีการแสดงออกสูงที่สุดในช่วงแรกเริ่มของการงอก และค่อย ๆ ลดลงจนกระทั่งอยู่ในระดับคงที่ในวันที่ 6 วัน หลังการงอก ในระยะข้าวออกรวง พบว่ายีน *Os1bglu4* มีการแสดงออกสูงที่สุดในช่อดอก รองลงมาคือ ราก ใบ

และกาบใบ สำหรับการแสดงออกของยีน *Os1bglu4* ในบริเวณอื่น ๆ พบการแสดงออกสูงสุดในวันที่ 14 ของการงอกของราก แต่แสดงออกได้น้อยในต้นอ่อน และใบ ในการวิเคราะห์รูปแบบการถอดรหัสของต้นข้าวที่เติมเกลือ (NaCl) และสารโพลีเอธิลีนไกลคอล (polyethyleneglycol; PEG) ในขณะที่ทำการปลูกข้าว ส่งผลให้มีการแสดงออกของยีน *Os1bglu4* ที่เพิ่มขึ้นแต่ไม่สามารถสังเกตเห็นการเปลี่ยนแปลงของฟีโนไทป์ได้ด้วยตาเปล่า การแสดงออกของยีน *Os1bglu4* เพิ่มมากขึ้นเมื่อข้าวเป็นโรคไหม้ (rice blast) โดยเฉพาะในข้าวปรับปรุงพันธุ์ที่ต้านทานต่อโรคไหม้ (near isogenic line) การแสดงออกมากกว่าปกติของยีน *Os1bglu4* ในข้าว ส่งผลให้ข้าวมีความต้านทานต่อโรคไหม้ได้มากขึ้น การลดการแสดงออกของยีน *Os1bglu4* ในข้าวก็ส่งผลต่อความต้านทานโรคไหม้ลดลงด้วย ยีน *Os1bglu4* มีการแสดงออกมากขึ้นในราก โดยพบการแสดงออกที่มากขึ้นเมื่อปริมาณขนรากมีมาก เมื่อวิเคราะห์ลักษณะทางฟีโนไทป์ พบว่าต้นกล้าข้าวดัดแปลงพันธุกรรมที่มีการแสดงออกของยีน *Os1bglu4* มากเกินปกตินั้น มีจำนวนของขนรากมากกว่าต้นกล้าข้าวดัดแปลงพันธุกรรมที่ลดการแสดงออกของยีนนี้ลงเมื่อเปรียบเทียบกับสายพันธุ์ปกติ จากผลการทดลองนี้ชี้ให้เห็นว่าโปรตีน Os1BGlu4 อาจมีบทบาทในการป้องกันการเกิดโรคไหม้ และการสร้างขนรากในข้าว

สาขาวิชาเทคโนโลยีชีวภาพ
ปีการศึกษา 2555

ลายมือชื่อนักศึกษา _____
ลายมือชื่ออาจารย์ที่ปรึกษา _____
ลายมือชื่ออาจารย์ที่ปรึกษาร่วม _____

CHEN ROUYI : FUNCTIONAL CHARACTERIZATION OF RICE β-GLUCOSIDASE Os1BGlu4. THESIS ADVISOR : ASSOC. PROF. MARIENA KETUDAT-CAIRNS, Ph.D., 194 PP.

RICE/BETA-GLUCOSIDASE/HYDROLYSIS KIENTICS/TRANSGENIC RICE/RNAi/TRANSCRIPTION PATTERN

Beta-glucosidases (β-D-glucopyranosideglucohydrolases, E.C. 3.2.1.21) are enzymes that hydrolyze glycosidic bonds to release nonreducing terminal glucosyl residues from glycosides and oligosaccharides. Thirty-fouractive rice β-glucosidase genes had been identified in the rice genome. Protein sequence based phylogenetic analysis showed that Os1BGlu4 along with *Arabidopsis* BGlu42 and *Heveabrasiliensis* latex cyanogenic β-glucosidase represented an independent cluster. To help narrow the possible functions of Os1BGlu4, recombinant Os1BGlu4 (rOs1BGlu4) was expressed in *E. coli* Origami B(DE3). The optimized expression conditions showed that 16 hrs incubation at 20 ^{o}C without isopropyl β-D-1-thiogalactopyranoside (IPTG) inducer was the optimum condition for the expression. Biochemical analyses showed that pH 6.5 and 45 ^{o}C were optimum condition for the hydrolysis activity of rOs1BGlu4. The rOs1BGlu4 efficiently hydrolyzed β-(1,3)-linked oligosaccharides of degree of polymerization (DP) 2-3 and β-(1, 4)-linked oligosaccharide of DP 3-4. The rOs1BGlu4 can hydrolyze *para*nitrophenyl-β-D-glucopyranoside (*p*NPG) and *p*NP-β-D-fucopyranoside efficiently, based on the kinetic parameters. Hydrolysis of natural substrates salicin, esculin and para-coumarylalcohol glucoside by rOs1BGlu4 can be detected by thin layer chromatography (TLC). The study of *p*NP-cellobioside sequential hydrolysis showed that the initial hydrolysis was

between the two glucosyl moieties. The transglycosylation studies showed that a high concentration of pNPG, rOs1BGlu4 has the ability to transfer the glucose group of *p*NPG to ethanol and *p*NPG. The inhibition study revealed that $HgCl_2$, delta-gluconolactone and $FeCl_3$ strongly inhibited the hydrolysis activity of rOs1BGlu4.

The *Os*1*bglu*4 had the highest expression level at the early stage of germination and decreased gradually to a steady level at 6 day after germination. In terms of spatial expression, *Os*1*bglu*4 had the highest expression in 14 day seedling root, low expression in shoot and leaf. The transcription pattern analysis of sodium chloride (NaCl) and polyethylene glycol (PEG) treated plants showed that the expression of *Os*1*bglu*4 increased, but no visible phenotype was observed. The expression of *Os*1*bglu*4 was also highly induced when treated with rice blast, especially in the rice blast resistant near isogenic line. The *Os*1*bglu*4 gene over-expression (oe) and knock-down transgenic rice were generated. Over-expression of *Os*1*bglu*4 gene in rice resulted in enhanced resistance to rice blast infection. Knock-down (RNAi) of *Os*1*bglu*4 in rice resulted in decreased resistance to rice blast infection. The expression of *Os*1-*bglu*4 was higher in root with more root hair than that with less root hair. Phenotype analysis showed that the oe lines had more root hair and the RNAi lines had lower root hair when compared to wild type rice seedling. These results suggest that Os1-BGlu4 might play some roles in rice blast defense and root hair formation in rice.

School of Biotechnology
Academic Year 2012

Student's Signature_____
Advisor's Signature_____
Co-advisor's Signature_____

ACKNOWLEDGEMENT

I would like to express my deepest gratitude to my advisor, Assoc. Prof. Dr. Mariena Ketudat-Cairns and my co-advisor, Prof. Dr. James R. Ketudat-Cairns for their kind supervision, valuable advice, support and giving me the opportunity to work on this project and also for providing resources for the experiments. I also thank research assistants Ton and Nim for their kind help with many experiments in molecular biology work and my lab mates Koi, Oa, Fai, Wan, Yee and Tam for all of their kind help and consideration. I also would like to thank all of the students in Prof. JKC's lab for their very kind help with biochemistry experiments. I wish to express my special thanks to Prof. Zheng Changxiang for providing the opportunity for me to study in Suranaree University of Technology (SUT) and Guizhou Upland Food Crop Institute. I also thank Guizhou Academy of Agricultural Science for providing the support for my study in SUT. I thank Prof. Li Shigui and Dr. Chen Weilan for their help and guidance in rice tissues culture and Agrobacterium-mediated transformation. Special thanks are extended to all my friends in SUT for their help. Finally, I would like to express my deepest gratitude to my parents, my wife and my younger brother for their love, understanding and encouragement.

Chen Rouyi

CONTENTS

Page

CONTENTS (Continued)

Page

CONTENTS (Continued)

Page

CONTENTS (Continued)

Page

CONTENTS (Continued)

Page

CONTENTS (Continued)

Page

CONTENTS (Continued)

Page

LIST OF TABLES

Table **Page**

LIST OF FIGURES

Figure **Page**

LIST OF FIGURES (Continued)

Figure **Page**

LIST OF FIGURES (Continued)

Figure **Page**

LIST OF FIGURES (Continued)

Figure **Page**

LIST OF FIGURES (Continued)

Figure **Page**

LIST OF ABBREVIATIONS

GA_4	=	Gibberellic acid 4
LB	=	Lysogeny broth
min	=	minute
Mw	=	Molecular weight
mRNA	=	Messenger ribonucleic acid
(n, μ) mole	=	(nano, micro) mole
(n, μ, m) g	=	(nano, micro, milli) gram
(n, μ, m) M	=	(nano, micro, milli) Molar
OD	=	Optical density
PAGE	=	Polyacrylamide gel electrophoresis
PCR	=	Polymerase chain reaction
PGO	=	Peroxidase-glucose oxidase
*p*NP	=	*para*-Nitrophenol
*p*NPG	=	*para*-Nitrophenyl-β-D-glucopyranoside
RNA	=	Ribonucleic acid
RNase	=	Ribonuclease
sec	=	second
SDS	=	Sodium dodecyl sulfate
TEMED	=	Tetramethylenediamine
TLC	=	Thin layer chromatography
Trx	=	Thioredoxin

LIST OF ABBREVIATIONS (Continued)

(μ, m) L	=	(micro, milli) Liter
V	=	Voltage
v/v	=	volume/volume
w/v	=	wight/volume

CHAPTER I

INTRODUCTION

1.1 Introduction

Beta-glucosidases (β-D-glucopyranoside glucohydrolases, EC 3.2.1.21) are enzymes that hydrolyze glycosidic bonds to release nonreducing terminal glucosyl residues from glycosides and oligosaccharides (Ketudat Cairns and Esen 2010). These enzymes are found in all kinds of organisms and involved in many fundamental life activities. The β-glucosidases hydrolyze the glycoside to release the aglycone from the conjugate. It is the nature of the aglycone that determines the functions of the β-glucosidase in plants (Ketudat Cairns and Esen 2010). The functions of β-glucosidase include plant defense (Poulton *et al.* 1994, Dakora *et al.* 1996, Soler-Rivas *et al.* 2000), plant-microbe and plant-insect interactions (Zagrobelny *et al.* 2004, Felton *et al.* 2008), cell wall catabolism and lignification (Akiyama *et al.* 1998, Opassiri *et al.* 2003), signal transduction (Matsushima *et al.* 2003), scent release (Yablonka-Reuveni *et al.* 1999), phytohormone conjugate activation (Smith *et al.* 1978, Zouhar *et al.* 1999, Lee *et al.* 2006, Xu *et al.* 2012) and plant secondary metabolism (Esen 1993, Barleben *et al.* 2005).

Forty GH1 genes have been identified from rice genomic databases, including 2 possible endophyte genes, 2 likely pseudogenes, 2 gene fragments, and 34 apparently competent rice glycosidase genes (Opassiri *et al.* 2006). The large number of rice GH1 enzymes may reflect different substrate specificity and expression patterns in rice

tissues and/or in response to environmental conditions among the GH1 members (Ketudat Cairns *et al*. 2010). Amino acid sequence alignment and phylogenetic analysis of GH1 proteins between rice, *Arabidopsis* and other type of plants showed that β-glucosidases with similar sequences clustered together and tend to inhabit on the same chromosome. Several experiment results indicated that the proteins in the same cluster tend to have similar functions (Leah *et al.* 1995, Hrmova *et al.* 1998, Opassiri *et al.* 2006).

BGlu1 (Os3BGlu7), which is highly expressed in flower and germinating shoot was cloned and characterized. The possible functions of the BGlu1 protein include hydrolysis and recycling of oligosaccharides generated from rapid cell wall expansion during seed germination and flower expansion, and release of the coenzyme pyridoxine from its glucose-conjugated storage form (Opassiri *et al.* 2003). The biochemical characteristics of the BGlu1 and BGlu1 homologs, which clustered together, were compared. Rice BGlu1, Os3BGlu8, and Os7BGlu26 hydrolyzed cello-oligosaccharides with increasing efficiency as the degree of polymerization (DP) increased from 2 to 6 (Kuntothom *et al.* 2009), while Os4BGlu12 showed little increase in activity with DP and Os3BGlu6 hydrolyzed disaccharides best (Opassiri *et al.* 2006, Seshadri 2009). The Os3BGlu7 and Os3BGlu8 isoenzymes are widely expressed in rice tissues, so they may be needed for release of glucose from oligosaccharides generated in cell wall remodeling at various stages of plant development. Since the rice β-glucosidase isoenzymes mentioned above also hydrolyze plant-derived glycosides, they may play other roles in the plant as well (Akiyama *et al.* 1998, Opassiri *et al.* 2003, Opassiri *et al.* 2004, Opassiri *et al.* 2006, Kuntothom *et al.* 2009).

Among the 34 rice GH1 glycosidase genes, there is only one gene predicted by bioinformatics to encode a protein without a signal peptide. This protein, Os1BGlu4,

should localize in the cytoplasm and may play an important and unique role in rice.

The EST database search showed that the *Os*1*blgu*4 is expressed in rice shoot, flower and panicle, flower and panicle in drought condition and blast infected 3-week leaf (Opassiri *et al*. 2006). The *Os*1*bglu*4 has the strongest expression in root and panicle from EST database http://www.ncbi.nlm.nih.gov/UniGene/ESTProfile Viewer analysis. The functions of its homologue BGlu42 in *Arabidopsis* and HB AAP51059 in *Hevea brasiliensis* have not been reported. So, figuring out the biochemical characteristics, functions and localization of the Os1BGlu4 will significantly increase to the knowledge of GH1 enzyme in plants, including its homologues AtBGlu42 and HB AAP51059. The knowledge may be useful for rice breeding and enzyme engineering.

1.2 Significance of the study

Thirty-four GH1 β-glucosidase-like enzymes have been identified in genomic sequences from rice. However, only a small number of these enzymes have been studied. A comprehensive approach is needed to study rice β-glucosidases in order to associate each of them with the physiological role that it plays in the plant, and to determine the precise substrate specificity in relation to the enzyme sequences and structures. The understanding of the biochemistry and mechanistic fundamentals of these enzymes can enrich the knowledge of glycoside hydrolases, which could be applied to the enzyme engineering. Possible applications include conversion of cellulosic biomass, an inexpensive renewable resource, into sugar derived high-value product, and crop breeding to improve the agronomic traits of crops.

1.3 Research objectives

1. To functionally express recombinant rice β-glucosidase Os1BGlu4 in *Escherichia coli*.

2. To purify the recombinant Os1BGlu4 and characterize the specific activities in terms of substrate-specificity and other important biochemical properties.

3. To study kinetics parameters of the recombinant rice Os1BGlu4 for hydrolysis of synthetic and natural substrates.

4. To generate transgenic rice with overexpression and knock down of the *Os1bglu4* gene in order to elucidate the biological functions of this enzyme in rice plants.

5. To determine the transcription pattern of the *Os1bglu4* gene.

6. To determine the localization of the Os1BGlu4 protein at the subcellular level.

1.4 References

Akiyama, T., H. Kaku and N. Shibuya (1998). A Cell Wall-Bound Beta-Glucosidase from Germinated Rice: Purification and Properties. **Phytochemistry** 48(1): 49-54.

Barleben, L., X. Ma, J. Koepke, G. Peng, H. Michel, *et al.* (2005). Expression, Purification, Crystallization and Preliminary X-Ray Analysis of Strictosidine Glucosidase, an Enzyme Initiating Biosynthetic Pathways to a Unique Diversity of Indole Alkaloid Skeletons. **Biochimica et Biophysica Acta-Proteins & Proteomics** 1747(1): 89-92.

Dakora, F. and D. Phillips (1996). Diverse Functions of Isoflavonoids in Legumes Transcend Anti-Microbial Definitions of Phytoalexins. **Physiological and Molecular Plant Pathology** 49(1): 1-20.

Esen, A. (1993). B-Glucosidase: Overview in β-Glucosidases: Biochemistry and Molecular Biology (Esen, A., Ed). **American Chemical Society, Washington, DC.**

Felton, G. W. and J. H. Tumlinson (2008). Plant–Insect Dialogs: Complex Interactions at the Plant–Insect Interface. **Current Opinion in Plant Biology** 11(4): 457-463.

Hrmova, M., E. A. Macgregor, P. Biely, R. J. Stewart and G. B. Fincher (1998). Substrate Binding and Catalytic Mechanism of a Barley Glucosidase/(1,4)-B-D-Glucan Exohydrolase. **The Journal of Biological Chemistry** 273(18): 11134-11143.

Ketudat Cairns, J. R. and A. Esen (2010). B-Glucosidases. **Cellular and Molecular Life Sciences** 67(20): 3389-3405.

Kuntothom, T., S. Luang, A. J. Harvey, G. B. Fincher, R. Opassiri*, et al.* (2009). Rice Family GH1 Glycoside Hydrolases with β-D-Glucosidase and B-D-Mannosidase Activities. **Archives of Biochemistry and Biophysics** 491(1): 85-95.

Leah, R., J. Kigel, I. Svendsen and J. Mundy (1995). Biochemical and Molecular Characterization of a Barley Seed-Glucosidase. **Journal of Biological Chemistry** 270(26): 15789-15797.

Lee, K. H., H. L. Piao, H. Y. Kim, S. M. Choi, F. Jiang*, et al.* (2006). Activation of Glucosidase Via Stress-Induced Polymerization Rapidly Increases Active Pools of Abscisic Acid. **Cell** 126(6): 1109-1120.

Matsushima, R., M. Kondo, M. Nishimura and I. Hara-Nishimura (2003). A Novel ER-Derived Compartment, the ER Body, Selectively Accumulates a β-Glucosidase with an ER-Retention Signal in *Arabidopsis*. **The Plant Journal** 33(3): 493-502.

Opassiri, R., Y. Hua, O. Wara-Aswapati, T. Akiyama, J. Svasti, *et al.* (2004). Beta-Glucosidase, Exo-Beta-Glucanase and Pyridoxine Transglucosylase Activities of Rice BGlu1. **Biochemical Journal** 379(Pt 1): 125-131.

Opassiri, R., J. R. Ketudat Cairns, T. Akiyama, O. Wara-Aswapati, J. Svasti, *et al.* (2003). Characterization of a Rice β-Glucosidase Highly Expressed in Flower and Germinating Shoot. **Plant Science** 165(3): 627-638.

Opassiri, R., B. Pomthong, T. Onkoksoong, T. Akiyama, A. Esen, *et al.* (2006). Analysis of Rice Glycosyl Hydrolase Family 1 and Expression of Os4BGlu12 Beta-Glucosidase. **BMC Plant Biology** 6: 33-33.

Poulton, J. E. and C. P. Li (1994). Tissue Level Compartmentation of (R)-Amygdalin and Amygdalin Hydrolase Prevents Large-Scale Cyanogenesis in Undamaged Prunus Seeds. **Plant Physiology** 104(1): 29-35.

Smith, A. and J. Van Staden (1978). Changes in Endogenous Cytokinin Levels in Kernels of *Zea* mays L. During Imbibition and Germination. **Journal of Experimental Botany** 29(5): 1067-1075.

Soler-Rivas, C., J. C. Espín and H. J. Wichers (2000). An Easy and Fast Test to Compare Total Free Radical Scavenger Capacity of Foodstuffs. **Phytochemical Analysis** 11(5): 330-338.

Xu, Z. Y., K. H. Lee, T. Dong, J. C. Jeong, J. B. Jin, *et al.* (2012). A Vacuolar B-Glucosidase Homolog That Possesses Glucose-Conjugated Abscisic Acid

Hydrolyzing Activity Plays an Important Role in Osmotic Stress Responses in *Arabidopsis*. **The Plant Cell** 24(5): 2184-2199.

Yablonka-Reuveni, Z., M. A. Rudnicki, A. J. Rivera, M. Primig, J. E. Anderson*, et al.* (1999). The Transition from Proliferation to Differentiation Is Delayed in Satellite Cells from Mice Lacking Myod. **Developmental Biology** 210(2): 440.

Zagrobelny, M., S. Bak, A. V. Rasmussen, B. Jørgensen, C. M. Naumann*, et al.* (2004). Cyanogenic Glucosides and Plant–Insect Interactions. **Phytochemistry** 65(3): 293-306.

Zouhar, J., E. Nanak and B. Brzobohatý (1999). Expression, Single-Step Purification, and Matrix-Assisted Refolding of a Maize Cytokinin Glucoside-Specific β-Glucosidase. **Protein Expression and Purification** 17(1): 153-162.

CHAPTER II

REVIEW OF LITERATURE

2.1 β-Glucosidases

2.1.1 Overview of β-glucosidases

β-Glucosidases (EC 3.2.1.21) are glycoside hydrolases (GH) which are found widely in all types of organisms (bacteria, archaea, and eukaryote). They play important roles in fundamental biological processes (Esen 1993). These enzymes hydrolyze the β-O-glycosidic bond at the anomeric carbon of glucosyl moieties, at the nonreducing end of carbohydrate or glycoside molecules.

According to the amino acid sequence similarity, glycoside hydrolases have been classfied into 95 families in 1997 (Henrissat *et al.* 1997), but the number of families increased steadily as the research moved on, so that 131 sequence-based families of GHs have been defined in the continuously updated CAZy (http://www.cazy.org.) in October 2012. The GH1, GH5, and GH30 β-glucosidases fall in GH Clan A, which possess the same tertiary structure which are $(\beta/\alpha)_8$-barrel with the catalytic acid/base on the C-terminal end of β-strands 4 and catalytic nucleophile on β-strand 7 (Henrissat *et al.* 1995, Jenkins *et al.* 1995). Catalysis by GH1 β-glucosidases involves these two catalytically active glutamic acid residues that are embedded in highly conserved TFNEP (catalytic acid/base) and I/VTENG (catalytic nucleophile) peptide motifs (Xu *et al.* 2004). These amino acid residues are important in catalysis and make up part of a crater-shaped active site (Henrissat *et al.* 1995, Czjzek *et al.* 2000).

2.1.2 Glycosides in plant

Glycosides are widely distributed throughout the plant and crucial to the physiological function of GH1 enzymes. Glycosides are inactive forms of many aglycones in plants, in which glycosylation can increase the solubility, stability and allow high accumulation in organelles like vacuoles (Esen 1993). So far, various glycosides have been reported to be hydrolyzed by plant β-glucosidases, including the defense-related glucosides, eg. linamarin, dhurrin, prunasin, and its precursor amygdalin, 2-O-β-D-glucopyranosyl-4-hydroxy-7-methoxy-1,4-benzoxazin-3-one (DIMBOAGlc) and the flavonoids apigenin 7-O-β-D-glucoside, diadzin and genistin, and phloridzin (Hsieh *et al.* 2001, Chuankhayan *et al.* 2005), the monolignol β-glucosides, coniferin and *para* coumaryl alcohol (Escamilla-Treviño *et al.* 2006), the phytohormones, abscissic acid-β-D-glucosyl ester, salicin and indoxyl β-D-glucoside, pyridoxin glucoside, the monoterpene alkaloid strictosidine, cell-wall-related oligosaccharides, eg, cellobiose, cellotriose, laminaribiose, laminaritriose (Hrmova *et al.* 1996, Akiyama *et al.* 1998), hydroxamic acid glucoside (Niemeyer 1988, Cicek *et al.* 1998, Sue *et al.* 2000). The structure of some glucoside compounds are shown in Figure 2.1.

The major glycosides found in various tissues of rice include glycosylsterols, flavonoid glucosides, hormone glucosides, a vitamin glucoside, and pantonic acid glucoside glycosylsterols, flavonoid glucosides, hormone glucosides, vitamin glucoside, and pantonic acid glucoside (Opassiri *et al.* 2006). Flavonoid glucosides is one of the major groups of compounds found in rice, including mainly anthocyanins (Ichikawa *et al.* 2001, Hu *et al.* 2003, Irakli *et al.* 2012, Lee *et al.* 2012, Matsuda *et al.* 2012), tricin-O-glucoside (Chung *et al.* 2005, Duarte-Almeida *et al.* 2007, Matsuda *et al.* 2012), the phenolic compounds addressed above possess antioxidant, anticancer

and antiviral biological activities as free radical scavengers and protein kinase C inhibitors (Ichikawa *et al.* 2001, Hu *et al.* 2003, Tian *et al.* 2005, Park *et al.* 2012, Soi-ampornkul *et al.* 2012).

Several phytohormone glucosides have been found in rice, including many kinds of gibberellin glucosides (Schliemann 1984, Hasegawa *et al.* 1994), salicylic glucosides (Chern *et al.* 2005), pyridoxine glycosides (Tadera *et al.* 1988, Opassiri *et al.* 2004), cytokinin O-glucosides (Kudo *et al.* 2012) and IAA-glucosiyl ester (Ruo-Zhong *et al.*, Morino *et al.* 2005).

Salicylic acid glucoside was found to play a role as a reservoir for free salicylic acid (Seo *et al.* 1995, Hennig *et al.* 2002) and salicylic acid glucoside levels may serve as a key factor in activating the rice defenses necessary for chemically induced disease resistance against blast fungus pathogens, and salicylic acid glucoside possibly contributes to systemic acquired resistance by serving as a natural regulator in rice plants (Iwai *et al.* 2007). Furthermore, endogenous salicylic acid was found to protect rice from oxidative damage caused by aging, as well as by biotic and abiotic stresses (Yang *et al.* 2004).

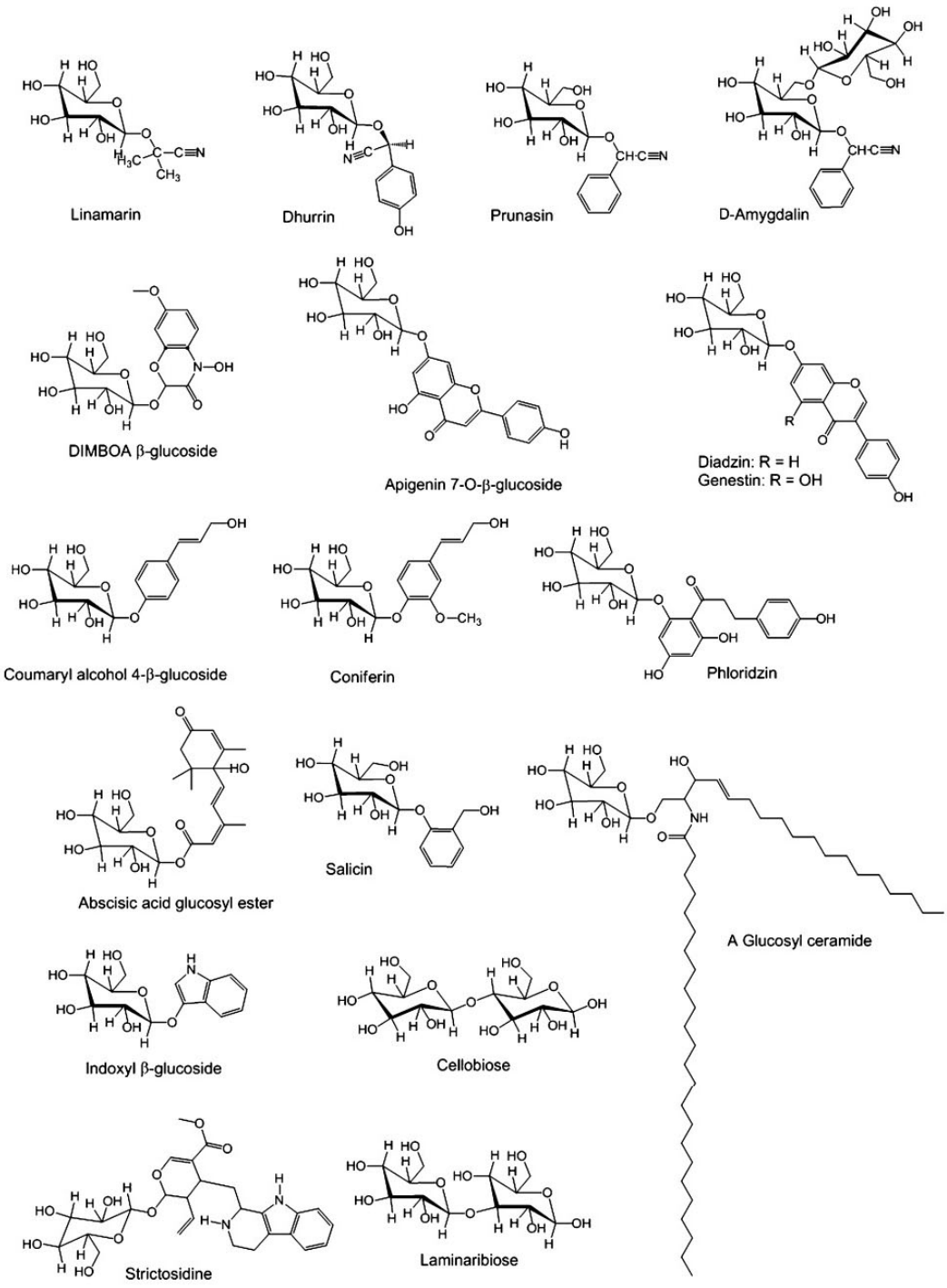

Figure 2.1 Structures of example β-glucosidase substrates. The plant cyanogenic glucosides linamarin, dhurrin, prunasin, and its precursor amygdalin. Other defense-related glycosides include 2-O-β-D-gluco-pyranosyl-4 -hydroxy-7-methoxy-1,4-benzoxazin-3-one (DIMBOAGlc) and the fla-

vornoids apigenin 7-O-β-D-glucoside, the isoflavonoids diadzin and genistin, and phloridzin. Coniferin and coumaryl alcohol represent monolignol β-glucosides, while abscissic acid glucosyl ester is a phytohormone glucoconjugate and salicin and indoxyl-β-D-glucoside are other plant glycosides with similarity to phytohormones. Strictosidine is the metabolic precursor to a wide array of monoterpene alkaloids. Cellobiose and laminaribiose represent plant cell-wall-derived oligosaccharides and can be extended with the same linkage to give the corres- ponding triose, tetraose, etc. In the lower right is an example of a glucosyl ceramide, one of the substrates for human acid β-glucosidase (GBA1) and other mammalian β-glucosidases (Ketudat Cairns and Esen 2010).

2.1.3 Functions of β-glucosidases in plants

β-Glucosidases have a variety of functions in plants, including cell wall remodeling, lignification, activation of metabolic intermediates, chemical defense, plant-microbe interactions, phytohormone activation, and release of volatiles from their glycosides (Ketudat Cairns and Esen 2010). They fulfill these roles by hydrolyzing the glycosidic bond at the nonreducing end of a glycoside or an oligosaccharide, thereby releasing the aglycones from the inactive glucosides. It is the nature of the aglycone that accounts for most of the physiological functions of β-glucosidases. The functions of aglycones released from the glycoside may be a monolignol to form the lignin (Dharmawardhana *et al.* 1995, Chapelle *et al.* 2012), a toxic compound to defend against pathogens and herbivores (Poulton 1990, Dakora *et al.* 1996, Mizutani *et al.*

2002, Morant *et al.* 2008), an active phytohormone to regulate the growth of the plant (Smith *et al.* 1978, Brzobohaty *et al.* 1993, Zouhar *et al.* 1999, Lee *et al.* 2006), a reactive metabolic intermediate to form further product (Esen 1993, Barleben *et al.* 2005), a volatile scent compound (Yablonka-Reuveni *et al.* 1999) or monosaccharides released from hydrolysis of the cell wall polysaccharide for reuse (Leah *et al.* 1995, Akiyama *et al*. 1998, Opassiri *et al.* 2003).

In defense against pathogens and herbivores, β-glucosidases act by releasing toxic defense compounds, such as hydrogen cyanide, isoflavones, and flavornoids produced by hydrolysis of their glucosides (Poulton *et al.* 1994, Dakora and Phillips 1996) and by releasing induced factors, such as volatiles that attract parasitoids of the herbivores to attack them (Mattiacci *et al.* 1995). In white clover, β-glucosidase is responsible for the cleavage of cyanogenic glucosides from leaf tissue after mechanical damage (Barrett *et al.* 1995). In maize, β-glucosidase is believed to act in defense against pests by releasing a toxic aglycone from the abundant natural β-glucoside-2-glucopyranosyl-4-hydroxy-7-methoxy-1,4-benzoxazin-3-one (DIMBOAGlc), which occurs mostly in young seedling parts of maize at millimolar concentrations (Babcock *et al.* 1994). The aglycone of DIMBOAGlc is DIMBOA, and it is the major defense compound in maize against aphids, the European corn borer and other pests (Kahler *et al.* 1986, Massardo *et al.* 1994). In olive leaf and fruit, β-glucosidase cleaves the oleuopein, a bitter phenol glucoside, to release an active aglycone in defense against pathogens (Amiot *et al.* 1989, Soler-Rivas *et al.* 2000). β-Glucosidase regulate the biological activity of plant phytohormones, such as cytokinins, gibberellins, auxins, salicylic acid and abscisic acids by releasing active forms from inactive hormone glucoside conjugates (Smith and Van Staden 1978, Schliemann *et al*. 1984, Zouhar *et al.* 1999). β-Glucosidases are also critical for activation of lignin

precursors by the hydrolysis of coniferin glycoside to the monolignol coniferyl alcohol (Dharmawardhana *et al.* 1995, Escamilla-Treviño *et al.* 2006). β-Glucosidases have also been reported to act in the depolymerization process of plant cell wall. Rice and barley β-glucosidases could hydrolyze cell wall hydrolysis products, including cellobiose, laminaribiose and other short-chain gluco-oligosaccharides (Leah *et al.* 1995, Akiyama *et al.* 1998, Opassiri *et al.* 2003). β-Glucosidases release molecules that act as intermediates during metabolic processes, such as of strictosidine, an intermediate in the synthesis of monoterpenoid indole alkaloids (Esen 1993, Barleben *et al.* 2005).

It seems evident that the substrate specificity, localization of the enzymes with respect to potential substrates, and the function of the substrates will determine the roles of these enzymes in living cells (Ketudat Cairns and Esen 2010).

2.1.4 Glycoside hydrolysis family 1

Glycoside hydrolysis famliy 1 enzymes were classified into many subfamilies, depending on their amino acid sequences. Despites the sequence similarity, these subfamilies display a wide range of activities, including phospho-β-galactosidases, β-galactosidases, β-mannosidases, phospho-β-glucosidases, hydroxyisourate hydrolase, myrosinases, disaccharidases and thioglucosidases besides β-glucosidases (Ketudat Cairns and Esen 2010). Some GH1 enzymes are capable of releasing multiple kinds of sugars from aglycones (Hösel *et al.* 1975, Chuankhayan *et al.* 2005). By contrast, some GH1 enzymes have high specificity for glucosides or fucosides, or may hydrolyze other glycosides, such as β-galactosides, β-mannosides, and β-xylosides, as well (Mizutani *et al.* 2002). Obviously, plant family 1 glycoside hydrolases show a

range of glycone specificities (Opassiri *et al.* 2006). Plant GH1 enzymes tend to show high specificity for their aglycones, though many hydrolyze synthetic, nonphysiological substrates, like p-nitrophenol (*p*NP)-β-glycosides. The aglycones span a wide range of structures, including hydroxaminic acids, isoflavonoids, rotenoids, alkaloids, hydroxyquinones, cyanogenic nitriles, etc. (Opassiri *et al.* 2006).

Forty-eight GH1 genes were identified from *Arabidopsis thaliana* genome (Xu *et al.* 2004). Later, forty GH1 genes were identified from rice databases, including 2 possible endophyte genes, 2 likely pseudogenes, 2 gene fragments, and 34 apparently competent rice glycosidase genes (Opassiri *et al.* 2006). The large size of both rice and *Arabidopsis* GH1 may reflect different substrate specificity and expression patterns in plant tissues and/or in response to environmental conditions (Ketudat-Cairns and Esen 2010).

Amino acid sequence alignment and phylogenetic analysis of GH1 proteins showed that many closely related members are located on the same chromosome. Comparison between rice and *Arabidopsis* GH1 members revealed that 8 clearly distinct clusters of plant-like GH1 genes (marked 1 to 8 in Figure 2.2) contain both *Arabidopsis* and rice genes that are clearly more closely related to each other than to other GH1 genes within their own species (Opassiri *et al.* 2006).

Phylogenetic analysis of rice GH1 members with other plant enzymes showed that some rice and *Arabidopsis* members that are clustered in the same groups were found to be closely related to β-glucosidases from other plants (Figure 2.3). For example, Os4BGlu14, Os4BGlu16 and Os4BGlu18, which cluster with *Arabidopsis* BGLU45, 46 and 47, are grouped with *Pinus contorta* coniferin/syringing β-glucosidase (PC AAC69619), suggesting that they may be involved in lignification.

Later, recombinantly expressed *Arabidopsis* BGLU45 and BGLU46 have been shown to hydrolyze lignin precursors (Escamilla-Treviño *et al.* 2006). Os1BGlu1, Os3BGlu7, Os3BGlu8, Os7BGlu26 and Os12BGlu38 β-glucosidases clearly grouped with barley BGQ60 β-glucosidase/β-mannosidase (Leah *et al.* 1995, Hrmova *et al.* 1998). Kinetic analysis showed that the hydrolytic activity of Os3BGlu7 toward β-linked glucose oligosaccharides is similar to that of the barley enzyme (Opassiri *et al.* 2004).

All the above analyses suggest that the same cluster may have the similar functions, so it is advisable and economical to clarify the function of one representative gene to help understand the functions of the whole cluster of genes.

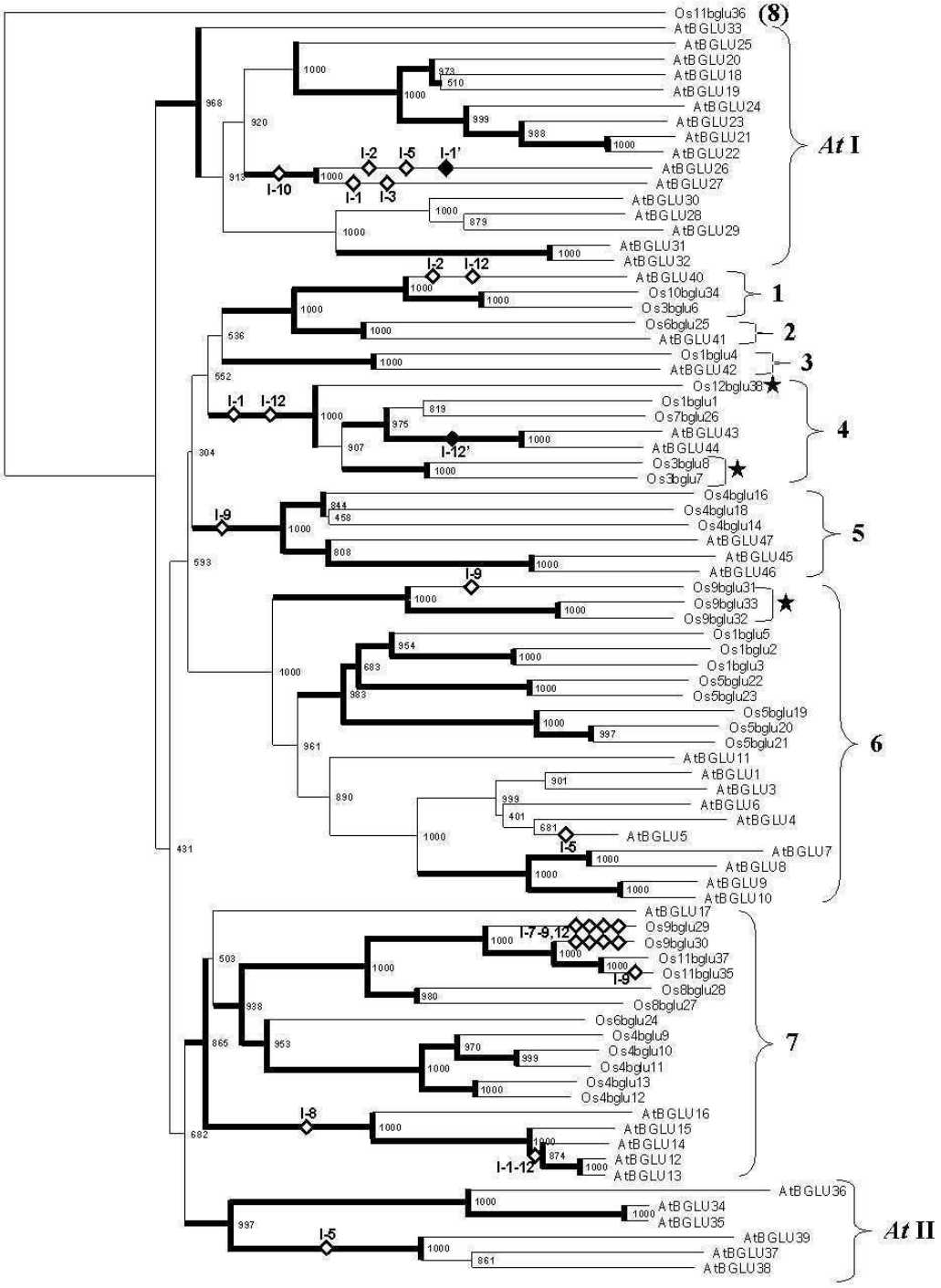

Figure 2.2 Phylogenetic tree of predicted protein sequences of rice and *Arabidopsis* Glycoside Hydrolase Family 1 genes. The tree was derived by the Neighbor-joining method from the protein sequence alignment made with Clustalx with default settings, followed by manual adjustment. Large gap

regions were removed for the tree calculation. The tree is drawn as an unrooted tree, but is rooted by the outgroup, *Os*11*bglu*36, for the other sequences. The boot-strap values are shown at the nodes. The clusters supported by a maximum parsimony analysis are shown as bold lines, and the loss and gain of introns are shown as open and closed diamonds, respectively. The 7 clusters that contain both *Arabidopsis* and rice sequences that are clearly more closely related to each other than to other *Arabidopsis* or rice sequences outside the cluster are numbered 1–7, while the outgroup cluster for which the *Arabidopsis* orthologue is not shown is numbered (8). Two *Arabidopsis* clusters that are more distantly diverged from the clusters containing both rice and *Arabidopsis* are numbered At I and At II, while rice genes and groups of genes that appear to have diverged before subclusters containing both rice and *Arabidopsis* are marked with stars (Copied from Opassiri *et al.* 2006).

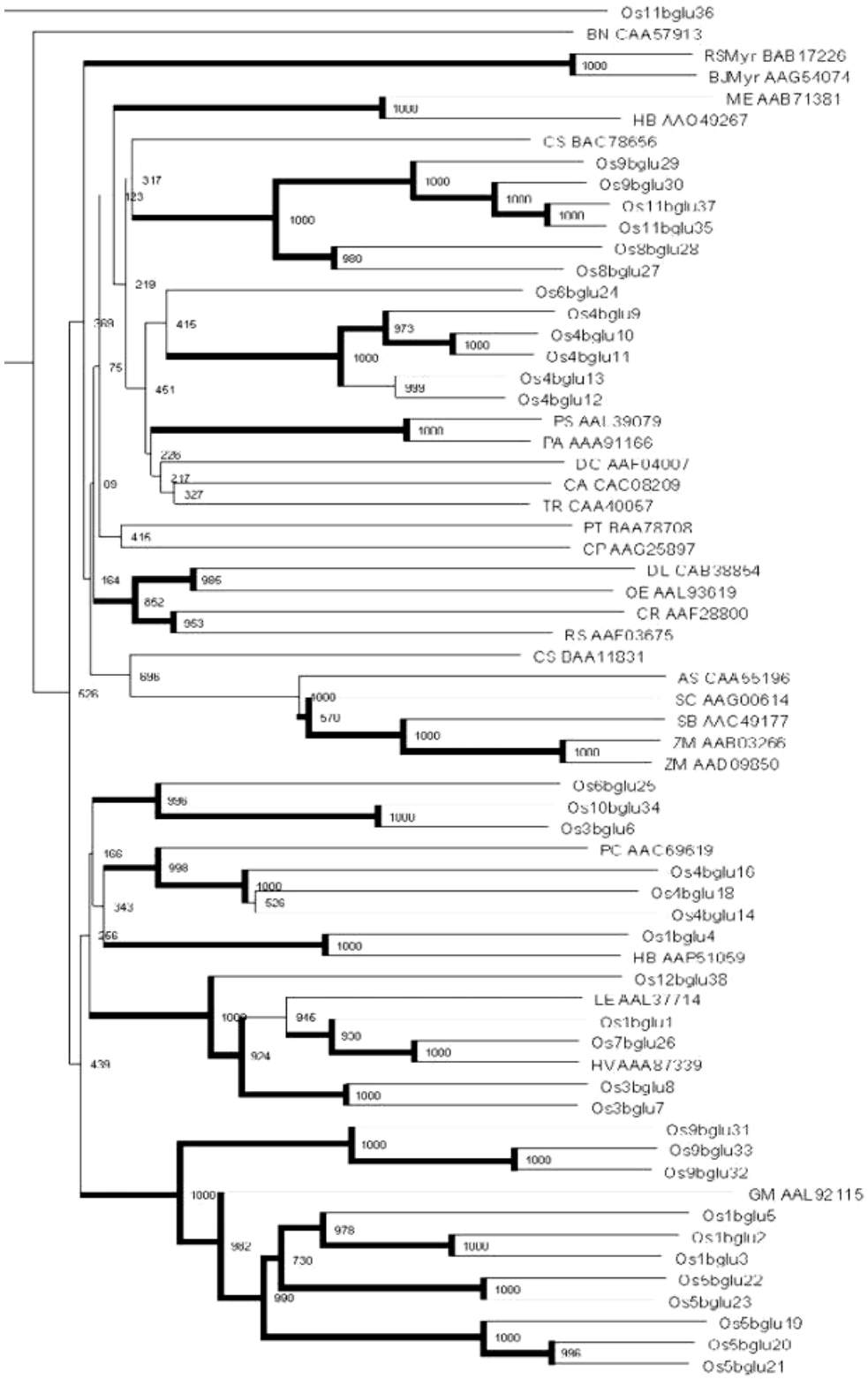

Figure 2.3 Relationship between rice and other plant GH1 protein sequences described by a phylogenetic tree rooted by Os11BGlu36. The sequences

were aligned with ClustalX, then manually adjusted, followed by removal of N-terminal, C-terminal and large gap regions to build the data model. The tree was produced by the neighbor joining method and analyzed with 1000 bootstrap replicates. The internal branches supported by a maximum parsimony tree made from the same sequences are shown as bold lines. The sequences other than rice include: ME AAB71381, *Manihot esculenta* linamarase; RSMyr BAB17226, *Raphanus sativus* myrosinase; BJMyr AAG54074, *Brassica juncea* myrosinase; BN CAA57913, *Brassica napus* zeatin-O-glucoside-degrading β-glucosidase; HB AAO49267, *Hevea brasiliensis* rubber tree β-glucosidase; CS BAA11831, *Costus speciosus* furostanol glycoside 26-O-β-glucosidase (F26G); PS AAL39079 *Prunus serotina* prunasin hydrolase isoform PHB precursor; PA AAA91166, *Prunus avium* ripening fruit β-glucosidase; TR CAA40057, *Trifolium repens* white clover linamarase; CA CAC08209, *Cicer arietinum* epicotyl β-glucosidase with expression modified by osmotic stress; DC AAF04007, *Dalbergia cochinchinensis* dalcochinin 8'-O-β-glucoside β-glucosidase; PT BAA78708, *Polygonum tinctorium* β-glucosidase; DL CAB38854, *Digitalis lanata* cardenolide 16-O-glucohydrolase; OE AAL93619, Olea europaea subsp. europaea β-glucosidase; CR AAF28800, *Catharanthus roseus* strictosidine β-glucosidase; RS AAF03675, *Rauvolfia serpentina* raucaffricine-O-β-D-glucosidase; CP AAG25897, *Cucurbita pepo* silverleaf whitefly induced protein 3; AS CAA55196, *Avena sativa* β-glucosidase; SC AAG00614, *Secale cereale* β-glucosidase; ZM AAB03266, *Zea mays* cytokinin β-glucosidase; ZM AAD09850, *Zea*

mays β-glucosidase; SB AAC49177, *Sorghum bicolor* dhurrinase; LE AAL37714, *Lycopersicon esculentum* β-mannosidase; HV AAA87339, barley BGQ60 β-glucosidase; HB AAP51059, *Hevea brasiliensis* latex cyanogenic β-glucosidase; PC AAC69619 *Pinus contorta* coniferin β-glucosidase; GM AAL92115, *Glycine max* hydroxyisourate hydrolase; CS BAC78656, *Camellia sinensis* β-primeverosidase. Os1BGlu4, the enzyme of this study is boxed (modified from Opassiri *et al.* 2006).

2.1.5 Rice β-glucosidases

Bioinformatics analysis indicated that all of the rice β-glucosidase ORFs, except *Os*1*bglu*4 and *Osbglu*39, were predicted to have signal peptides ranging in length from 18 to 44 amino acids, which would target them to the secretory pathway. The predicted cellular locations for rice β-glucosidases included the cell exterior, cytoplasm, peroxisome, vacuole, ER lumen, ER membrane, plasma membrane, and mitochondrial matrix. Predicted precursor protein lengths vary from 458-647 amino acids, which correspond to protein molecular weights of 55.3 to 73.2 kD. Isoelectric points (pI) of predicted proteins are divided into 3 groups, acidic (4.96–6.66), neutral (6.99-7.78), and basic (8.36-8.96) and 21 of 34 of these proteins are in the acidic group. All rice GH1 members except Os1BGlu4 were predicted to contain one to six N-linked glycosylation sites. The protein properties predicted for the rice GH1 members are similar to *Arabidopsis* GH1 proteins in the average numbers of glycosylation sites, pI and predicted MW of precursor proteins and mature proteins (Opassiri *et al.* 2006).

In 1973, rice β-glucosidase activity against the synthetic substrate pNP-β-D-glucoside was reported (Palmiano *et al.* 1973). Later, partially purified rice β-glucosidases were shown to hydrolyze gibberellin glucosides (Schliemann 1984).

A β-glucosidase was reported to hydrolyze the derivative of pantoic acid, R (-) pantoyllactone-β-D-glucopyranoside from rice seedlings (Menegus *et al.* 1995). Thorough characterization was later done for a rice cell wall-bound β-glucosidase and Os3BGlu7 (BGlu1) β-glucosidases cloned from rice seedlings (Akiyama *et al.* 1998, Opassiri *et al.* 2003, Opassiri *et al.* 2004). Later, the Os3BGlu7 β-glucosidase was found to hydrolyze β-1,4-linked oligosaccharides with increasing catalytic efficiency (k_{cat} /K_m) values as the degree of polymerization (DP) increased from 2 to 6 (Opassiri *et al.* 2004). In contrast, hydrolysis of β-1,3-linked oligosaccharides decreased from DP 2 to 3, and polymers with a DP greater than 3 were not hydrolyzed. The enzyme also hydrolysed *p*-nitrophenyl β-D-glycosides and some natural glucosides but with lower catalytic efficiency than β-linked oligosaccharides. Pyridoxine 5-O-β-D-glucoside was the most efficiently hydrolysed natural glycoside tested. Os3BGlu7 also had high transglucosylation activity towards pyridoxine, producing pyridoxine 5'-O-β-D-glucopyranoside in the presence of the glucose donor *p*-nitrophenyl-β-D-glucoside. Besides, rice Os3BGlu7, Os3BGlu8, and Os7BGlu26 hydrolyzed cello-oligosaccharides with increasing efficiency as the degree of polymerization (DP) increased from 2 to 6, while Os4BGlu12 showed little increase in activity with DP and Os3BGlu6 hydrolyzed disaccharides best. The Os3BGlu7 and Os3BGlu8 isoenzymes are widely expressed in rice tissues, so they may be needed for release of glucose from oligosaccharides generated in cell wall remodeling at various stages of plant development (Ketudat Cairns and Esen 2010). The Os4BGlu12 was found to be a cell wall-bound enzyme, the cDNA of the Os4BGlu12 gene was isolated by RT-PCR from rice seedlings, a thioredoxin-Os4BGlu12 fusion protein expressed in *E. coli* efficiently hydrolyzed β-(1, 4)-linked oligosaccharides of 3-6 glucose residues and laminaribiose (Opassiri *et al.* 2006). Later, rice Os4BGlu12 was found to be a wound-induced β-glucosidase that hydrolyzes cell wall-β-glucan-derived

oligosaccharides and glycosides (Opassiri *et al.* 2010). The structure of rice BGlu1 β-glucosidase has been solved at 2.2 Å resolution. The structures were similar to the known structures of other glycosyl hydrolase family 1 (GH1) β-glucosidases, but showed several differences in the loops around the active site, which lead to an open active site with a narrow slot at the bottom, compatible with the hydrolysis of long β-1,4-linked oligosaccharides (Chuenchor *et al.* 2010). The crystal structure of Os3BGlu6 was solved at 1.83Å. The side chain of methionine-251 in the mouth of the active site appeared to block the binding of extended β-(1/4)-linked oligosaccharides and interact with the hydrophobic aglycone of n-octyl-β-D-thioglucopyranoside (Seshadri *et al.* 2009). Besides, the crystal structure of Os4BGlu12 was solved at 2.50 Å resolution, the result showed that the overall structure of rice Os4BGlu12 is typical of GH1 enzymes (Sansenya *et al.* 2011).

2.2 Recombinant β-glucosidase expression

Availability of highly purified β-glucosidase is a basic requirement for analysis of enzyme kinetics and structure function relationships. However, there are many factors that affect soluble recombinant β-glucosidase expression, such as temperature, chaperonin proteins, induction time and IPTG application and expression host strains.

It has also been suggested that an increasing growth temperature is one parameter to promote aggregation of a recombinant protein as an inclusion body (Strandberg *et al.* 1991, Chrunyk *et al.* 1993). Cicek and Esen (2000) expressed the maize β-glucosidases, rGlu1 and rGlu2, from the pET21 vector in *E. coli* strain BL21 pLysS and indicated that a higher percentage of total expressed β-glucosidase was soluble when the cultures were grown and induced at room temperature (25 ^{o}C) than at 37 ^{o}C. Higher temperatures (30 ^{o}C and 37 ^{o}C) did not favor production of higher active

protein, while lower temperatures (20 ^{o}C and 25 ^{o}C) favored production of Os3BGlu6 in the active form (Seshadri 2008). Appropriate induction temperature promoted the correct folding of the protein (Dinner *et al.* 1999) and increased the percentage of the soluble protein. So far, many β-glucosidases have been produced and induced at 20-30 ^{o}C (Opassiri *et al.* 2003, Opassiri *et al.* 2004, Opassiri *et al.* 2007, Chuenchor *et al.* 2008, Kuntothom *et al.* 2009, Seshadri *et al.* 2009, Opassiri *et al.* 2010).

It has been demonstrated that the folding of many proteins can be facilitated by proteins called molecular chaperones, and the aggregation of overexpressed protein may be prevented by fusion with small protein molecules, such as Thioredoxin (Trx), Glutathione S-transferase (GST), Maltose binding protein (MBP), The *Escherichia coli* heat shock protein complex (GroEL/ES) and small ubiquitin-like modifier (SUMO), as has been reported for several proteins (Liu *et al.* 2005, Purbey *et al.* 2006). Among these small proteins, the Trx, in the pET32 vector system, has been extensively used in the expression of β-glucosidases (Cicek and Esen 1998, Opassiri *et al.* 2003, Opassiri *et al.* 2006, Opassiri *et al.* 2007, Kuntothom *et al.* 2009, Gomez *et al.* 2010, Zhang *et al.* 2011).

In the expression of recombinant protein using the pET systems, IPTG should be added into the medium so the *Lac* operon can initiate the expression of T7 polymerase. However, different IPTG concentrations result in variable amounts of active protein. Many beta-glucosidases, for example Os3BGlu8, Os3BGlu7, Os7BGlu26, Os4BGlu12, can be induced to express at the IPTG concentration from 0.1 mM to 0.5 mM. There were no significant differences in the activity of Trx-Os4bglu12 expressed in *E. coli* in the presence of 0.1-0.5 mM IPTG at 20, 25 and 30 ^{o}C, for 8-16 hr. The expression of pET32a(+)-bglu1 (BGlu1) was induced in the presence of 0.4 mM IPTG, at 20 ^{o}C for 8 hr (Opassiri *et al.* 2003). Strangely, in the

expression of rice Os3BGlu6, after 16 hr of incubation at 20 ^{o}C, soluble extracts of induced cells with 0.4 mM IPTG and with no addition of IPTG had similar β-glucosidase activity, which means the protein can be expressed well even without the IPTG inducer (Seshadri 2008).

Many *E. coli* strains can be used as the host strains for pET vector protein expression system, such as BL21(DE3), Origami(DE3), Origami B(DE3), Rosetta-(DE3), Rosettagami(DE3). Amonog these *E. coli* strains, Origami(DE3) had been used for expressing Os3BGlu7, Os3BGlu8 and Os7BGlu26 (Kuntothom *et al.* 2009). OrigamiB (DE3) had been used for the expression of Os4BGlu12 and GH5BG (Opassiri *et al.* 2006, Chantarangsee *et al.* 2007, Opassiri *et al.* 2007). The *E. coli* strain Rosetta(DE3) was used for the expression of two intracellular β-glucosidases belonging to the glycoside hydrolase family 1 from the basidiomycete *Phanerochaete chrysosporium* (Tsukada *et al.* 2006).

2.3 RNAi technique

RNA interference (RNAi) is an RNA-dependent gene silencing process initiated by the double-stranded RNA (dsRNA), also known as post transcriptional gene silencing (PTGS) in plants. The enzyme dicer trims the dsRNA into short fragments of 21-25 base pairs, namely small interfering RNA strands (siRNA), and degrades its homologous mRNA and thus inhibits the expression of target genes (Fire *et al.* 1998, Fire 1999). When a double-stranded RNA of the gene of interest is formed and introduced into a cell or organism, where it is recognized as exogenous genetic material, it induces the RNAi reaction. Using this mechanism, a dramatic decrease in the expression of a targeted gene can be achieved. Studying the effects of this decrease

can show the physiological role of the gene product (Hoffmann *et al.* 2006). Since RNAi may not totally abolish expression of the gene, this technique is sometimes referred as a "knock down", to distinguish it from "knock out" procedures in which expression of a gene is entirely eliminated (Voorhoeve *et al.* 2003). Knock down the expression of target genes can be achieved by expressing dsRNA through stable or transient transformation with RNAi constructs (Wesley *et al.* 2001, Zentella *et al.* 2002, Miki *et al.* 2004).

The selective and robust effect of RNAi on gene expression makes it a valuable research tool widely applied to study gene function. With the completion of the entire rice genome sequences, RNAi provides a powerful approach for functional genomics study and genetic improvement of rice (Leung *et al.* 2004, Crane *et al.* 2007).

The pOpOff2 vector allows dexamethasone-inducible RNAi against plant genes was reported (Wielopolska *et al.* 2005). The pOpOff2 vector utilizes a modified pHELLSGATE vector, under the control of the pOp6 promoter, and the synthetic transcription factor, LhGR (Wielopolska *et al.* 2005). The production of RNAi-inducing hairpin RNA from this system can be regulated by the application and removal of dexamethasone. Silencing of a target gene encoding phytoene desaturase in *Arabidopsis* was highly effective 24 hr after application of dexamethasone. In the presence of the hormone silencing was maintained for at least 5 days, while removal of the inducer resulted in significant recovery within 24 hr (Wielopolska *et al.* 2005). Insertion of target gene sequences into this vector is mediated by GATEWAY™ recombination, facilitating the use for high-throughput applications, such as gene discovery or validation. The inducibility of RNAi from this system may be useful in helping to identify the functions of genes which when constitutively silenced give

embryo lethality or pleiotropic phenotypes (Wielopolska *et al.* 2005). So, in this research, the RNAi technique using pOpOff2 RNAi vector was adopted to determine the function of *Os*1*bglu*4.

2.4 *Agrobacterium* mediated rice transformation

Agrobacterium EHA105 is "super-virulence" strain and has been reported to be effective for rice transformation (Cao *et al.* 1998, Cheng *et al.* 1998, He *et al.* 2008). Many research papers have proven the success of rice transformation by this *Agrobacterium* strain (Trick *et al.* 1998, Yamada *et al.* 2001, Yancheva *et al.* 2006, Jin *et al.* 2007). Therefore, *Agrobacterium* strain EHA105 was used to construct the transgenic plants in this research.

The first reliable *Agrobacterium*-mediated transformation system for rice was reported in 1994 (Hiei *et al.* 1994). Since then, efficient transformation and regeneration of *O. sativa* L. japonica varieties have been reported widely (Abe *et al.* 1986, Aldemita *et al.* 1996, Zhang *et al.* 1997, Gelvin 2003). However, tissue browning and necrosis following *Agrobacterium* infection is still a critical problem in genetic transformation in rice. Many factors, such as rice variety, binary vector, selectable marker gene and promoter, inoculation and co-culture conditions, medium, desiccation, *Agrobacterium* density and surfactants were found to affect the recovery of stably transformed plant cells after *Agrobacterium* infection (Cheng *et al.* 2004). Many efforts have been conducted to improve the efficiency of transformation (Toki 1997, Toki *et al.* 2006, Zhao *et al.* 2011, Chen 2012, Chen *et al.* 2012, Duan *et al.* 2012, Ozawa 2012). The competency of scutellum tissue from 1-day pre-cultured seeds for *Agrobacterium*-mediated transformation was reported; early infection of rice seeds

with *Agrobacterium* enhanced efficient selection of transformed calli. Transgenic rice plantlets were successfully regenerated within a month from the start of the aseptic culture of mature seeds (Toki *et al.* 2006). This protocol was adopted to use for rice transformation in this research.

2.5 Reporter gene application

GUS is encoded by the *E. coli uidA* gene (Jefferson *et al.* 1987), has a molecular weight of 68.2 kDa. 5-Bromo-4-chloro-3-indolyl glucuronide (X-Gluc) is the typical substrate for histochemical localization of β-glucuronidase activity in tissues and cell. The indolyl derivative produced from glucuronidase activity on X-Gluc must undergo an oxidative dimerization to form an insoluble and highly colored indigo dye which can be visualized. GUS staining can be used to acess the activity of the promoter, to determine where and how strong the promoter is expressed. For example, The AtBG1 upstream region was placed in front of the β-glucuronidase (GUS) coding region, and the resulting construct was introduced into plants, GUS expression was detected in seed cells. In vegetative tissues, GUS expression was low and highly specific to hydathodes of rosette and cauline leaves, and dehydration stress strongly induced GUS expression in hydathodes and the vasculature of rosette and cauline leaves, suggesting that AtBG1 participates in drought response (Lee *et al.* 2006). Ning *et al.* 2010 fused DSM1 gene promoter with GUS, the expression patterns in transgenic rice plants was checked. The result indicated that GUS staining was detected in hull, pistil, stamen, root, and mature leaves. In this study, the GUS staining was used to assess the activity of pOp6 promoter in transgenic rice.

Green fluorescent proteins (GFPs) are a unique type of protein involved in

the bioluminescence of many jellyfish (Prendergast *et al.* 1978). The GFP from *Aequorea victoria* is a 26.9 kDa protein (238 amino acid) which can fluoresce green upon excitation with blue light (Prasher *et al.* 1992). Native GFP from *A. victoria* absorbs optimally at 395 nm and emits at 509 nm (Gilroy 1997). The *GFP* gene can be introduced into organisms and maintained in their genome through breeding, injection with a viral vector, or cell transformation (Chudakov *et al.* 2005, Baker *et al.* 2008, Joo *et al.* 2008). Tagging proteins with GFP is as simple as attaching the gene for GFP to one end of the gene that encodes a protein of interest. Normally, the resulting GFP fusion protein behaves in the same way as the original protein (Inouye *et al.* 1994), and its movement can be monitored by following its fluorescence inside the cell by fluorescent microscopy (Yuste 2005). Today large numbers of proteins are being tracked in living cells by this method (Llopis *et al.* 1998, Chen *et al.* 2006, Ozawa 2009, Du *et al.* 2010, Chen *et al.* 2011, Yi *et al.* 2011, Ding *et al.* 2012).

With the aim of providing tools for high throughput gene analysis, pMDC83, a vector derived from pCambia T-DNA cloning vectors, was designed for *Agrobacterium* mediated transformation of a wide range of plant species. The pMDC83 vector is a Gateway-compatible *Agrobacterium* binary vector that facilitates fast and reliable DNA cloning drived by the 35S promoter. The GFP protein was designed to be fused at the C terminal of the target protein. The subcellular localization of the protein can be traced in the transgenic cells (Curtis *et al.* 2003). In this research, the pMDC83 vector was adopted to achieve the *Os*1*bglu*4 gene overexpression and subcellular localization.

2.6 Real time PCR technique

The profile of mRNA transcription has become a frequent research field in recent years. Changes in mRNA transcription levels are crucial to many developmental

processes (Mackay *et al.* 2002). The quantification of mRNA becomes indispensable procedure in biological research. Common methods for RNA detection include: northern blotting, *in situ* hybridisation, qualitative RT-PCR, RNase protection assay, competitive RT-PCR, microarray analysis, and quantitative real-time PCR (qPCR). The qPCR has become the most popular method for quantification of mRNA transcription levels in recent years due to its outstanding accuracy, broad dynamic range, and sensitivity. Moreover, qPCR is fast, easy to use, and highly reproducible, requiring a minimal amount of RNA and no post-PCR handling, and it avoids the use of radioactivity (Bustin 2002, Ginzinger 2002, Wong *et al.* 2005).

The real-time reverse transcription polymerase chain reaction (qRT-PCR) combines the nucleic acid amplification and detection steps into one homogeneous assay and obviates the need for gel electrophoresis to detect amplification products (Bustin *et al.* 2005).

Many reference genes have been studied to select the reference gene with stable expression under various environment conditions and across all tissue samples (Radonić *et al.* 2004). Normally, housekeeping genes are selected as the reference gene, for example, 18S Ribosomal RNA (*18S rRNA*), 25S Ribosomal RNA (*25S rRNA*), ubiquitin-conjugating enzyme E2 (*UBC*), ubiquitin 5 (*UBI 5*), ubiquitin 10 (*UBI 10*), actin 11 (*ACT 11*), eukaryotic elongation factor 1-alpha (*eEF-1α*), glyceral dehyde-3-phosphate dehydrogenase (*GAPDH*), eukaryotic initiation factor 4a (*eIF-4a*), and β-tubulin (*β-TUB*) (Schmittgen *et al.* 2000, Bas *et al.* 2004, Jain *et al.* 2006, Infante *et al.* 2008, Komiya *et al.* 2008, Hu *et al.* 2009). Among these reference genes, the *actin* gene showed the most stable expression among almost all the tested samples from two rice varieties, including different temporal and spatial specific tissues, especially in seeds at different developmental stages (Qi *et al.* 2002, Ma *et al.* 2006,

Caldana *et al.* 2007, Li *et al.* 2010). However, some researchers find that *actin* is not that stable in some conditions and suggest that *ubiquitin* is a better reference gene than *actin* (Jain *et al.* 2006). Ubiquitin reference gene has been used extensively as a reference gene in recent years (Miki *et al.* 2005, Sayler *et al.* 2007, Tamaki *et al.* 2007, Yu *et al.* 2007, Jiao *et al.* 2010). However, the uses of more than one reference gene were strongly recommended (Radonić *et al.* 2004, Reid *et al.* 2006, Tong *et al.* 2009). In this study, both *ubiquitin* and *actin* were used as reference genes.

2.7 References

Abe, T. and Y. Futsuhara (1986). Genotypic Variability for Callus Formation and Plant Regeneration in Rice (*Oryza sativa* L.). **Theoretical and Applied Genetics** 72(1): 3-10.

Ahn, Y. O., M. Mizutani, H. Saino and K. Sakata (2004). Furcatin Hydrolase from *Viburnum furcatum* Blume Is a Novel Disaccharide-Specific Acuminosidase in Glycosyl Hydrolase Family 1. **Journal of Biological Chemistry** 279(22): 23405-23414.

Akiyama, T., H. Kaku and N. Shibuya (1998). A Cell Wall-Bound Beta-Glucosidase from Germinated Rice: Purification and Properties. **Phytochemistry** 48(1): 49-54.

Akiyama, T. H. K. N. S. (1998). A Cell Wall-Bound β-Glucosidase from Germinating Rice. **Phytochemistry** 48(1): 49-54.

Aldemita, R. R. and T. K. Hodges (1996). *Agrobacterium tumefaciens*-Mediated Transformation of Japonica and Indica Rice Varieties. **Planta** 199(4): 612-617.

Amiot, M. J., A. Fleuriet and J. J. Macheix (1989). Accumulation of Oleuropein Derivatives During Olive Maturation. **Phytochemistry** 28(1): 67-69.

Babcock, G. D. and A. Esen (1994). Substrate Specificity of Maize β-Glucosidase. **Plant Science** 101(1): 31-39.

Baker, B., H. Mutoh, D. Dimitrov, W. Akemann, A. Perron*, et al.* (2008). Genetically Encoded Fluorescent Sensors of Membrane Potential. **Brain Cell Biology** 36(1): 53-67.

Barleben, L., X. Ma, J. Koepke, G. Peng, H. Michel*, et al.* (2005). Expression, Purification, Crystallization and Preliminary X-Ray Analysis of Strictosidine Glucosidase, an Enzyme Initiating Biosynthetic Pathways to a Unique Diversity of Indole Alkaloid Skeletons. **Biochimica et Biophysica Acta-Proteins & Proteomics** 1747(1): 89-92.

Barrett, T., C. Suresh, S. Tolley, E. Dodson and M. Hughes (1995). The Crystal Structure of a Cyanogenic B-Glucosidase from White Clover, a Family 1 Glycosyl Hydrolase. **Structure** 3(9): 951-960.

Bas, A., G. Forsberg, S. Hammarström and M. L. Hammarström (2004). Utility of the Housekeeping Genes 18s Rrna, B-Actin and Glyceraldehyde-3-Phosphate‐Dehydrogenase for Normalization in Real-Time Quantitative Reverse Transcriptase-Polymerase Chain Reaction Analysis of Gene Expression in Human T Lymphocytes. **Scandinavian Journal of Immunology** 59(6): 566-573.

Biswas, S., D. Sircar, A. Mitra and B. De (2011). Phenolic Constituents and Anti-oxidant Properties of Some Varieties of Indian Rice. **Nutrition & Food Science** 41(2): 123-135.

Brzobohaty, B., I. Moore, P. Kristoffersen, L. Bako, N. Campos*, et al.* (1993). Release of Active Cytokinin by a Beta-Glucosidase Localized to the Maize Root Meristem. **Science** 262(5136): 1051-1054.

Bustin, S. (2002). Quantification of mRNA Using Real-Time Reverse Transcription PCR (RT-PCR): Trends and Problems. **Journal of Molecular Endocrinology** 29(1): 23-39.

Bustin, S., V. Benes, T. Nolan and M. Pfaffl (2005). Quantitative Real-Time RT-PCR–a Perspective. **Journal of Molecular Endocrinology** 34(3): 597-601.

Caldana, C., W. R. Scheible, B. Mueller-Roeber and S. Ruzicic (2007). A Quantitative Rt-Pcr Platform for High-Throughput Expression Profiling of 2500 Rice Transcription Factors. **Plant Methods** 3(1): 7.

Cantarel, B. L., P. M. Coutinho, C. Rancurel, T. Bernard, V. Lombard*, et al.* (2009). The Carbohydrate-Active Enzymes Database (Cazy): An Expert Resource for Glycogenomics. **Nucleic Acids Research** 37 (suppl 1): D233-D238.

Cao, X., Q. Liu, L. Rowland and F. Hammerschlag (1998). Gus Expression in Blueberry (Vaccinium Spp.): Factors Influencing *Agrobacterium*-Mediated Gene Transfer Efficiency. **Plant Cell Reports** 18(3): 266-270.

Chantarangsee, M., W. Tanthanuch, T. Fujimura, S. C. Fry and J. Ketudat Cairns (2007). Molecular Characterization of B-Galactosidases from Germinating Rice (*Oryza sativa*). **Plant Science** 173(2): 118-134.

Chapelle, A., K. Moreel, R. Vanholme, P. Le-Bris, H. Morin*, et al.* (2012). Impact of Absence of Stem-Specific Beta-Glucosidases on Lignin and Monolignols. **Plant Physiology**.

Chen, M. (2012). Optimization of *Agrobacterium*-Mediated Transformation Method for Rice. **Journal of Anhui Agricultural Sciences** 7: 014.

Chen, M., J. Jing and S. JinLei (2012). Optimization of *Agrobacterium*-Mediated Rice Transformation. **Agricultural Biotechnology** 1(1): 12-13.

Chen, N., Y. Xu, X. Wang, C. Du, J. Du*, et al.* (2011). Osran2, Essential for Mitosis, Enhances Cold Tolerance in Rice by Promoting Export of Intranuclear Tubulin and Maintaining Cell Division under Cold Stress. **Plant, Cell & Environment** 34(1): 52-64.

Chen, S., L. Tao, L. Zeng, M. E. Vega-Sanchez, K. Umemura*, et al.* (2006). A Highly Efficient Transient Protoplast System for Analyzing Defence Gene Expression and Protein–Protein Interactions in Rice. **Molecular Plant Pathology** 7(5): 417-427.

Cheng, M., B. A. Lowe, T. M. Spencer, X. Ye and C. L. Armstrong (2004). Factors Influencing *Agrobacterium*-Mediated Transformation of Monocotyledonous Species. **In Vitro Cellular & Developmental Biology-Plant** 40(1): 31-45.

Cheng, X., R. Sardana, H. Kaplan and I. Altosaar (1998). *Agrobacterium*-Transformed Rice Plants Expressing Synthetic cryIA (b) and cryIA (c) Genes Are Highly Toxic to Striped Stem Borer and Yellow Stem Borer. **Proceedings of the National Academy of Sciences of the United States of America** 95(6): 2767-2772.

Chern, M., H. A. Fitzgerald, P. E. Canlas, D. A. Navarre and P. C. Ronald (2005). Overexpression of a Rice Npr1 Homolog Leads to Constitutive Activation of Defense Response and Hypersensitivity to Light. **Molecular Plant-Microbe Interactions** 18(6): 511-520.

Chrunyk, B., J. Evans, J. Lillquist, P. Young and R. Wetzel (1993). Inclusion Body Formation and Protein Stability in Sequence Variants of Interleukin-1 Beta. **Journal of Biological Chemistry** 268(24): 18053-18061.

Chuankhayan, P., Y. Hua, J. Svasti, S. Sakdarat, P. A. Sullivan*, et al.* (2005). Purification of an Isoflavonoid 7-O-B-Apiosyl-Glucoside β-Glycosidase and Its Substrates from *Dalbergia nigrescens* Kurz. **Phytochemistry** 66(16): 1880-1889.

Chudakov, D. M., S. Lukyanov and K. A. Lukyanov (2005). Fluorescent Proteins as a Toolkit for *in Vivo* Imaging. **Trends in Biotechnology** 23(12): 605-613.

Chuenchor, W., S. Pengthaisong, R. C. Robinson, J. Yuvaniyama, W. Oonanant*, et al.* (2008). Structural Insights into Rice Bglu1 Beta-Glucosidase Oligosaccharide Hydrolysis and Transglycosylation. **Journal of Molecular Biology** 377(4): 1200-1215.

Chung, I. M., S. J. Hahn and A. Ahmad (2005). Confirmation of Potential Herbicidal Agents in Hulls of Rice, *Oryza sativa*. **Journal of Chemical Ecology** 31(6): 1339-1352.

Cicek, M. and A. Esen (1998). Structure and Expression of a Dhurrinase (Beta-Glucosidase) from Sorghum. **Plant Physiology** 116(4): 1469-1478.

Coutinho, P. M. (1999). Carbohydrate-Active Enzymes: An Integrated Database Approach. **Recent Advances in Carbohydrate Bioengineering**.

Crane, Y. M. and S. B. Gelvin (2007). RNAi-Mediated Gene Silencing Reveals Involvement of *Arabidopsis* Chromatin-Related Genes in *Agro-bacterium*-Mediated Root Transformation. **Proceedings of the National Academy of Sciences of the United States of America** 104(38): 15156-15161.

Curtis, M. D. and U. Grossniklaus (2003). A Gateway Cloning Vector Set for High-Throughput Functional Analysis of Genes in Planta. **Plant Physiology** 133(2): 462-469.

Czjzek, M., M. Cicek, V. Zamboni, D. R. Bevan, B. Henrissat*, et al.* (2000). The Mechanism of Substrate (Aglycone) Specificity in Beta -Glucosidases Is Revealed by Crystal Structures of Mutant Maize Beta-Glucosidase-DIMBOA, -DIMBOAGLC, and -Dhurrin Complexes. **Proceedings of the National Academy of Sciences of the United States of America** 97(25): 13555-13560.

Dakora, F. and D. Phillips (1996). Diverse Functions of Isoflavonoids in Legumes Transcend Anti-Microbial Definitions of Phytoalexins. **Physiological and Molecular Plant Pathology** 49(1): 1-20.

Dharmawardhana, D. P., B. E. Ellis and J. E. Carlson (1995). A Beta-Glucosidase from Lodgepole Pine Xylem Specific for the Lignin Precursor Coniferin. **Plant Physiology** 107(2): 331-339.

Dharmawardhana, D. P., B. E. Ellis and J. E. Carlson (1995). A β-Glucosidase from Lodgepole Pine Xylem Specific for the Lignin Precursor Coniferin. **Plant Physiology** 107(2): 331-339.

Ding, B., M. del Rosario Bellizzi, Y. Ning, B. C. Meyers and G. L. Wang (2012). HDT701, a Histone H4 Deacetylase, Negatively Regulates Plant Innate Immunity by Modulating Histone H4 Acetylation of Defense-Related Genes in Rice. **The Plant Cell** (9): 1-12.

Dinner, A. R., V. Abkevich, E. Shakhnovich and M. Karplus (1999). Factors That Affect the Folding Ability of Proteins. **Proteins: Structure, Function, and Bioinformatics** 35(1): 34-40.

Du, H., N. Wang, F. Cui, X. Li, J. Xiao, *et al.* (2010). Characterization of the Beta-Carotene Hydroxylase Gene DSM2 Conferring Drought and Oxidative Stress Resistance by Increasing Xanthophylls and Abscisic Acid Synthesis in Rice. **Plant Physiology** 154(3): 1304-1318.

Duan, Y., C. Zhai, H. Li, J. Li, W. Mei, *et al.* (2012). An Efficient and High-Throughput Protocol for *Agrobacterium*-Mediated Transformation Based on Phosphomannose Isomerase Positive Selection in Japonica Rice (*Oryza Sativa* L.). **Plant Cell Reports**: 1-14.

Duarte-Almeida, J. M., G. Negri, A. Salatino, J. E. de Carvalho and F. M. Lajolo (2007). Antiproliferative and Antioxidant Activities of a Tricin Acylated Glycoside from Sugarcane (*Saccharum officinarum*) Juice. **Phytochemistry** 68(8): 1165-1171.

Escamilla-Treviño, L. L., W. Chen, M. L. Card, M. C. Shih, C. L. Cheng, *et al.* (2006). *Arabidopsis thaliana* β-Glucosidases BGLU45 and BGLU46 Hydrolyse Monolignol Glucosides. **Phytochemistry** 67(15): 1651-1660.

Esen, A. (1993). B-Glucosidase: Overview in B-Glucosidases: Biochemistry and Molecular Biology (Esen, A., Ed). **American Chemical Society, Washington, DC.**

Fire, A. (1999). Rna-Triggered Gene Silencing. **Algorithms** 14: 25-39.

Fire, A., S. Q. Xu, M. K. Montgomery, S. A. Kostas, S. E. Driver, *et al.* (1998). Potent and Specific Genetic Interference by Double-Stranded Rna in Caenorhabditis Elegans. **Nature** 391(6669): 806-811.

Gelvin, S. B. (2003). *Agrobacterium*-Mediated Plant Transformation: The Biology Behind the "Gene-Jockeying" Tool. **Microbiology and Molecular Biology Reviews** 67(1): 16-37.

Gilroy, S. (1997). Fluorescence Microscopy of Living Plant Cells. **Annual Review of Plant Biology** 48(1): 165-190.

Ginzinger, D. G. (2002). Gene Quantification Using Real-Time Quantitative Pcr: An Emerging Technology Hits the Mainstream. **Experimental Hematology** 30(6): 503-512.

Gomez, J. A., J. Chen, J. Ngo, D. Hajkova, I. J. Yeh*, et al.* (2010). Cell-Penetrating Penta-Peptides (CPP5s): Measurement of Cell Entry and Protein-Transduction Activity. **Pharmaceuticals** 3(12): 3594-3613.

Hasegawa, M., M. Nakajima, K. Takeda, I. Yamaguchi and N. Murofushi (1994). A Novel Gibberellin Glucoside 16α,17-Dihydroxy-16, 17-Dihydrogibberellin A4-17-O-B-D-Glucopyranoside, from Rice Anthers. **Phytochemistry** 37(3): 629-634.

He, X., S. C. Miyasaka, M. M. M. Fitch, P. H. Moore and Y. J. Zhu (2008). *Agrobacterium tumefaciens*-Mediated Transformation of Taro (*Colocasia esculenta* (L.) Schott) with a Rice Chitinase Gene for Improved Tolerance to a Fungal Pathogen Sclerotium Rolfsii. **Plant Cell Reports** 27(5): 903-909.

Hennig, J., J. Malamy, G. Grynkiewicz, J. Indulski and D. F. Klessig (2002). Interconversion of the Salicylic Acid Signal and Its Glucoside in Tobacco. **The Plant Journal** 4(4): 593-600.

Henrissat, B. (1991). A Classification of Glycosyl Hydrolases Based on Amino Acid Sequence Similarities. **Biochemical Journal** 280 (Pt 2): 309-316.

Henrissat, B., I. Callebaut, S. Fabrega, P. Lehn, J. P. Mornon*, et al.* (1995). Conserved Catalytic Machinery and the Prediction of a Common Fold for Several Families of Glycosyl Hydrolases. **Proceedings of the National Academy of Sciences of the United States of America** 92(15): 7090-7094.

Henrissat, B. and G. Davies (1997). Structural and Sequence-Based Classification of Glycoside Hydrolases. **Current Opinion in Structural Biology** 7(5): 637-644.

Hiei, Y., S. Ohta, T. Komari and T. Kumashiro (1994). Efficient Transformation of Rice (*Oryza sativa* L.) Mediated by *Agrobacterium* and Sequence Analysis of the Boundaries of the T-DNA. **The Plant Journal: for Cell and Molecular Biology** 6(2): 271-282.

Hoffmann, T., G. Kalinowski and W. Schwab (2006). Rnai‐Induced Silencing of Gene Expression in Strawberry Fruit (Fragaria x Ananassa) by Agroinfiltration: A Rapid Assay for Gene Function Analysis. **The Plant Journal** 48(5): 818-826.

Hösel, W. and W. Barz (1975). β-Glucosidases from *Cicer arietinum* L. **European Journal of Biochemistry** 57(2): 607-616.

Hrmova, M., A. J. Harvey, J. Wang, N. J. Shirley, G. P. Jones*, et al.* (1996). Barley Beta-D-Glucan Exohydrolases with Beta-D-Glucosidase Activity. Purification, Characterization, and Determination of Primary Structure from a cDNA Clone. **The Journal of Biological Chemistry** 271(9): 5277-5286.

Hrmova, M., E. A. Macgregor, P. Biely, R. J. Stewart and G. B. Fincher (1998). Substrate Binding and Catalytic Mechanism of a Barley Glucosidase/(1,4)-β-D-Glucan Exohydrolase. **The Journal of Biological Chemistry** 273(18): 11134-11143.

Hsieh, M. C. and T. L. Graham (2001). Partial Purification and Characterization of a Soybean β-Glucosidase with High Specific Activity Towards Isoflavone Conjugates. **Phytochemistry** 58(7): 995-1005.

Hu, C., J. Zawistowski, W. Ling and D. D. Kitts (2003). Black Rice (*Oryza sativa* L. Indica) Pigmented Fraction Suppresses Both Reactive Oxygen Species and

Nitric Oxide in Chemical and Biological Model Systems. **Journal of Agricultural and Food Chemistry** 51(18): 5271-5277.

Hu, R., C. Fan, H. Li, Q. Zhang and Y. F. Fu (2009). Evaluation of Putative Reference Genes for Gene Expression Normalization in Soybean by Quantitative Real-Time RT-PCR. **BMC Molecular Biology** 10(1): 93.

Ichikawa, H., T. Ichiyanagi, B. Xu, Y. Yoshii, M. Nakajima*, et al.* (2001). Antioxidant Activity of Anthocyanin Extract from Purple Black Rice. **Journal of Medicinal Food** 4(4): 211-218.

Infante, C., M. P. Matsuoka, E. Asensio, J. P. Cañavate, M. Reith*, et al.* (2008). Selection of Housekeeping Genes for Gene Expression Studies in Larvae from Flatfish Using Real-Time PCR. **BMC Molecular Biology** 9(1): 28.

Inouye, S. and F. Tsuji (1994). Aequorea Green Fluorescent Protein. Expression of the Gene and Fluorescence Characteristics of the Recombinant Protein. **FEBS Letters** 341(2-3): 277.

Irakli, M. N., V. F. Samanidou, C. G. Biliaderis and I. N. Papadoyannis (2012). Simultaneous Determination of Phenolic Acids and Flavonoids in Rice Using Solid‐Phase Extraction and RP‐HPLC with Photodiode Array Detection. **Journal of Separation Science** 35(13): 1603-1611.

Iwai, T., S. Seo, I. Mitsuhara and Y. Ohashi (2007). Probenazole-Induced Accumulation of Salicylic Acid Confers Resistance to *Magnaporthe grisea* in Adult Rice Plants. **Plant and Cell Physiology** 48(7): 915-924.

Jain, M., A. Nijhawan, A. K. Tyagi and J. P. Khurana (2006). Validation of Housekeeping Genes as Internal Control for Studying Gene Expression in Rice by Quantitative Real-Time PCR. **Biochemical and Biophysical Research Communications** 345(2): 646-651.

Jefferson, R. A., T. A. Kavanagh and M. W. Bevan (1987). Gus Fusions: Beta-Glucuronidase as a Sensitive and Versatile Gene Fusion Marker in Higher Plants. **The EMBO Journal** 6(13): 3901.

Jenkins, J., L. Lo Leggio, G. Harris and R. Pickersgill (1995). Beta-Glucosidase, Beta-Galactosidase, Family a Cellulases, Family F Xylanases and Two Barley Glycanases Form a Superfamily of Enzymes with 8-Fold Beta/Alpha Architecture and with Two Conserved Glutamates near the Carboxy-Terminal Ends of Beta-Strands Four and Seven. **FEBS Letters** 362(3): 281-285.

Jiao, Y., Y. Wang, D. Xue, J. Wang, M. Yan, *et al.* (2010). Regulation of Ossp14 by Osmir156 Defines Ideal Plant Architecture in Rice. **Nature Genetics** 42(6): 541-544.

Jin, Y., D. Ma, J. Dong, D. Li, C. Deng, *et al.* (2007). The HC-Pro Protein of Potato Virus Y Interacts with NtMind of Tobacco. **Molecular Plant-Microbe Interactions** 20(12): 1505-1511.

Joo, C., H. Balci, Y. Ishitsuka, C. Buranachai and T. Ha (2008). Advances in Single-Molecule Fluorescence Methods for Molecular Biology. **Annual Review of Biochemistry** 77: 51-76.

Kahler, A. and C. Wehrhahn (1986). Associations between Quantitative Traits and Enzyme Loci in the F2 Population of a Maize Hybrid. **Theoretical and Applied Genetics** 72(1): 15-26.

Ketudat Cairns, J. R. and A. Esen (2010). β-Glucosidases. **Cellular and Molecular Life Sciences** 67(20): 3389-3405.

Komiya, R., A. Ikegami, S. Tamaki, S. Yokoi and K. Shimamoto (2008). Hd3a and Rft1 Are Essential for Flowering in Rice. **Development** 135(4): 767-774.

Kudo, T., N. Makita, M. Kojima, H. Tokunaga and H. Sakakibara (2012). Cytokinin Activity of Cis-Zeatin and Phenotypic Alterations Induced by Overexpression of Putative Cis-Zeatin-O-Glucosyltransferase in Rice. **Plant Physiology** 160(1): 319-331.

Kuntothom, T., S. Luang, A. J. Harvey, G. B. Fincher, R. Opassiri*, et al.* (2009). Rice Family GH1 Glycoside Hydrolases with Beta-D-Glucosidase and Beta-D-Mannosidase Activities. **Archives of Biochemistry and Biophysics** 491(1-2): 85-95.

Leah, R., J. Kigel, I. Svendsen and J. Mundy (1995). Biochemical and Molecular Characterization of a Barley Seed-Glucosidase. **The Journal of Biological Chemistry** 270(26): 15789-15797.

Lee, D. Y., S. Shrestha, W. D. Seo, M. H. Lee, T. S. Jeong*, et al.* (2012). Structural and Quantitative Analysis of Antioxidant and Low-Density Lipoprotein-Antioxidant Flavonoids from the Grains of Sugary Rice. **Journal of Medicinal Food** 15(4): 399-405.

Lee, K. H., H. L. Piao, H.-Y. Kim, S. M. Choi, F. Jiang*, et al.* (2006). Activation of Glucosidase Via Stress-Induced Polymerization Rapidly Increases Active Pools of Abscisic Acid. **Cell** 126(6): 1109-1120.

Leung, H. and G. An (2004). Rice Functional Genomics: Large-Scale Gene Discovery and Applications to Crop Improvement. **Advance in Agronomy** 82: 55-111.

Li, Q. F., S. S. M. Sun, D. Y. Yuan, H. X. Yu, M. H. Gu*, et al.* (2010). Validation of Candidate Reference Genes for the Accurate Normalization of Real-Time Quantitative Rt-Pcr Data in Rice During Seed Development. **Plant Molecular Biology Reporter** 28(1): 49-57.

Liu, Y., T. J. Zhao, Y. B. Yan and H. M. Zhou (2005). Increase of Soluble Expression in *Escherichia coli* Cytoplasm by a Protein Disulfide Isomerase Gene Fusion System. **Protein Expression and Purification** 44(2): 155-161.

Llopis, J., J. M. McCaffery, a. Miyawaki, M. G. Farquhar and R. Y. Tsien (1998). Measurement of Cytosolic, Mitochondrial, and Golgi Ph in Single Living Cells with Green Fluorescent Proteins. **Proceedings of the National Academy of Sciences of the United States of America** 95(12): 6803-6808.

Ma, J. F., K. Tamai, N. Yamaji, N. Mitani, S. Konishi*, et al.* (2006). A Silicon Transporter in Rice. **Nature** 440(7084): 688-691.

Mackay, I. M., K. E. Arden and A. Nitsche (2002). Real-Time PCR in Virology. **Nucleic Acids Research** 30(6): 1292-1305.

Massardo, L., M. E. Martínez, S. Jacobelli, L. Villarroel, H. Rosenberg*, et al.* (1994). Survival of Chilean Patients with Systemic Lupus Erythematosus. **Seminars in Arthritis and Rheumatism** 24(1): 1-11.

Matsuda, F., Y. Okazaki, A. Oikawa, M. Kusano, R. Nakabayashi*, et al.* (2012). Dissection of Genotype–Phenotype Associations in Rice Grains Using Metabolome Quantitative Trait Loci Analysis. **The Plant Journal** 70(4): 624-636.

Mattiacci, L., M. Dicke and M. A. Posthumus (1995). B-Glucosidase: An Elicitor of Herbivore-Induced Plant Odor That Attracts Host-Searching Parasitic Wasps. **Proceedings of the National Academy of Sciences of the United States of America** 92(6): 2036-2040.

Menegus, F., L. Cattaruzza, E. Ragg and L. Scaglioni (1995). R(−) Pantoyllactone-β-D-Glucopyranoside: Characterization of a Metabolite from Rice Seedlings. **Phytochemistry** 40(6): 1617-1621.

Miki, D., R. Itoh and K. Shimamoto (2005). RNA Silencing of Single and Multiple Members in a Gene Family of Rice. **Plant Physiology** 138(4): 1903-1913.

Miki, D. and K. Shimamoto (2004). Simple RNAi Vectors for Stable and Transient Suppression of Gene Function in Rice. **Plant and Cell Physiology** 45(4): 490-495.

Mizutani, H., S. J. Degrado and A. H. Hoveyda (2002). Cu-Catalyzed Asymmetric Conjugate Additions of Alkylzinc Reagents to Acyclic Aliphatic Enones. **Journal of the American Chemical Society** 124(5): 779-781.

Morant, A. V., N. Bjarnholt, M. E. Kragh, C. H. Kjaergaard, K. Jorgensen*, et al.* (2008). The Beta-Glucosidases Responsible for Bioactivation of Hydroxynitrile Glucosides in Lotus Japonicus. **Plant Physiology** 147(3): 1072-1091.

Morino, K., F. Matsuda, H. Miyazawa, A. Sukegawa, H. Miyagawa*, et al.* (2005). Metabolic Profiling of Tryptophan-Overproducing Rice Calli That Express a Feedback-Insensitive A Subunit of Anthranilate Synthase. **Plant and Cell Physiology** 46(3): 514-521.

Niemeyer, H. M. (1988). Hydroxamic Acids (4-Hydroxy-1, 4-Benzoxazin-3-Ones), Defence Chemicals in the Gramineae. **Phytochemistry** 27(11): 3349-3358.

Opassiri, R., Y. Hua, O. Wara-Aswapati, T. Akiyama, J. Svasti*, et al.* (2004). Beta-Glucosidase, Exo-Beta-Glucanase and Pyridoxine Transglucosylase Activities of Rice BGlu1. **Biochemical Journal** 379(Pt 1): 125-131.

Opassiri, R., J. R. Ketudat Cairns, T. Akiyama, O. Wara-Aswapati, J. Svasti*, et al.* (2003). Characterization of a Rice B-Glucosidase Highly Expressed in Flower and Germinating Shoot. **Plant Science** 165(3): 627-638.

Opassiri, R., J. Maneesan, T. Akiyama, B. Pomthong, S. Jin*, et al.* (2010). Rice Os4bglu12 Is a Wound-Induced β-Glucosidase That Hydrolyzes Cell Wall-

β-Glucan-Derived Oligosaccharides and Glycosides. **Plant Science** 179(3): 273-280.

Opassiri, R., B. Pomthong, T. Akiyama, M. Nakphaichit, T. Onkoksoong*, et al.* (2007). A Stress-Induced Rice (*Oryza sativa* L.) Beta-Glucosidase Represents a New Subfamily of Glycosyl Hydrolase Family 5 Containing a Fascin-Like Domain. **The Biochemical Journal** 408(2): 241-249.

Opassiri, R., B. Pomthong, T. Onkoksoong, T. Akiyama, A. Esen*, et al.* (2006). Analysis of Rice Glycosyl Hydrolase Family 1 and Expression of Os4BGlu12 Beta-Glucosidase. **BMC Plant Biology** 6: 33-33.

Ozawa, K. (2009). Establishment of a High Efficiency *Agrobacterium*-Mediated Transformation System of Rice (*Oryza sativa* L.). **Plant Science** 176(4): 522-527.

Ozawa, K. (2012). A High-Efficiency *Agrobacterium*-Mediated Transformation System of Rice (*Oryza sativa* L.). **Method in Molecular Biology (Clifton, NJ)** 847: 51-57.

Palmiano, E. P. and B. O. Juliano (1973). Changes in the Activity of Some Hydrolases, Peroxidase, and Catalase in the Rice Seed During Germination. **Plant Physiology** 52(3): 274-277.

Park, S. Y., S. H. Ha, S. H. Lim, J. Y. Jung, S. M. Lee*, et al.* (2012). Determination of Phenolic Acids in Korean Rice (*Oryza sativa* L.) Cultivars Using Gas Chromatography-Time-of-Flight Mass Spectrometry. **Food Science and Biotechnology** 21(4): 1141-1148.

Poulton, J. E. (1990). Cyanogenesis in Plants. **Plant Physiology** 94(2): 401-405.

Poulton, J. E. and C. P. Li (1994). Tissue Level Compartmentation of (R)-Amygdalin and Amygdalin Hydrolase Prevents Large-Scale Cyanogenesis in Undamaged Prunus Seeds. **Plant Physiology** 104(1): 29-35.

Prasher, D. C., V. K. Eckenrode, W. W. Ward, F. G. Prendergast and M. J. Cormier (1992). Primary Structure of the *Aequorea victoria* Green-Fluorescent Protein. **Gene** 111(2): 229.

Prendergast, F. G. and K. G. Mann (1978). Chemical and Physical Properties of Aequorin and the Green Fluorescent Protein Isolated from *Aequorea forskalea*. **Biochemistry** 17(17): 3448-3453.

Purbey, P. K., P. C. Jayakumar, M. S. Patole and S. Galande (2006). PC6-2/Caspase-6 System to Purify Glutathione-S-Transferase-Free Recombinant Fusion Proteins Expressed in *Escherichia coli*. **Nature Protocols** 1(4): 1820-1827.

Qi, M. and Y. Yang (2002). Quantification of Magnaporthe Grisea During Infection of Rice Plants Using Real-Time Polymerase Chain Reaction and Northern Blot/Phosphoimaging Analyses. **Phytopathology** 92(8): 870-876.

Radonić, A., S. Thulke, I. M. Mackay, O. Landt, W. Siegert*, et al.* (2004). Guideline to Reference Gene Selection for Quantitative Real-Time PCR. **Biochemical and Biophysical Research Communications** 313(4): 856-862.

Raychaudhuri, A. and P. A. Tipton (2002). Cloning and Expression of the Gene for Soybean Hydroxyisourate Hydrolase. Localization and Implications for Function and Mechanism. **Plant Physiology** 130(4): 2061-2068.

Reid, K. E., N. Olsson, J. Schlosser, F. Peng and S. T. Lund (2006). An Optimized Grapevine Rna Isolation Procedure and Statistical Determination of Reference Genes for Real-Time Rt-Pcr During Berry Development. **BMC Plant Biology** 6(1): 27.

Ruo-Zhong, W., Z. Min, D. Jun-Hui and X. Lang-Tao Relationship between Endogenous Hormones and Phytic Acid Concentrations of Intersubspecific Hybrid Rice.**Accerlerating Hybrid Rice Development**: 207.

Sansenya, S., R. Opassiri, B. Kuaprasert, C. J. Chen and J. R. Ketudat Cairns (2011). The Crystal Structure of Rice (*Oryza sativa* L.) Os4BGlu12, an Oligosaccharide and Tuberonic Acid Glucoside-Hydrolyzing β-Glucosidase with Significant Thioglucohydrolase Activity. **Archives of Biochemistry and Biophysics** 510(1): 62-72.

Sayler, R. J. and Y. Yang (2007). Detection and Quantification of Rhizoctonia Solani Ag-1 Ia, the Rice Sheath Blight Pathogen, in Rice Using Real-Time Pcr. **Plant Disease** 91(12): 1663-1668.

Schliemann, W. (1984). Hydrolysis of Conjugated Gibberellins by B-Glucosidases from Dwarf Rice (*Oryza sativa* L. cv.«Tan-Ginbozu»). **Journal of Plant Physiology** 116(2): 123-132.

Schmittgen, T. D. and B. A. Zakrajsek (2000). Effect of Experimental Treatment on Housekeeping Gene Expression: Validation by Real-Time, Quantitative Rt-Pcr. **Journal of Biochemical and Biophysical Methods** 46(1): 69-81.

Seo, S., K. Ishizuka and Y. Ohashi (1995). Induction of Salicylic Acid B-Glucosidase in Tobacco Leaves by Exogenous Salicylic Acid. **Plant and Cell Physiology** 36(3): 447-453.

Seshadri, S. (2008). Functional and Structural Studies of Rice β-Glucosidase. **Suranaree University of Technology.**

Seshadri, S., T. Akiyama, R. Opassiri, B. Kuaprasert and J. K. Cairns (2009). Struc- tural and Enzymatic Characterization of Os3BGlu6, a Rice Beta-Glucosi- dase Hydrolyzing Hydrophobic Glycosides and (1->3)- and (1->2)-Linked Disaccharides. **Plant Physiology** 151(1): 47-58.

Smith, A. and J. Van Staden (1978). Changes in Endogenous Cytokinin Levels in Kernels of *Zea mays* L. During Imbibition and Germination. **Journal of Experimental Botany** 29(5): 1067-1075.

Soi-ampornkul, R., S. Junnu, S. Kanyok, S. Liammongkolkul, W. Katanyoo*, et al.* (2012). Antioxidative and Neuroprotective Activities of the Pre-Germinated Brown Rice Extract. **Food and Nutrition** 3: 135-140.

Soler-Rivas, C., J. C. Espín and H. J. Wichers (2000). An Easy and Fast Test to Compare Total Free Radical Scavenger Capacity of Foodstuffs. **Phytochemical Analysis** 11(5): 330-338.

Strandberg, L. and S. O. Enfors (1991). Factors Influencing Inclusion Body Formation in the Production of a Fused Protein in *Escherichia coli*. **Applied and Environmental Microbiology** 57(6): 1669-1674.

Sue, M., A. Ishihara and H. Iwamura (2000). Purification and Characterization of a Hydroxamic Acid Glucoside β-Glucosidase from Wheat (*Triticum aestivum* L.) Seedlings. **Planta** 210(3): 432-438.

Sue, M., A. Ishihara and H. Iwamura (2000). Purification and Characterization of a B-Glucosidase from Rye (*Secale cereale* L.) Seedlings. **Plant Science** 155(1): 67-74.

Tadera, K., T. Kaneko and F. Yagi (1988). Isolation and Structural Elucidation of Three New Pyridoxine-Glycosides in Rice Bran. **Journal of Nutritional Science and Vitaminology** 34(2): 167.

Tamaki, S., S. Matsuo, H. L. Wong, S. Yokoi and K. Shimamoto (2007). Hd3a Protein Is a Mobile Flowering Signal in Rice. **Science Signalling** 316(5827): 1033.

Tian, S., K. Nakamura, T. Cui and H. Kayahara (2005). High-Performance Liquid Chromatographic Determination of Phenolic Compounds in Rice. **Journal of Chromatography A** 1063(1): 121-128.

Toki, S. (1997). Rapid and Efficient *Agrobacterium*-Mediated Transformation in Rice. **Plant Molecular Biology Reporter** 15(1): 16-21.

Toki, S., N. Hara, K. Ono, H. Onodera, A. Tagiri*, et al.* (2006). Early Infection of Scutellum Tissue with *Agrobacterium* Allows High‐Speed Transformation of Rice. **The Plant Journal** 47(6): 969-976.

Tong, Z., Z. Gao, F. Wang, J. Zhou and Z. Zhang (2009). Selection of Reliable Reference Genes for Gene Expression Studies in Peach Using Real-Time PCR. **BMC Molecular Biology** 10(1): 71.

Toonkool, P., P. Metheenukul, P. Sujiwattanarat, P. Paiboon, N. Tongtubtim*, et al.* (2006). Expression and Purification of Dalcochinase, a Beta-Glucosidase from Dalbergia Cochinchinensis Pierre, in Yeast and Bacterial Hosts. **Protein Expression and Purification** 48(2): 195-204.

Trick, H. and J. Finer (1998). Sonication-Assisted *Agrobacterium*-Mediated Transformation of Soybean [*Glycine max* (L.) Merrill] Embryogenic Suspension Culture Tissue. **Plant Cell Reports** 17(6): 482-488.

Tsukada, T., K. Igarashi, M. Yoshida and M. Samejima (2006). Molecular Cloning and Characterization of Two Intracellular Beta-Glucosidases Belonging to Glycoside Hydrolase Family 1 from the Basidiomycete *Phanerochaete chrysosporium*. **Applied Microbiology and Biotechnology** 73(4): 807-814.

Voorhoeve, P. M. and R. Agami (2003). Knockdown Stands Up. **Trends in Biotechnology** 21(1): 2-4.

Wakuta, S., S. Hamada, H. Ito, H. Matsuura, K. Nabeta*, et al.* (2010). Identification of a β-Glucosidase Hydrolyzing Tuberonic Acid Glucoside in Rice *(Oryza sativa* L.). **Phytochemistry** 71(11): 1280-1288.

Wesley, S. V., C. A. Helliwell, N. A. Smith, M. B. Wang, D. T. Rouse*, et al.* (2001). Construct Design for Efficient, Effective and High‐Throughput Gene Silencing in Plants. **The Plant Journal** 27(6): 581-590.

Wielopolska, A., H. Townley, I. Moore, P. Waterhouse and C. Helliwell (2005). A High-Throughput Inducible Rnai Vector for Plants. **Plant Biotechnology Journal** 3(6): 583-590.

Wong, M. L. and J. F. Medrano (2005). Real-Time PCR for mRNA Quantitation. **Biotechniques** 39(1): 75.

Xu, Z., L. Escamilla-Treviño, L. Zeng, M. Lalgondar, D. Bevan*, et al.* (2004). Functional Genomic Analysis of *Arabidopsis thaliana* Glycoside Hydrolase Family 1. **Plant Molecular Biology** 55(3): 343-367.

Yablonka-Reuveni, Z., M. A. Rudnicki, A. J. Rivera, M. Primig, J. E. Anderson*, et al.* (1999). The Transition from Proliferation to Differentiation Is Delayed in Satellite Cells from Mice Lacking Myod. **Developmental Biology** 210(2): 440.

Yamada, T., M. Teraishi, K. Hattori and M. Ishimoto (2001). Transformation of Azuki Bean by *Agrobacterium tumefaciens*. **Plant Cell, Tissue and Organ Culture** 64(1): 47-54.

Yancheva, S., L. Shlizerman, S. Golubowicz, Z. Yabloviz, A. Perl*, et al.* (2006). The Use of Green Fluorescent Protein (Gfp) Improves *Agrobacterium*-Mediated Transformation of 'Spadona'pear (*Pyrus communis* L.). **Plant Cell Reports** 25(3): 183-189.

Yang, Y., M. Qi and C. Mei (2004). Endogenous Salicylic Acid Protects Rice Plants from Oxidative Damage Caused by Aging as Well as Biotic and Abiotic Stress. **The Plant Journal** 40(6): 909-919.

Yi, N., S.-J. Oh, Y. S. Kim, H.-J. Jang, S.-H. Park*, et al.* (2011). Analysis of the Wsi18, a Stress-Inducible Promoter That Is Active in the Whole Grain of Transgenic Rice. **Transgenic Research** 20(1): 153-163.

Yu, B., Z. Lin, H. Li, X. Li, J. Li*, et al.* (2007). Tac1, a Major Quantitative Trait Locus Controlling Tiller Angle in Rice. **The Plant Journal** 52(5): 891-898.

Yuste, R. (2005). Fluorescence Microscopy Today. **Nature Methods** 2(12): 902-904.

Zentella, R., D. Yamauchi and T. D. Ho (2002). Molecular Dissection of the Gibberellin/Abscisic Acid Signaling Pathways by Transiently Expressed RNA Interference in Barley Aleurone Cells. **The Plant Cell** 14(9): 2289-2301.

Zhang, J., R. Xu, M. C. Elliott and D. F. Chen (1997). *Agrobacterium*-Mediated Transformation of Elite Indica and Japonica Rice Cultivars. **Molecular Biotechnology** 8(3): 223-231.

Zhang, Z., Y. Zhang, H. Tan, Y. Wang, G. Li, *et al.* (2011). Rice Morphology Determinant Encodes the Type II Formin FH5 and Regulates Rice Morphogenesis. **The Plant Cell** 23(2): 681-700.

Zhao, W., S. Zheng and H. Q. Ling (2011). An Efficient Regeneration System and *Agrobacterium*-Mediated Transformation of Chinese Upland Rice Cultivar Handao297. **Plant Cell, Tissue and Organ Culture** 106(3): 475-483.

Zouhar, J., E. Nanak and B. Brzobohatý (1999). Expression, Single-Step Purification, and Matrix-Assisted Refolding of a Maize Cytokinin Glucoside-Specific β-Glucosidase. **Protein Expression and Purification** 17(1): 153-162.

CHAPTER III

RECOMBINANT EXPRESSION AND BIOCHEMICAL CHARACTERIZATION OF RICE β-GLUCOSIDASE Os1BGlu4

3.1 Abstract

The coding sequence of the *Os*1*bglu*4 β-glucosidase gene was amplified from a cDNA library of rice seedlings, and subcloned into the pET32a(+) *E. coli* expression vector, the recombinant pET32a(+) was transformed into the *E.coli* strain OrigamiB(DE3). Sequence analysis showed that the mature Os1BGlu4 included 483 amino acids, and suggested its subcellular localization is in the cytoplasm. The recombinant Thioredoxin-6Histidine-Os1BGlu4 (Trx-His6-rOs1BGlu4) fusion protein was functionally expressed. The expression conditions were optimized; the result showed that 16 hr incubation at 20 ^{o}C without IPTG inducer was the best condition to express the Trx-His6-rOs1BGlu4. The Trx-His6-rOs1BGlu4 was purified by immobilized metal affinity chromatography (IMAC), and the thioredoxin was cut from the Trx-His6-rOs1BGlu4 to release the rOs1BGlu4. The purified rOs1BGlu4 was used to determine its biochemical characteristics. The result showed that the optimum pH for hydrolysis activity of rOs1BGlu4 is 6.5, the rOs1BGlu4 was stable over the pH range of 6.0 to 8.0 after 24 hr incubation and the optimum temperature is 45 ^{o}C. The rOs1BGlu4 was stable at 20 and 30 ^{o}C for 1 hr.

The rOs1BGlu4 efficiently hydrolyzed β-(1, 3)-linked oligosaccharides of degree of polymerization (DP) 2- 3, and β-(1, 4)-linked oligosaccharide of DP 3-4. Cellopentaose and cellohexaose can be hydrolyzed with lower efficiency, while laminari-oligosaccharides with DP more than 3 are not hydrolyzed. The rOs1BGlu4 can hydrolyze *p*NP-β-D-glucopyranoside (*p*NPG) efficiently, while *p*NP-β-D-fucopyranoside was hydrolyzed with about 50% hydrolysis efficiency of the *p*NPG. Based on the kinetic parameters, others *p*NP-derivatives can be hydrolyzed with low efficiency. Thin Layer Chromotography (TLC) showed that the natural substrates salicin, esculin and *para*-coumaryl alcohol glucoside can be hydrolyzed by rOs1BGlu4. The hydrolysis activity of rOs1BGlu4 was strongly inhibited by $HgCl_2$, delta-glucono-lactone and $FeCl_3$. Analysis of the hydrolysis of *p*NP-cellobioside showed that the initial hydrolysis was between the two glucose molecules. The transglycosylation study showed that at 10 mM concentration of *p*NPG, the rOs1BGlu4 can transfer the glucosyl group of *p*NPG to ethanol and *p*NPG.

3.2 Introduction

Beta-glucosidases (β-D-glucopyranoside glucohydrolases, E.C. 3.2.1.21) are enzymes that hydrolyze glycosidic bonds to release nonreducing terminal glucosyl residues from glycosides and oligosaccharides (Ketudat Cairns and Esen 2010).

Glycoside hydrolases (GH) have been classified to 131 glycoside hydrolase families based on amino acid sequence and structural similarity, the families that have similar catalytic domain structures and conserved catalytic amino acids, are grouped into clans (http://www.cazy.org) (Henrissat and Davies 1997). Of these, clan A has the largest number of families, all members have catalytic domains with $(\alpha/\beta)_8$

structures, which typically have the catalytic acid/base residing at the end of β-strand 4 and the nucleophile at the end of β-stand 7 (Henrissat *et al.* 1995, Jenkins *et al.* 1995). Of the GH families containing β-glucosidases, Clan A includes families GH1, GH5, and GH30. Most of the plant β-glucosidases fall into GH1.

In plants, these enzymes are involved in variety of processes, such as release of glucose from cell-wall derived oligosaccharides, defense against herbivores and fungi by release of toxic compounds from inactive glycosides, activation of lignin precursors in lignification, release of phytohormones from inactive glycosides, release of scent compounds, and general activation of glucose-blocked intermediates in metabolism (Esen 1993). The properties of the substrate specificity, their tissue and subcellular localization, and the conditions under which they come into contact with their physiological substrates will determine the roles of these enzymes (Ketudat Cairns and Esen 2010).

Forty rice genes homologous to GH1 β-glucosidase have been identified from rice genome databases, and 34 of these are likely to form active glycosidases (Opassiri *et al.* 2006). Phylogenetic analysis revealed that many members that contain closely related sequences are located on the same chromosome and clustered in the same subfamilies. The relationship between rice and *Arabidopsis* GH1 protein sequences have been described by a phylogenetic tree rooted by Os11bglu36 (Figure 2.2, Chapter 2), in which the β-glucosidase from rice and *Arabidopsis* were classified to 8 clusters, and 2 clusters special for *Arabidopsis*. Since it is plausible that genes in the same cluster may have the similar functions, it is advisable and economical to clarify the function of one representative gene to help understand the functions of all genes in each cluster.

So far, several cell wall related rice β-glucosidases have been isolated and characterized, Os3BGlu7 (BGlu 1) and its close relatives Os3BGlu8 and Os7BGlu26,

were found to be involved in the release of glucose and mannose from oligosaccharides generated in cell wall remodeling at various stages of plant development (Opassiri *et al.* 2003, Kuntothom *et al.* 2009). Another possible function of Os3BGlu7 is the release of the coenzyme pyridoxine from its glucose-conjugated storage form (Opassiri *et al.* 2003). Recently, Os4BGlu13 (OsTAGG1) and its close relative Os4BGlu12 were found to act as tuberonic acid glucoside β-glucosidases, Os4BGlu12 was possibly involved in hydrolysis of cell wall-derived oligosaccharides (Opassiri *et al.* 2006, 2010, Wakuta *et al.* 2010).

Os1BGlu4, the only rice GH1 β-glucosidase sequence without signal peptide, clustered with *Arabidopsis* BGlu42 and *Hevea brasiliensis* latex cyanogenic β-glucosidase in an independent cluster (Opassiri *et al.* 2006). So, it would be interesting to determine the substrate specificity and characteristics of a representative member in this cluster, which can enrich the knowledge of the GH1 β-glucosidases and help, narrow the possible biological function of Os1BGlu4.

3.3 Materials and methods

3.3.1 Plasmids and bacterial strain

The pET32a(+) is designed for high-level expression of peptide sequence fused with 109aa Trx·Tag™ thioredoxin protein which can help the efficient translation and folding of the target protein. The pET32a(+) was used for Os1BGlu4 protein expression in *E. coli.*

DH5α, a recombination-deficient suppressing strain, was used for cloning plasmids. Origami B(DE3) host strain, a K-12 derivative mutated in both the thioredoxin reductase (*trxB*) and glutathione reductase (*gor*) genes, which greatly enhances

disulfide bond formation and has been used to express the soluble and active β-glucosidase (Opassiri *et al.* 2007), was used for the expression of recombinant Os1BGlu4. Origami B(DE3) has both the tetracycline and kanamycin resistance genes.

3.3.2 Bioinformatics analysis of *Os1bglu4*

The National Center for Biotechnology Information Web site was used to search the pubic DNA sequence database for Os1BGlu4 cDNA sequence accession number AK243365.1 (http://www.ncbi.nlm.nih.gov/). Protein analyses were done at the Expasy proteomics server (http://www.expasy.org/). The protein structure was predicted by SWISS-MODEL program using the Os3BGlu6 structure (PDB code: 3GNP) as template.

3.3.3 Transformation of recombinant plasmid into the expression host cells

3.3.3.1 Target gene preparation

Fourteen days rice leaf cDNA was kindly provided by Ms. Supaporn Baiya and Dr. James R. Ketudat-Cairns. The coding sequence of the rice Os1BGlu4 gene was amplified. The 25 µL PCR reaction was consisted of 13.5 µL distilled H_2O, 1×Green Go*Taq*® Reaction buffer, 2 mM $MgCl_2$, 0.4 mM dNTP, 0.4 µM bglu-f (CACCATGGGGAGCACGGGGCGC) which contains the *Nco*I site, 1 µL 10 µM bglu-r (AGGGAATTCCTAGTTCATGTCAGC) which contains the *EcoR*I site, 2.5 U Go*Taq*® DNA Polymerase, and 1 µL cDNA template. The amplification condition was 94 ^{o}C 4 min, 30 cycles of 94 ^{o}C 30 sec, 55 ^{o}C 30 sec, 72 ^{o}C 110 sec, and finally 8 min extra extension. The PCR product was purified with a QIA quick extraction kit following the protocol of the company (QIAGEN).

3.3.3.2 Expression vector construction

The PCR product was digested with *Nco*I and *Eco*RI, and then ligated into pET32a(+), which had been digested with the same restriction enzymes, using T4 DNA ligase, and the recombinant pET32a+ was transformed into *E. coli* DH5α by electroporation. Positive clones were selected on a 100 μg/mL ampicillin LB plate. Colony PCR method with gene specific primers was used to check the positive clone. Recombinant plasmids were extracted from positive clones with QIAGEN Plasmid Prep Kits. The forward primer 393F (GAAAGAGTTCCTCGACGC) and reverse primer T7 terminator (GCTAGTT ATTGCTCAGCGG) were used to sequence the plasmid pET32-*Os*1*bglu*4 to confirm the correct reading frame and sequence.

3.3.4 Recombinant protein expression in *E. coli* Origami B(DE3)

To produce recombinant thioredoxin-Os1BGlu4 fusion protein, the plasmid pET32-*Os*1*bglu*4 was transformed into the *E. coli* Origami B(DE3) by electroporation and the bacteria was spread onto an LB plate containing 100 μg/mL ampicillin, 15 μg/mL kanamycin and 12.5 μg/mL tetracycline and incubated at 37 ^{o}C overnight. Positive clones were singled out and grown overnight in 3 mL LB broth containing the same antibiotics at 37 ^{o}C with shaking at 200 rpm. The fresh starter cultures was inoculated into LB broth containing the same antibiotics and then the culture was grown at 37 ^{o}C with shaking at 200 rpm for 3-5 hr until the optical density of 600 nm reached 0.5-0.6. IPTG was added to final concentrations of 0, 0.1, 0.2, 0.3, 0.4 and 0.5 mM to find the optimum IPTG concentration. The cultures were shaken at 200 rpm at 10, 20 and 30 ^{o}C with different induction time of 8, 12, 16, 20 and 24 hr. The induced cultures were centrifuged at 5,000 *g* for 10 min at 4 ^{o}C. The cell pellets were kept

at -70 ^{o}C. To monitor the total protein expression levels, 5 mL aliquots of the cell cultures were sampled at the different culture temperatures induction times and IPTG concentrations, the cultured cells were collected by centrifugation at 12,000 *g* for 5 min, and the cell pellet was weighed. The cell pellet was resuspended with protein extraction buffer (20 mM Tris-Cl buffer, pH 8.0, 200 µg/mL lysozyme, 1% Triton-X 100, 1 mM PMSF, 40 µg/mL DNase I) in a ratio of 1 g cell pellet to 5 mL extraction buffer. The resuspended cells were incubated at room temperature for 30 min. Then, the soluble protein was recovered by centrifugation at 12,000 *g* at 4 ^{o}C for 10 min. The soluble protein fraction was kept on ice for protein purification in the next step. Eight microliter aliquots were mixed with 2 µl 5×loading buffer (2.5 M Tris-HCl, 10% SDS, 0.5% bromophenol blue, 50% glycerol, 20% 2-mercaptoethanol) and boiled for 5 min to denature proteins. Then, the samples were loaded onto 15% SDS polyacrylamide gels (SDS-PAGE).

3.3.5 Purification of Os1BGlu4

Firstly, the resin was washed with 10 column volumes (CV) 0.2 mM EDTA, pH 8.0, followed by 10 CV deionized water. Then, the resin was regenerated with 10 CV 50 mM of $CoCl_2$, followed by 7 CV deionized water. Again, the column was washed by 3 CV 300 mM NaCl, followed by 3 CV deionized water. Finally, the column was equilibrated with 10 CV equilibration buffer (20 mM Tric-Cl and 150 mM NaCl).

The soluble protein fraction was purified by immobilized metal affinity chromatography (IMAC) on the prepared BD TALON cobalt resin. Ten mL of soluble protein fraction was loaded onto a 2 mL bed volume of pre-equilibrated cobalt resin. The soluble protein and the cobalt resin were incubated for 30 min on ice with shaking. The resin was packed and washed with 5 CV W0 buffer (20 mM Tris-Cl+

150 mM NaCl) and 5 CV W1 buffer (W0+5 mM imidazole), followed by 5 CV W2 buffer (W0+10 mM imidazole). The Trx-His6-rOs1BGlu4 was eluted with 5 CV of Elution buffer 1 (W0+50 mM imidazole) and 5 CV of Elution buffer 2 (W0+100 mM imidazole). After the elution of the protein, the column was washed with 5 CV Mes, pH 5.0, followed by 5 CV deionized water. Then, 20% ethanol was added to preserve the resin until the next use.

The eluted Trx-His6-rOs1BGlu4 was concentrated and the buffer was changed to 20 mM Tris-Cl, pH 8.0, using a Millipore regenerated cellulose amicon ultra centrifugal filter (with PLGC Ultracel-10 Membrane, 15 mL Capacity, 10 kDa NMWL, 29.7 mm Diameter x 122 mm Length, 7.6 sq cm Membrane) with 1500 *g* centrifugation.

3.3.6 Elimination of the fused thioredoxin

3.3.6.1 Protein assay

The purified protein concentration was determined by protein assay kit (Bio-Rad Protein Assay Kit I), using bovine serum albumin (BSA) as standard. Diluted Trx-His6-rOs1BGlu4 (0.8 mL) was mixed with 0.2 mL protein assay solution (Appendix table 1). The reaction was incubated at room temperature for 10 min and the absorbance of 595 nm was measured. Triplicate samples were measured according to the BSA standard (Appendix figure 1).

3.3.6.2 Thioredoxin elimination

The purified Trx-His6-rOs1BGlu4 was incubated with the entero-kinase (NEB) for 16 hr at 23 ^{o}C in a ratio of 0.00016 μg of enterokinase per 20 μg

Trx-His6-rOs1BGlu4 according to the instruction of the manufacture. After incubation, the reaction was loaded onto 4 mL of pre-equilibrated cobalt resin. The flow through and W0 solution were collected as recombinant Os1BGlu4 (rOs1BGlu4), thioredoxin was eluted using E1 and E2 to wash the resin. An aliquot of each faction was loaded onto SDS-PAGE.

3.3.7 SDS-PAGE analysis of protein expression and purification

The composition of a 12% SDS-PAGE separating gel (Appendix table 4) were mixed and poured into the gap between a pair of glass plates assembled in a Hoefer vertical gel cassette up to a level of three fourths of the height of the lower plate. Deionized water was layered over the separating gel solution, which was allowed to polymerize for 30 min at room temperature. The components of a 5% stacking SDS-PAGE gel (Appendix table 4), were mixed and layered on the separating gel, the comb was inserted into the gap between the two glasses immediately. After polymerization for 30 min, the polyacrylamide gel plates were assembled in a Hoefer gel electrophoresis apparatus and filled with 1X Tris-glycine electrode buffer (pH 8.3).

Protein samples were mixed with 1X loading buffer (0.05 M Tris-HCl, pH 6.8, 10% SDS, 0.2 mg/mL bromophenol blue, 50% glycerol, 20% 2-mercaptoethanol) and boiled for 5 min to denature proteins. Denatured protein (10 μL) was loaded into sample wells, and electrophoresed at a constant voltage of 120 V for 90 min. Then, the gels was stained with staining solution for 10 min and destained with destaining solution for 30 min, twice. The molecular mass of the protein band was estimated by comparison to the Fermentas Protein Molecular Weight Markers.

3.3.8 Optimum pH and pH stability

To determine the pH optimum of the rOs1BGlu4 enzyme, two different sets of buffer was prepared to 50 mM concentration. The first set ranging from pH 3.5 to 10.5 (formate pH 3.5-4.0; sodium acetate pH 4.5-5.5; sodium phosphate pH 6.0-8.5; CAPS pH 9.0-10.5), at 0.5 pH increments (Opassiri *et al.* 2003); the second set was prepared by citric acid-disodium hydrogen phosphate, from pH 2.0 to pH 9.0 (Seshadri *et al.* 2009). One hundred microliter reaction consisted of 10 µL 0.025 µg/µL Os1BGlu4, 80 µL different pH buffer and 10 µL 10 mM *p*NPG (Opassiri *et al.* 2007). The reactions were incubated for 10 min at 30 ^{o}C, then 70 µL 0.4 M Na_2CO_3 were added to stop the reaction, the *p*NP released was measured at 405 nm.

The pH stability for the rOs1BGlu4 was determined by incubating the concentrated rOs1BGlu4 in 50 mM buffers ranging from pH 4 to 10 (the first set of buffers mentioned above) as above at increment of 1.0 pH unit for 10 min, 1, 3, 6, 12 and 24 hr at 30 ^{o}C. The rOs1BGlu4 at each time point was sampled. After incubation, the enzyme was diluted to 0.025 µg, 10 µL protein aliquot was incubated with 10 µL 10 mM *p*NPG in 80 µL 50 mM phosphate buffer, pH 6.5. The reaction was incubated for 10 min at 30 ^{o}C, then 70 µL 0.4 M Na_2CO_3 was added to stop the reaction, and the *p*NP released was measured at 405 nm.

3.3.9 Optimum temperature and thermostability

The optimum temperature for enzyme activity was determined by incubuting 0.25 µg rOs1BGlu4 with 1 mM *p*NPG in 50 mM phosphate buffer, pH 6.5, in a reaction volume of 100 µL at temperatures ranging from 5 ^{o}C to 90 ^{o}C in 5 ^{o}C increments for 10 min, and then 70 µL 0.4 M Na_2CO_3 was added to stop the reaction, and the *p*NP released was measured at 405 nm.

The thermostability of the enzyme was checked by incubating enzyme in 50 mM phosphate buffer, pH 6.5, at different temperatures in the range of 20 ^{o}C to 60 ^{o}C at 10 ^{o}C intervals for 10, 20, 30, 40, 50 and 60 min. The rOs1BGlu4 was sampled at each time point, and a 10 µL 0.025 µg/µL Os1BGlu4 aliquot was assayed as above.

3.3.10 Activity assays and kinetics study

3.3.10.1 Glucose standard

In order to measure the amount of glucose which was released from the reaction, 0.0025 to 0.03 µmole of glucose was incubated with the phosphate buffer (Appendix table 2), pH 6.5, for 15 min at 30 ^{o}C, 50 µL of 2, 2'-azino-bis (3-ethylbenzothiazoline-6-sulphonic acid) ABTS and 100 µL of peroxidase-glucose oxidase (PGO) solutions were added to the reactions and they were incubated at 37 ^{o}C for 10 min. The OD at 405 nm was measured. The glucose standard was plotted (Appendix figure 2).

3.3.10.2 *p*NP standard

The *p*NP (0.0025 µmole to 0.03µmole) was incubated with phosphate buffer (Appendix table 3), pH 6.5, for 15 min at 30 ^{o}C, then, 70 µL Na_2CO_3 was added to the reaction, the OD at 405 nm was measured. The *p*NP standard was plotted (Appendix figure 3).

3.3.10.3 Substrate specificity assay

The enzyme activity on various substrates was determined by measuring either (1) the *p*-nitrophenol (*p*NP) liberated from the *p*NP derivatives of

monosaccharides or disaccharides, or (2) glucose released from natural or artificial substrates. All substrate solutions were prepared in 50 mM sodium phosphate, pH 6.5. The glycone specificity of rOs1BGlu4 β-glucosidase was tested with synthetic *p*NP-glycoside substrates inculuding *p*NP-β-D-glucopyranoside (*p*NPG), *p*NP-β-L-fucopyranoside, *p*NP-α-D-glucopyranoside, *p*NP-β-D-cellobioside, *p*NP-β-D-mannopyranoside, *p*NP-α-L-arabionopyranoside, *p*NP-β-D-xylopyranoside, *p*NP-β-D-fucopyranoside, *p*NP-β-D-galactopyranoside). rOs1BGlu4 (0.25 μg) was incubated with 1 mM *p*NP- derivatives in 50 mM phosphate buffer, pH 6.5, at 30 ^{o}C for 15 min, then, 70 μL 0.4 M Na_2CO_3 was added to stop the reaction, and the absorbance of the liberated *p*NP was measured at 405 nm. A reaction mixture of the same composition but without the enzyme was used as a blank.

The rOs1BGlu4 was also tested with oligosaccharides. The oligosaccharides include laminaripentaose, laminaritetraose, laminaritriose, laminaribiose, cellohexaose, cellohexaose, cellopentaose, cellotetraose, cellotriose and cellobiose, gentiobiose and chitopentaose. In 50 μL reactions, rOs1BGlu4 (0.0125 μg) was incubated with 1 mM oligosaccharide in 50 mM phosphate buffer, pH 6.5, at 30 ^{o}C for 20 min. A reaction mixture of the same composition but without the enzyme was used as a blank. The reaction was stopped by heating to 100 ^{o}C for 10 min, the reaction was transferred to microtiter plate, 50 μL ABTS and 100 μL PGO were added to the reaction, and incubated at 37 ^{o}C for 10 min. the OD at 405 nm was measured with a spectrophotometer (Opassiri *et al.* 2006).

The products of rOs1BGlu4 hydrolysis of cello- and laminarioligosaccharides and natural substrates were detected by TLC. In the 50 μL reaction system, 0.125 μg enzyme was incubated with 1 mM oligosaccharide in 50 mM phosphate buffer, pH 6.5, at 30 ^{o}C for 20 min. The reaction mixture (2 μL) was spotted

on silica-gel 60 F254 plates and chromatographed vertically with solvent consisted of ethyl acetate, acetic acid and water (2:2:1, v/v). The products was detected by spraying with developer solution (10% H_2SO_4 in ethanol, v/v) and baked at 120 ^oC for 5 min to visualize the sugar.

3.3.10.4 Kinetic parameter determination

Kinetic parameters, K_m and V_{max} of purified rOs1BGlu4 with *p*NP- glycosides and oligosaccharides were determined in triplicate. The initial velocity of hydrolysis for each substrate was initially determined using 3-4 substrate concentrations and incubation times (10-30 min) to find conditions that yield 0.1 to 1.0 absorbance units. The rate versus time was plotted and an appropriate time and enzyme amount was chosen for kinetic studies. The reactions containing phosphate buffer and 5-8 different substrate concentrations ranging from 1/4-4 fold of the K_m value were pre-incubated on ice, and then appropriately diluted enzyme was added to the reaction, the reaction was incubated immediately at 30 ^oC for 10 to 30 min, depending on each substrate, to establish the initial velocity (V_0).

One unit of enzyme activity was defined as the amount of enzyme that produced 1 μmole of product per min. The activity values for disaccharides were determined by dividing the amount of glucose released by two, since two glucose molecules are released per molecule of disaccharides hydrolyzed. The number of micromoles of the product formation for oligosaccharides is defined in terms of total glucose released, although oligosaccharides may also have more than one glucose released per substrate molecule due to sequential cleavage. The kinetic parameters were calculated by nonlinear regression of the Michaelis-Menlen curves with the Grafit 5.0 program.

3.3.11 The inhibition study

The inhibition of rOs1BGlu4 activity by many chemicals was studied. Various 10 mM inhibitors was mixed with 1 mM *p*NPG in 50 mM phosphate buffer, pH 6.5, followed by adding rOs1BGlu4, and incubated for 10 min at 30 ^{o}C. The reaction was stopped by adding 70 µL of 0.4 M Na_2CO_3, and the absorbance was read at 405 nm. The same reaction without the substrate was used as the blank; the same volume of buffer was supplemented to the reaction. The strong inhibitors, such as $HgCl_2$ and delta-glucono-lactone, were diluted to explore the inhibition effect.

3.3.12 Sequential hydrolysis to *p*NP-cellobioside

In order to investigate the sequential hydrolysis of *p*NP-cellobioside, 50 µL reaction of 0.125 µg rOs1BGlu4 was incubated with 5mM *p*NP-cellobioside in 50 mM phosphate buffer, pH 6.5, at 30 ^{o}C.The hydrolysis time ranging from 5 min to 1 hr with 5 or 10 min intervals. The reaction was sampled at the designated time points and the reaction in the samples stopped by boiling. The reaction (2 µL) was loaded on silica-gel 60 F254 plates and chromatographed vertically with a solvent that consisted of ethyl acetate, methanol and water (7:2.5:1, v/v). The plate was detected first by UV light to detect the *p*NP, followed by spraying with solution (10% H_2SO_4 in ethanol, v/v) and baked at 120 ^{o}C for 5 min to visualize the sugar.

3.3.13 Transglycosylation activity of rOs1BGlu4

In order to investigate the translgycosylation activity of the rOs1BGlu4, the *p*NPG was used as the glycosyl group donor, while ethanol and *p*NPG were used as glucosyl group acceptors, respectively. Different concentrations of ethanol acceptors

(10%, 20%, 30% and 50%, v/v), and 10 mM or 20 mM final concentration of *p*NPG as donor was compared.

The effect of different incubation times and *p*NPG concentrations on the product of the transglycosylation reaction was studied. 0.5, 5, 10, 20 and 40 mM *p*NPG concentrations at 1, 2 and 3 hr incubation times were compared. The reaction products were loaded on a silica gel-coated F_{254} aluminium plates, (Merck) and chromatographed vertically with solvents of 2:1:1 ethyl acetate:acetic acid:water. The TLC was visualized by UV light and sulfuric acid as described in 3.3.13.

3.4 Results and Discussion

3.4.1 Sequence analysis of rice *Os*1*bglu*4

The coding sequence, and 5' and 3' untranslated regions of *Os*1*bglu*4 are shown in Figure 3.2. The 1731 bp long nucleotide sequence includes a 1449 bp open reading frame, which encodes a 483 amino acid long protein.

The deduced protein was predicted by Signal P (Bendtsen *et al.* 2004) to have no signal peptides and the subcellular localization predicted by PSORT is in the Cytoplasm (Horton and Nakai 1999). Unlike many putative rice β-glucosidases, which were predicted to enter the secretary pathway, Os1BGlu4 should exist in the cytoplasm.

The pI is predicted to be 5.16 and the molecular weight is 55.3 kD according to the Compute pI/Mw at the EXPASY Server. There is no N-glycosylation site by prediction of NetNGlyc. The predicted pI of Os1BGlu4 is different from the pI of many cell wall bound beta-glucosidases, eg, rice Os4BGlu12, protein purified from the cell wall of rice seedlings (pI 10) (Akiyama *et al.* 1998), and germinated barley seeds (pI 9-9.5) (Leah *et al.* 1995, Hrmova *et al.* 1996).

The analysis of the cDNA sequence indicated that the protein was classified into glycoside hydrolase family 1 and had the conserved catalytic core and active site sequences of this family. The EST expression indicates that the *Os*1*bglu*4 is expressed in callus, flower, leaf, panicle, root and stem (Figure 3.1).

Tissue	TPM	Matches/Total
callus	18	3 / 162069
flower	7	1 / 134391
leaf	22	4 / 175658
panicle	51	7 / 136249
root	74	5 / 67194
seed	0	0 / 32409
stem	16	2 / 124773
vegetative meristem	0	0 / 4537

Figure 3.1 The EST expression profile of rice *Os*1*bglu*4 gene (http://www.ncbi.nlm.nih.gov/UniGene/ESTProfileViewer). The number before the spot is transcripts per million (TPM), the spot intensity is based on the TPM, the number in the last column is gene EST/total EST.

The structure of Os1BGlu4 was modeled by the SWISS-MODEL Server (Schwede *et al.* 2003) with the Os3BGlu6 structure, PDB code 3GNP as the template. The overall structure of Os1BGlu4 is a $(\alpha/\beta)_8$-barrel, which corresponds to the typical structure of GH1 family (Figure 3.3). The Os1BGlu4 polypeptide contains Glu residues at positions 177 and 380 that lie within the sequences TFNEP and ITENG, respectively, which matches the consensus motifs in family 1 β-glucosidases (Czjzek *et al.* 2001).

The two consensus motifs lie at the ends of β-strand 4 and 7 of Os1BGlu4, and are important in catalysis and makeup part of a crater-shaped active site (Henrissat

et al. 1995, Czjzek *et al.* 2000). The substrate binding site lies in a funnel-shaped pocket on the C-terminal end of the β-barrel, and residues found in the region dictate the substrate-specificity of the enzyme (Henrissat *et al.* 1995, Burmeister *et al.* 1997, Czjzek *et al.* 2000).

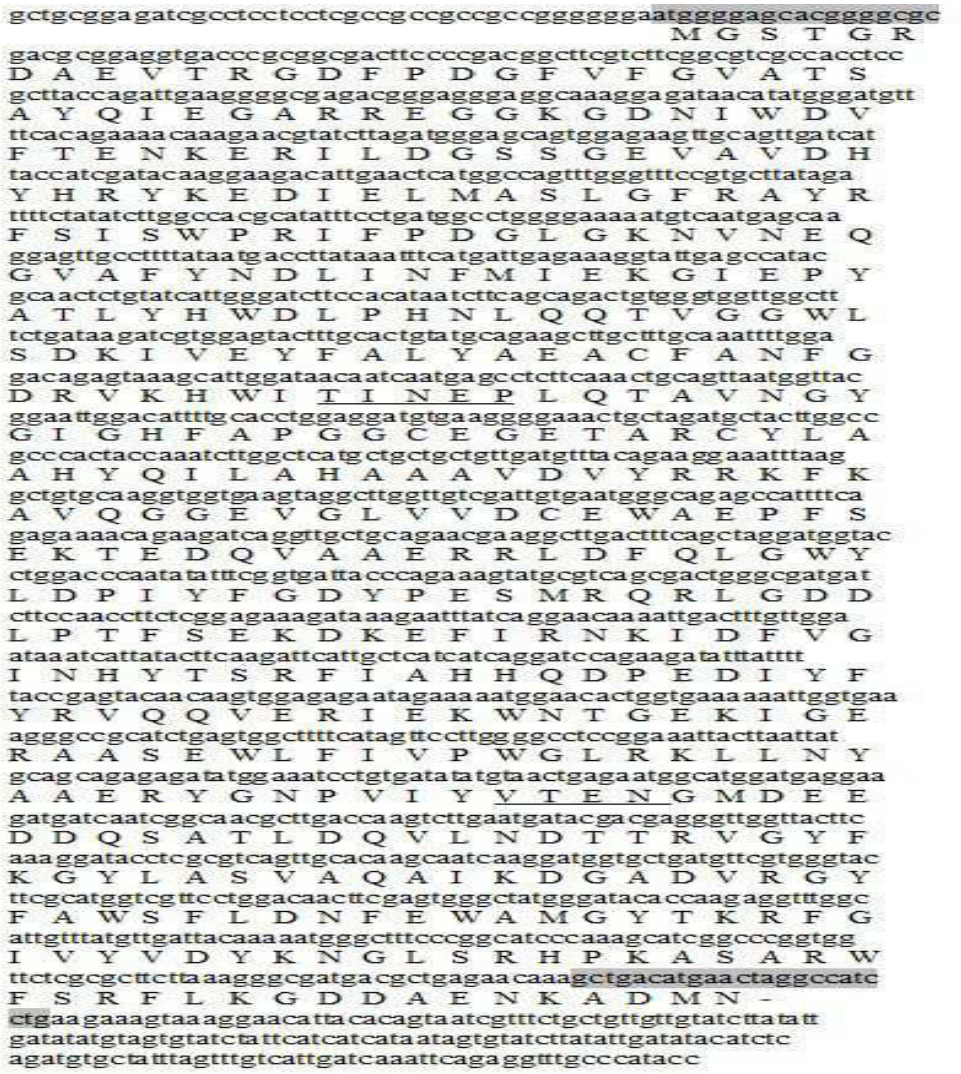

Figure 3.2 The nucleotide and deduced amino acid sequences of the AK243365.1 accession. The highlighted letters correspond to the sequence used for designing the primers used for amplifying the coding sequence of *Os*1*bglu*4. The underlined amino acids are the predicted catalytic acid/ base and nucleophile concensus sequences.

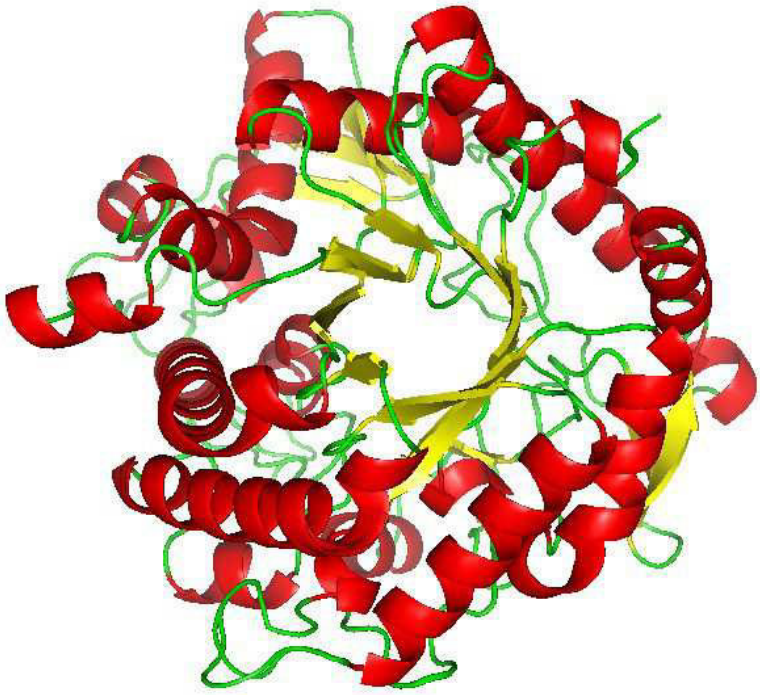

Figure 3.3 The predicted structure of Os1BGlu4 modeled by the Swiss-model software with the Os3BGlu6 template. The structure contains an $(\alpha/\beta)_8$-barrel, which is the typical structure of GH1 family. The red color helix is α-helix, the yellow strand is β-strand. The blue sticks are the two glutamic acids in the catalytic acid/base and nucleophile consensus motif.

3.4.2 Construction of *E. coli* expression vector

3.4.2.1 Amplification of coding sequence of *Os*1*bglu*4 from rice cDNA

The coding sequence of *Os*1*bglu*4 gene was amplified from 14 day rice seedlings cDNA library. A single intense band near 1.5 kb was observed (Figure 3.4). The PCR product was preliminarily checked by restriction digest with *Bam*HI. The *Os*1*bglu*4 gene sequence contains one site for *Bam*HI at the position 965 bp. The result showed that the *Os*1*bglu*4 amplicon was cut into two bands which were near 1 kb and 500 bp, corresponding to the expected size (Figure 3.5).

Figure 3.4 PCR product amplified with gene specific primers. Lane 1, DNA marker, lanes 2 and lane 3, PCR product.

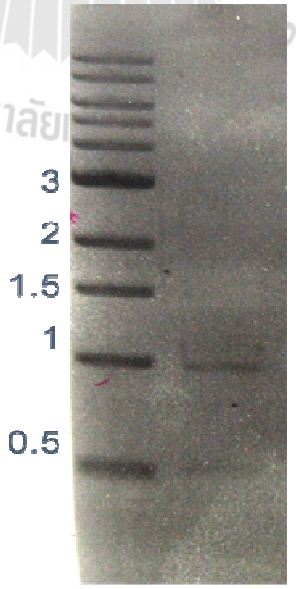

Figure 3.5 Target sequence check by restriction enzyme *Bam*HI digestion. Lane 1, DNA marker, lane 2, PCR product after *Bam*HI digestion.

3.4.2.2 Construction of *E. coli* expression vector

The pET32a(+) expression system was chosen, because it facilitates disulfide bond formation in the reducing environment of *E. coli* cytoplasm (Stewart *et al.* 1998), and many β-glucosidases have been expressed as active and soluble enzyme with the pET32a(+) vector, such as Os4BGlu12 and GB5BG (Opassiri *et al.* 2007), BGlu1 (Opassiri *et al.* 2003), rHvBII, Os7BGlu26, Os3BGlu6 and Os3BGlu8 (Kuntothom *et al.* 2009, Seshadri *et al.* 2009). Fusion of enzymes to soluble fusion partners, such as TRX, GST and MBP, is thought to help to overcome the aggregation of insoluble protein forms by promoting the proper folding of the attached protein into its biologically active conformation (Kapust and Waugh 1999).

The *Os*1*bglu*4 sequence of the cloned gene and the sequence in the database were aligned (Figure 3.6), all of the 3 point mutations were silent mutations, such that the cloned coding sequence of *Os*1*bglu*4 has no amino acid changes and could be used to express the target protein. The mutations were from the using of *Taq* DNA polymerase which has no proofreading ability over the nucleotide extension. Some researchers use the *Pfu* DNA polymerase to amplify the sequence instead to avoid the mutations despite its low amplification efficiency (Lundberg *et al.* 1991, Kroutil *et al.* 1996). To increase the efficiency, a small percentage of *Pfu* mixed with *Taq* polymerase to do the amplification was recommended (Cline *et al.* 1996).

Figure 3.6 The alignment between the sequence of *Os1bglu4* in the database (AK243365.1) (Sbjct) and the sequence from the constructed plasmid (Query). The letters stand for the mutant.

3.4.3 Expression the Os1BGlu4 in *E. coli* Origami B(DE3)

The substrate specificities and kinetic parameters of recombinant HvBII and HvBII isolated from germinated seeds were almost the same (Hrmova *et al.* 1996, Hrmova *et al.* 1998, Kuntothom *et al*. 2009), suggesting that the substrate specificities which was determined by the enzyme expressed in the *E. coli* expression system, are likely to comply to those of the corresponding native enzymes *in vivo*. This background authorizes us to assess the plant enzyme parameters through the recombinant enzyme expressed by *E. coli*.

The pET32-*Os*1*bglu*4 was introduced into competent Origami B(DE3) by electroporation. The transformed bacteria were induced to express the protein by adding the 0.3 mM of IPTG at 20 ^{o}C, 200 rpm for 20 hr. The results showed that all clones can express the Trx-His6-rOs1BGlu4 (lane 2-7) which is about 66 kD (Figure 3.7). By contrast, no intense band was observed at the same position of Origami B(DE3).

In order to get the large amount of the active protein, the IPTG concentration, induction time and induction temperature was investigated to optimize the expression of the protein. In the experiment, the protein production was found to be different when cultured at the different induction temperatures. So, the effects of the induction conditions on cell growth were investigated. The results showed that the induction temperature had significant effect on the cell growth. Because the low temperature decreased the metabolism of the cell, the 10 ^{o}C treatment had the lowest cell pellet weight. The 20 ^{o}C and 30 ^{o}C treatments had much higher amount of cell pellet than the 10 ^{o}C treatment. That means the 20 ^{o}C and 30 ^{o}C treatments had faster growth rate than the 10 ^{o}C treatment.

As the induction time increased from 12 to 16 hr, the weight of cell pellet increased significantly (Figure 3.8). By contrast, the weight of cell pellet increased little when the induction time increase from 16 to 24 hr, which may result from the dynamic equilibrium of the *E. coli* population in a limited space after sufficient growth time of 16 hr.

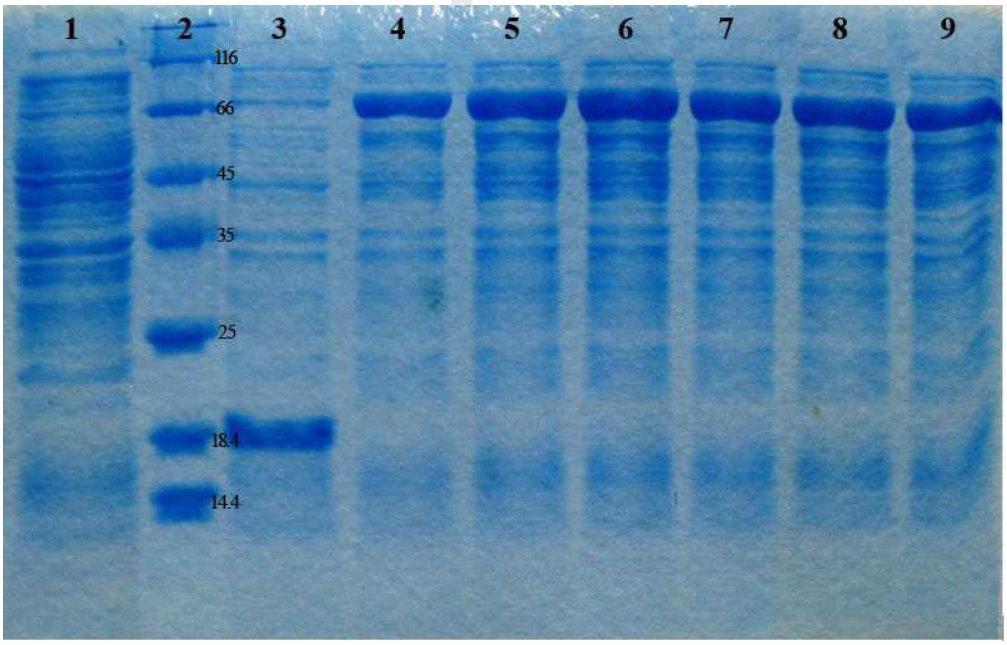

Figure 3.7 The protein expression profile of Origami B(DE3) transformed with the pET32-*Os*1*bglu*4. Lane 1 is proteins extracted from Origami B(DE3) colony, lane 2, protein marker, lane 3 is proteins extracted from Origami B(DE3)+pET32a colony, lanes 4-9 are proteins extracted from Origami B(DE3)+pET32-*Os*1*bglu*4 colonies.

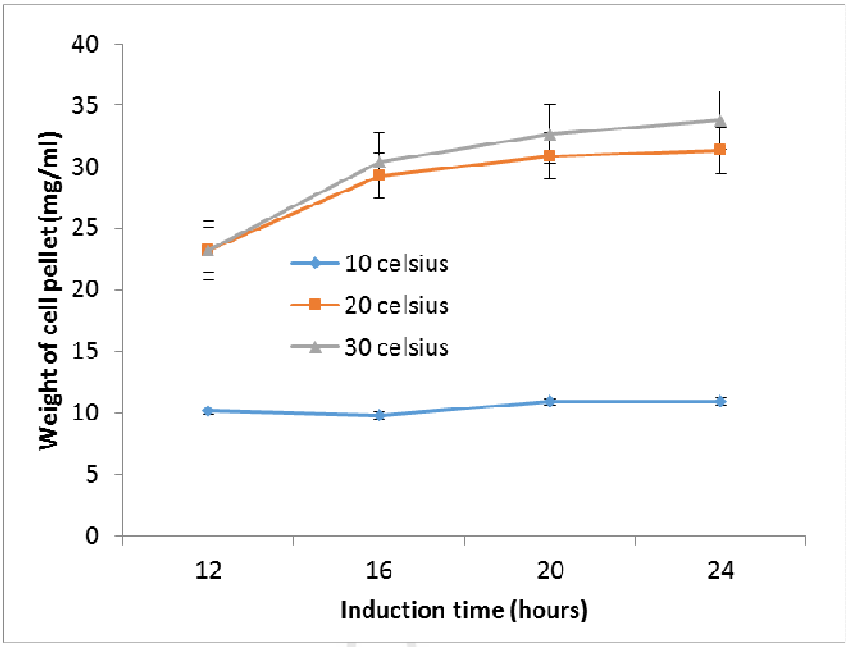

Figure 3.8 The effect of induction time and induction temperature to the weight of cell pellet.

The extraction buffer was added to the cell pellet in the ratio of 1 gram cell pellet to 5 mL extraction buffer. After centrifugation, the soluble part was used as the crude enzyme to do the activity assay. The same amount of crude Trx-His6-rOs1BGlu4 was incubated with 1 mM *p*NPG in sodium acetate, pH 5.0 (Opassiri *et al.* 2006). The results showed that the Trx-His6-rOs1BGlu4 extracted from 10 ^{o}C and 20 ^{o}C treatments have higher 'activity' than that of 30 ^{o}C (Figure 3.9). The 'activity' determined by both the Trx-His6-rOs1BGlu4 activity and the soluble protein percentage. The ratio of soluble protein and insoluble Trx-His6-rOs1BGlu4 induced by 0.3 mM IPTG under 10, 20 and 30 ^{o}C for 16 hr showed that 10 and 20 ^{o}C treatments have a bit more soluble Trx-His6-rOs1BGlu4 than 30 ^{o}C treatment (Figure 3.10), which means the different 'activity' of Trx-His6-rOs1BGlu4 among different temperature may be from the different amounts of soluble Trx-His6-rOs1BGlu4.

The optimum expression temperature is different for each protein, most proteins are expressed well from 10-40 ^{o}C, for example, CcBglA can be expressed at 13 ^{o}C, NkBgl can be expressed at 16 ^{o}C (Jeng *et al.* 2011). OsEGL1 and OsEGL2 can be expressed at 30 ^{o}C (Akiyama *et al.* 2009). GH5BG and Os4BGlu12 were induced at 20 ^{o}C (Opassiri *et al.* 2006, 2007). HvExoI was expressed successfully at 20 ^{o}C (Luang *et al.* 2010). The recombinant linamarase of cassava (Keresztessy *et al.* 1996) and primeverosidase of tea leaves (Mizutani *et al.* 2002) in *E. coli* were also not soluble and directed to inclusion bodies when cultures were grown and induced at 37 ^{o}C. This suggested that the recombinant proteins tend to form inclusion bodies when synthesis was induced at higher temperature. rOs1BGlu4 is expressed well at 20 ^{o}C, the activity of the enzyme decrease at 30 ^{o}C, and this phenomenon was observed in the expression of Os3BGlu6 (Seshadri *et al.* 2009). This is caused by the higher percentage of insoluble protein which are not folded properly due to fast expression under higher temperature (Baneyx 1999, Baneyx and Mujacic 2004).

The induction time had no significant effect to the activity of 6His-Trx-rOs1BGlu4 from 12 hr to 24 hr (Figure 3.9).

The IPTG concentration had no significant effect on the weight of cell pellet in the 10 ^{o}C treatment (Figure 3.11), because the cell growth of 10 ^{o}C treatment was very low. In contrast, the cell growth of the 20 ^{o}C and 30 ^{o}C treatments was inhibited by the adding of IPTG. Many proteins expressed in the pET system need the IPTG to induce the expression of the protein. The concentration is between 0.1-0.5 mM in the expression of some rice β-glucosidases despite the 1 mM concentration recommended by the manufacture (Opassiri *et al.* 2006, Jeng *et al.* 2011). However, the expression of Trx-His6-rOs1BGlu4 did not need IPTG; the IPTG inhibited the growth of the cells instead, which resulted in the decrease in the weight of cell pellet (Figure

3.11). However, the presences of IPTG have no significant effect on the specific activity of Trx-His6-rOs1BGlu4 (Figure 3.12). This phenomenon was also observed during the expression of Os3BGlu6 (Seshadri *et al.* 2009).

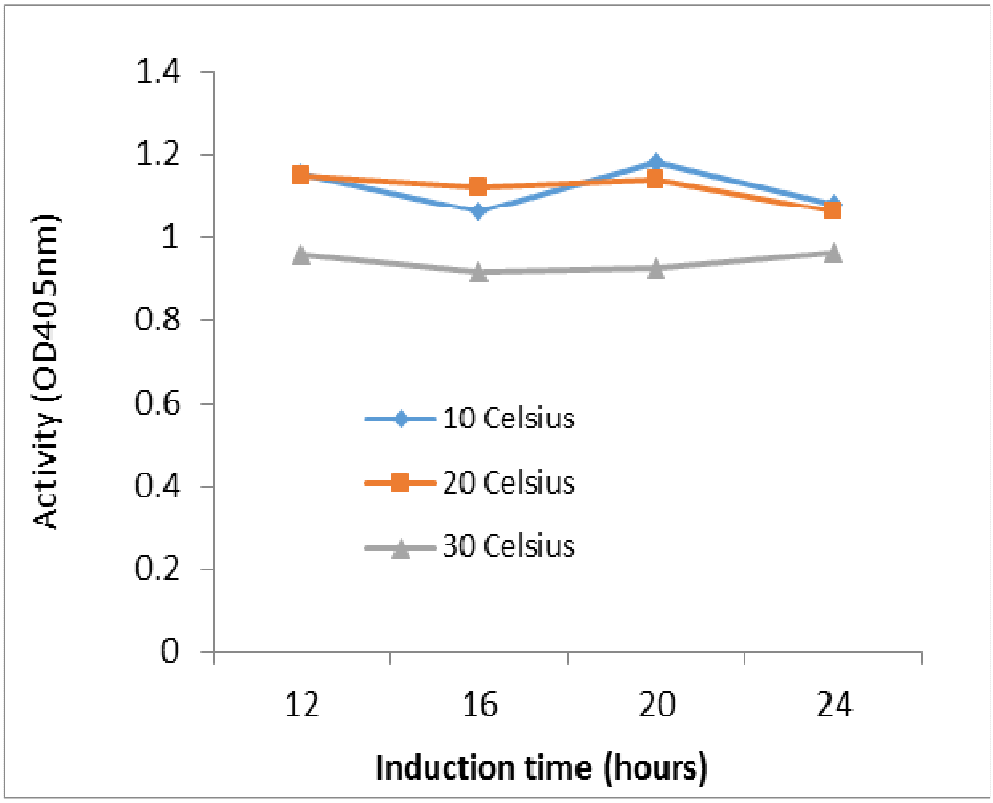

Figure 3.9 The effect of induction time and induction temperature to the 'activity' of crude Trx-His6-rOs1BGlu4. The 100 µL reaction included 10 µL of crude protein (1 g cell pellet/3 ml extraction buffer), 1 mM *p*NPG and 50 mM sodium acetate buffer; pH 5.0, the reaction was incubated at 30 ^{o}C for 15 min. The *p*NP release was measured at OD 405 nm.

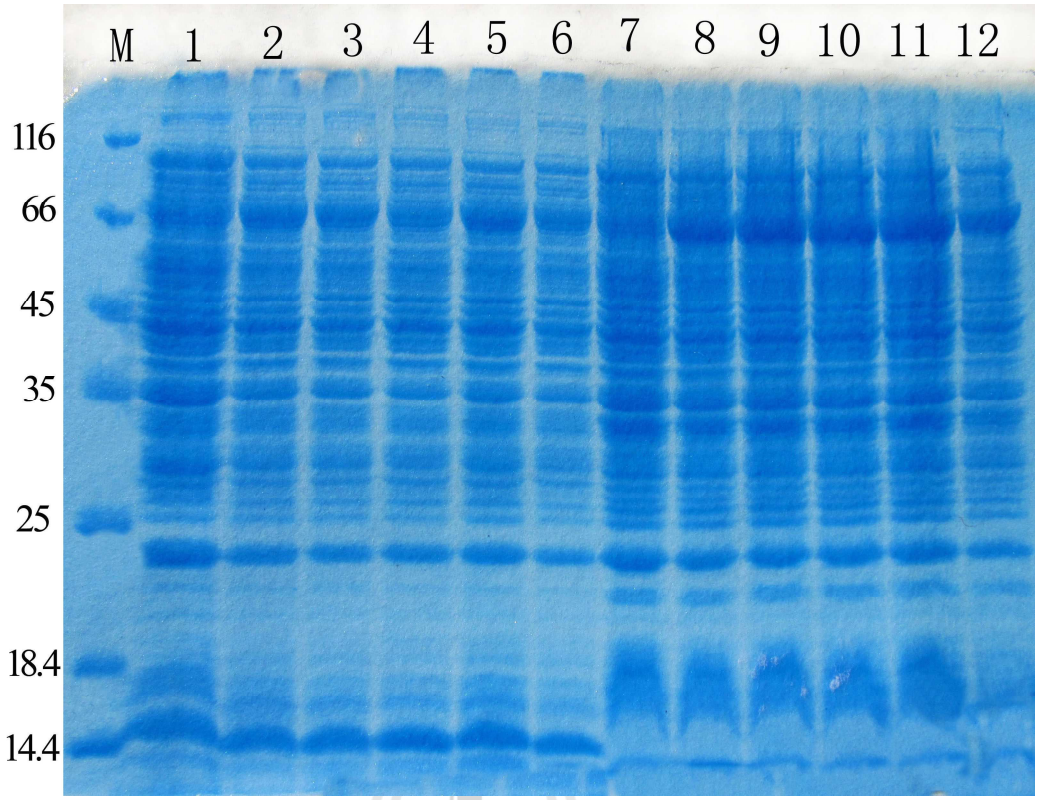

Figure 3.10 The soluble and insoluble Trx-His6-rOs1BGlu4 under different temperature under 0.3 mM IPTG induction for 16 hr. M, protein marker, lanes 1 and 4, soluble Trx-His6-rOs1BGlu4 induced at 10 ^{o}C, lanes 2 and 5, soluble Trx-His6-rOs1BGlu4 induced at 20 ^{o}C, lanes 3 and 6, soluble Trx-His6-rOs1BGlu4 induced at 30 ^{o}C, lanes 7 and 10, insoluble Trx-His6-rOs1BGlu4 induced at 10 ^{o}C, lanes 8 and 11, insoluble Trx-His6-rOs1BGlu4 induced at 20 ^{o}C, lanes 9 and 12, insoluble Trx-His6-rOs1-BGlu4 induced at 30 ^{o}C.

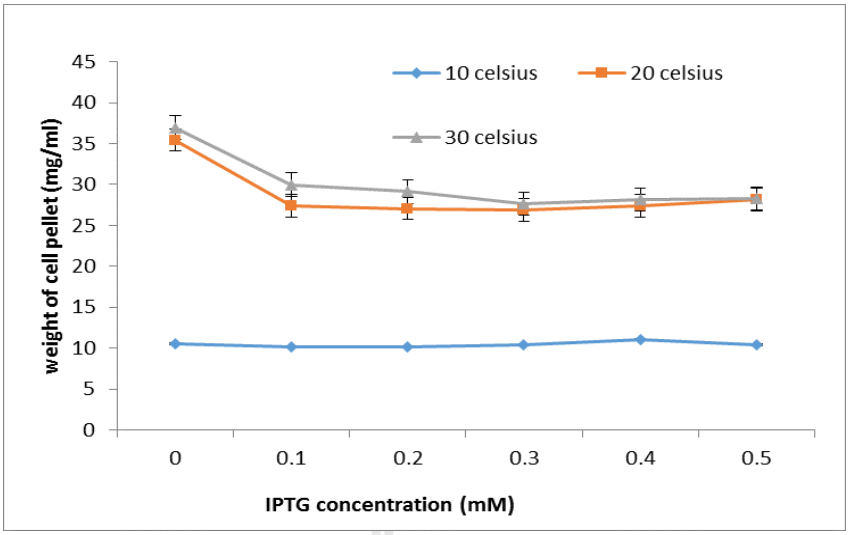

Figure 3.11 The effect of IPTG concentration to the weight of the cell pellet. The 100 µL reaction included 10 µL of crude protein (1 g cell pellet/3 ml extraction buffer), 1 mM *p*NPG and 50 mM sodium acetate buffer, pH 5.0, the reaction was incubated at 30 ^{o}C for 15 min. The *p*NP release was measured at OD 405 nm.

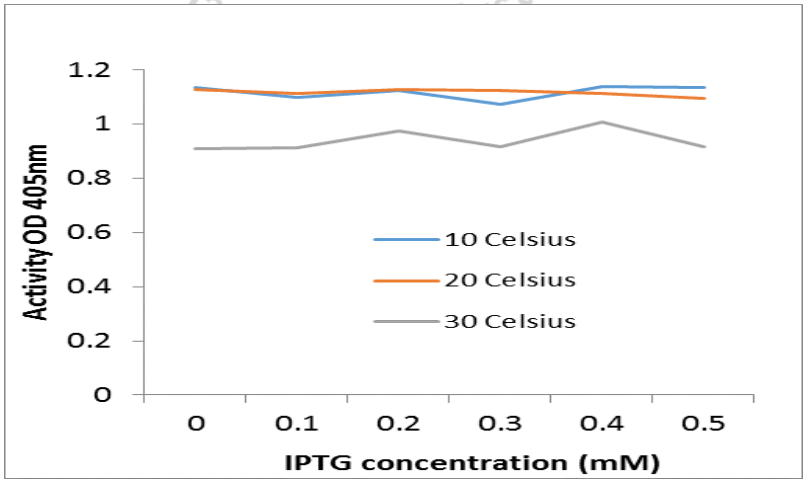

Figure 3.12 The effect of IPTG concentration to the 'activity' of crude Trx-His6-rOs1BGlu4.

3.4.4 Extraction and purification of the Trx-His6-rOs1BGlu4

Purification of the recombinant protein was designed to allow easy and fast, single step purification. 6His tag in the pET system facilitates the use of affinity chromatography. The recombinant Trx-His6-rOs1BGlu4 was purified by IMAC on BD Talon^{TM} (immobilized cobalt) metal affinity column to obtain approximately 85% pure protein and an intense band at 66 kD was observed on SDS-PAGE (Figure 3.13). After concentrated and changing the buffer, the concentration of Trx-His6-rOs1BGlu4 was 3.4 mg/mL. Approximately 2.8 mg of purified Trx-His6-rOs1BGlu4 could be obtained per liter of bacterial expression culture. The purified Trx-His6-rOs1BGlu4 was cut by the enterokinase and the recombinant Os1BGlu4 (rOs1BGlu4) which is about 55 kD, and the thioredoxin tag were released (Figure 3.14). The size of rOs1BGlu4 by experimental estimate is almost identical to the predicted molecular weight (55.3 kD). After a second IMAC purification step, the pure rOs1BGlu4 was obtained as a single band on SDS-PAGE (Figure 3.13). The buffer of rOs1BGlu4 was changed to 20 mM Tris-Cl, pH 8.0, the concentration was 2.2 mg/mL. This rOs1BGlu4 was aliquotted and kept in -20℃ and used to characterize the biochemical properties.

3.4.5 pH optimum and pH stability of rOs1BGlu4

When the pure rOs1BGlu4 was obtained, the rOs1BGlu4 was characterized. The results showed that rOs1BGlu4 was most active at pH 6.5 when assayed with 1 mM *p*NPG for 10 min (Figure 3.15). When compared with others pH buffers, rOs1BGlu4 had higher activity at pH 6.0-pH 7.0 buffers. The rOs1BGlu4 had almost no activity when the enzyme was assayed in buffers with pH below 5.0. The enzyme activity also decreased dramatically at pH above 8.0. The activity of rOs1BGlu4 had the similar change trend between the two sets of the buffer (Figure 3.16). The pH

optima of most β-glucosidases ranged between pH 4 and 7.5, depending on their source and cellular location, and they tend to be stable over a range of pH from 4 to 9 (Ketudat Cairns and Esen 2010). The pH optimum of the purified rOs1BGlu4 was pH 6.5, which is reasonable even it is different to many others β-glucosidases (Os3BGlu8, pH5.0, Os7BGlu26, pH 4.5, Os3BGlu7, pH 5.0, rHvBII, pH 4.0) (Esen 1993, Hrmova *et al.* 1998, Opassiri *et al.* 2003). This pH is related to the pH environment of the catalytic reaction, since Os1BGlu4 was predicted to localize to the cytoplasm, the pH of which should be near neutral pH 7 (Berrin *et al.* 2002).

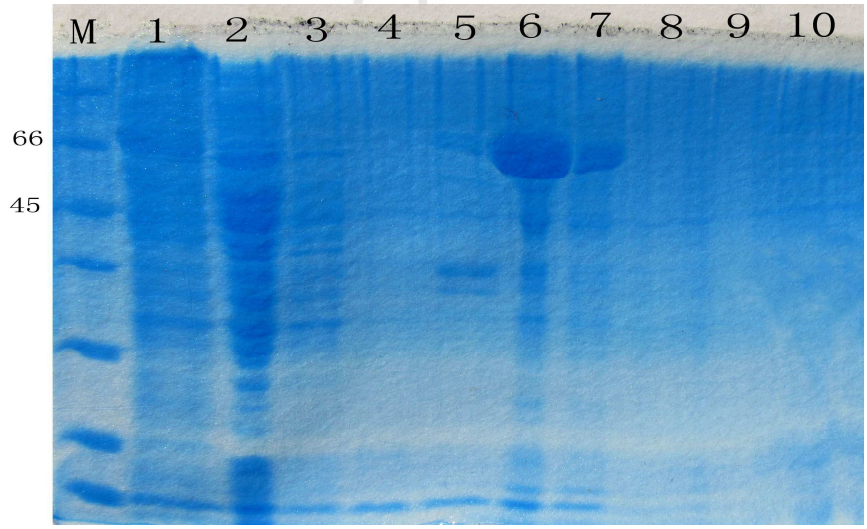

Figure 3.13 SDS-PAGE profiles of Trx-His6-rOs1BGlu4 purification using IMAC. M, standard marker (Bio-RAD), lane 1, crude protein, lane 2, flow through, lane 3, solution washed by W0, lane4, solution washed by W0+5 mM imidazole, lane 5, solution washed by W0+20 mM imidazole, lane 6, solution washed by W0+50 mM imidazole, lane 7, solution washed by W0+100 mM imidazole, lane 8, solution washed by W0+250 mM imidazole, lane 9, solution washed by 500 mM imidazole, lane 10, solution washed by 50 mM MES, pH5.0.

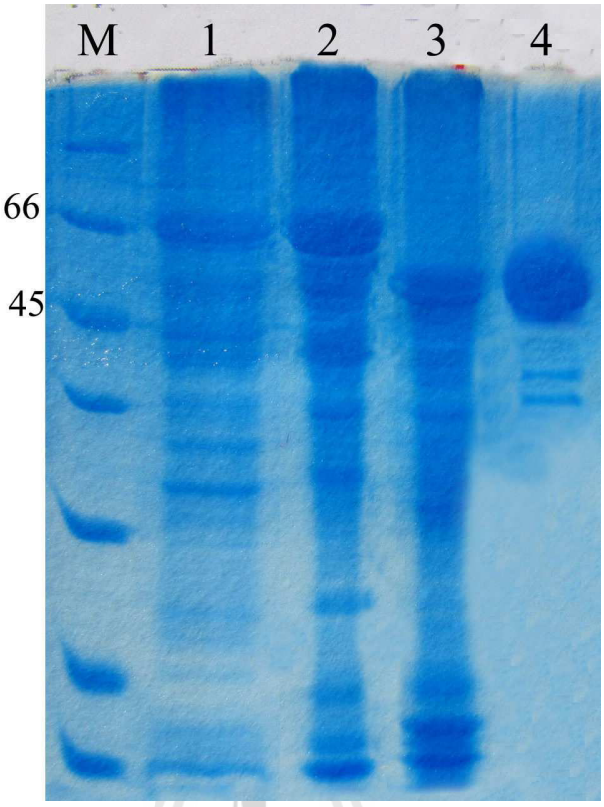

Figure 3.14 SDS-PAGE profiles of Trx-His6-rOs1BGlu4 recombinant protein expressed in Origami B(DE3) after incubation at 20 for 16 hr. M, standard protein marker (Bio-RAD), Lane 1, crude Trx-His6-rOs1BGlu4, lane 2, purified Trx-His6-rOs1BGlu4, lane 3, Trx-His6-rOs1BGlu4 digested by enterokinase, lane 4, purified rOs1BGlu4.

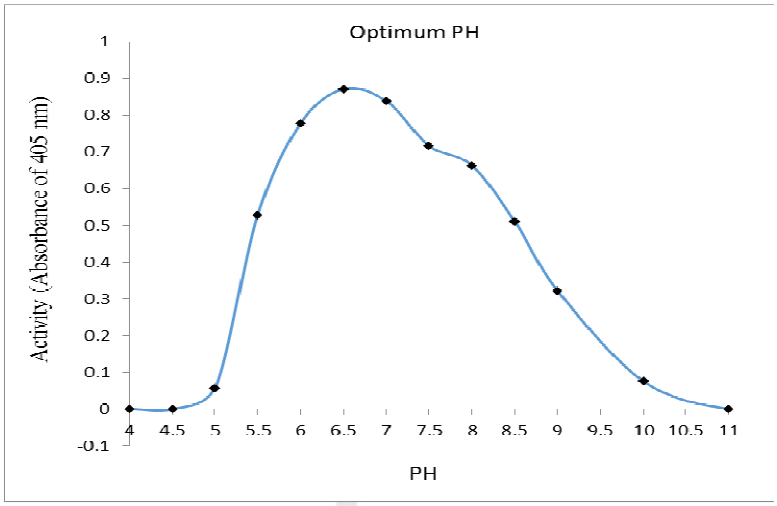

Figure 3.15 The activity versus pH profile for rOs1BGlu4 over the pH range of 4.0 to 11 (formate pH 3.5-4.0; sodium acetate pH 4.5-5.5; sodium phosphate pH 6.0-7.5; Tris pH 8.0-9.5 CAPS pH10.0-11.0). rOs1BGlu4 (0.25 µg) was assayed with 1 mM *p*NPG in different 50 mM pH buffers at 30 ^{o}C for 10 min.

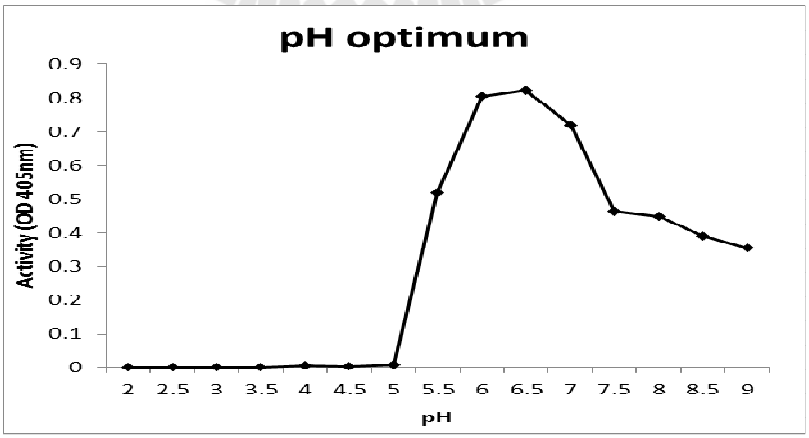

Figure 3.16 The pH optimum for rOs1BGlu4 over the pH range of 2.0 to 9.0 (50 mM citric acid and disodium hydrogen phosphate buffers with pH ranging from pH 2.0 to pH 9.0). Os1BGlu4 (0.25 µg) was assayed with 1 mM *p*NPG in different pH buffers at 30 ^{o}C for 10 min.

The rOs1BGlu4 was relatively stable over the pH range of 6.0 to 8.0, when incubated for up to 24 hr (Figure 3.17). As the time increased from 10 min to 24 hr, the activity of rOs1BGlu4 decreased in all the pH buffers, but the descent of the activity was relatively slight in pH 6.0- pH 8.0 when compared with the other pH buffers. pH 7-8, temperature 0-4 ^{o}C are normal storage condition for many proteins, when major protease contaminants have been removed (Ketudat Cairns and Esen 2010). As with other proteins, pH extremes, co-purifying proteases, and microbial contamination may result in degradation, although many β-glucosidases are resistant to proteases due to their tightly folded core structure (Ketudat Cairns and Esen 2010). The purified rOs1BGlu4 showed two bands on the SDS page accasionally (Figure 3.18), which may result from internal cleavage but leaves the fold intact (Ketudat Cairns and Esen 2010).

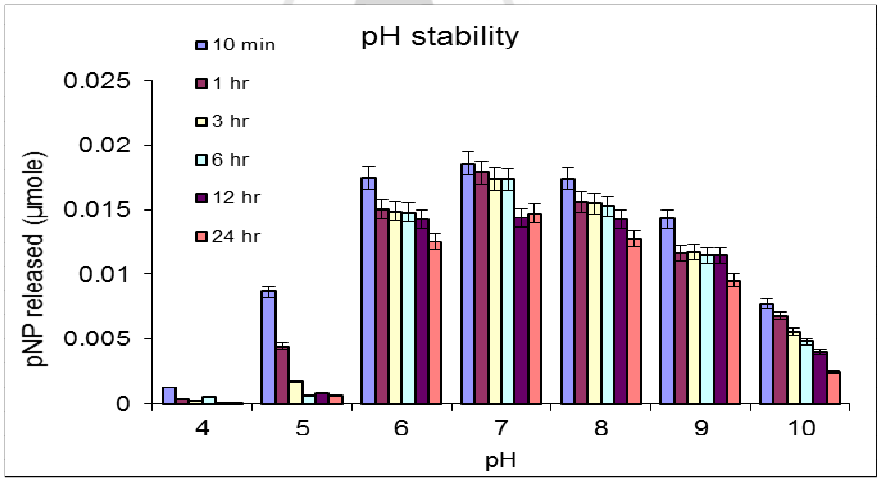

Figure 3.17 The pH stability of rOs1BGlu4 after incubation for 10 min to 24 hr at 30 ^{o}C over the pH range of 4.0 to 10.0 (formate pH 4.0; sodium acetate pH 5.0; sodium phosphate pH 6.0-8.0; CAPS pH 9.0-10.0). Aliquots of enzyme in each pH buffer were sampled at the designated times and diluted 5 fold and assayed in 50 mM phosphate buffer, pH 6.5, and incubated with 1 mM *p*NPG at 30 ^{o}C for 10 min.

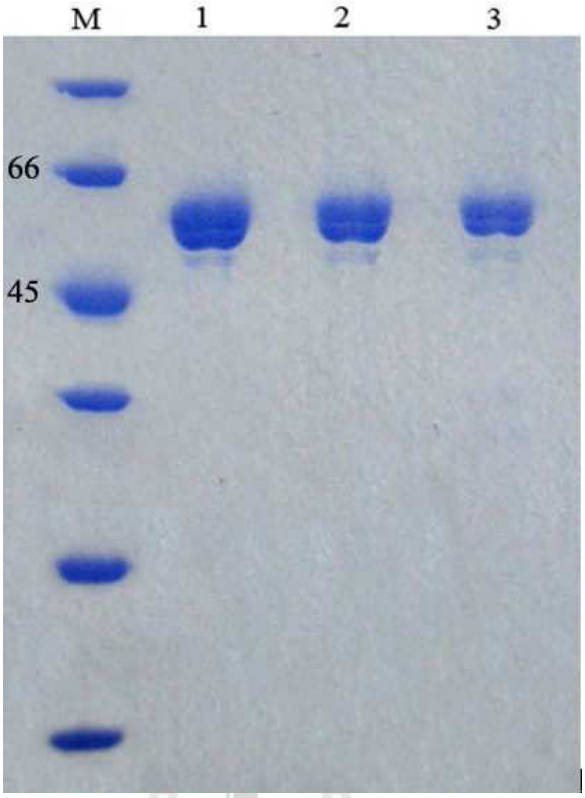

Figure 3.18 SDS-PAGE profile of purified rOs1BGlu4 showed two band. M, protein marker, lane 1-3, purified rOs1BGlu4.

3.4.6 Temperature optimum and thermostability of rOs1BGlu4

The temperature optimum for rOs1bglu4 was determined by incubating the enzyme with 1 mM *p*NPG for 10 min at different temperatures ranging from 5 ^{o}C to 90 ^{o}C. The activity of rOs1BGlu4 at different temperature was normal distribution (Figure 3.19), the peak was 45 ^{o}C. As the temperature increased from 5 ^{o}C to 45 ^{o}C, the activity of rOs1BGlu4 increased correspondingly, as the temperature continued to increase from 45 ^{o}C to 90 ^{o}C, the activity of rOs1BGlu4 decreased gradually. The optimum point was 45 ^{o}C, which corresponded to the results that many β-glucosidases have temperature optima near 50 ^{o}C (Konno *et al.* 1996, Akiyama 1998, Riou *et al.* 1998). However some β-glucosidases have higher optimal temperatures, such as the

Thai rosewood and *Dalbergia nigrescens* β-glucosidases, which have a temperature optima of 60 and 65 °C, respectively (Srisomsap *et al.* 1996, Chuankhayan *et al.* 2005). Because high activity at temperatures above the extremes of the enzyme's natural environment is not physiologically relevant and these temperatures may result in rapid heat denaturation, assays are often run at 30-40 °C (Ketudat Cairns and Esen 2010).

The thermostability study was performed by incubating the enzyme with the phosphate buffer pH 6.5, at temperatures ranging from 20-60℃ from 10 min to 60 min, and then aliquots of rOs1BGlu4 was assayed with 1 mM *p*NPG at pH 6.5 for 10 min. Figure 3.20 showed that the enzyme was stable at 20 °C and 30 °C for up to 1 hr incubation. The rOs1BGlu4 lost about 20% of its activity when incubated at 40 °C for 20 minutes, rOs1BGlu4 was unstable at 50 °C and 60 °C, 70% of the activity was lost with the 50 °C treatment after only in 10 min incubation, 83% of the activity was lost in 20 min. At 60 °C, only 10 min incubation resulted in almost complete loss of rOs1BGlu4 activity.

For rOs1BGlu4, the activity decreased even after 10 min incubation at 40, 50 and 60 °C, which indicated that irreversible inactivation of the enzyme, occurred at temperatures higher than 40 °C. However, the Os4BGlu12 and BGlu1 were more stable than Os1BGlu4, the irreversible inactivation happened at 50 °C (Opassiri *et al.* 2003, 2006).

The maximum temperature for a given enzyme depends on a balance between the rate of the catalytic reaction and enzyme denaturation. β-Glucosidases from different organisms might have different optimum temperatures and stability, which would reflect different interactions stabilizing the enzymes (Dixon and Webb 1979).

According to above analysis, 30 °C was used as the standard incubation tem- perature in this experiment.

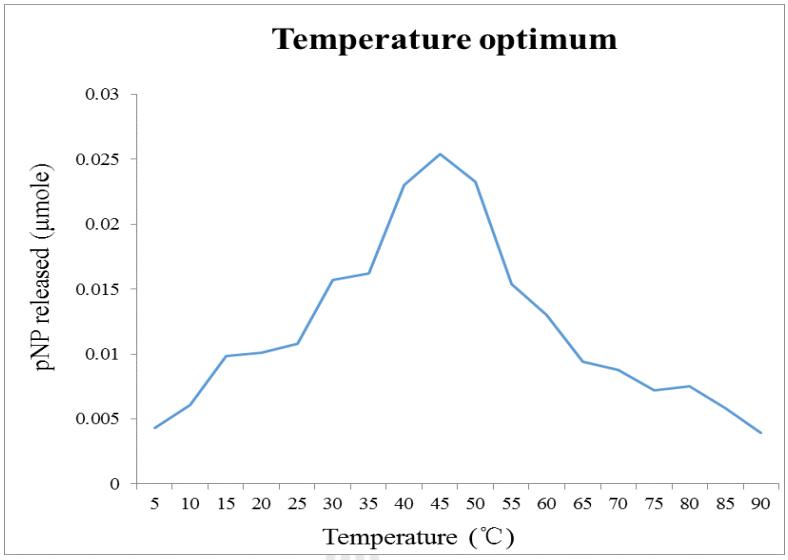

Figure 3.19 Activity of rOs1BGlu4 over the temperature range from 5 to 90 °C. rOs1BGlu4 (0.25 µg) was assayed with 1 mM *p*NPG for 10 min at the designated temperature.

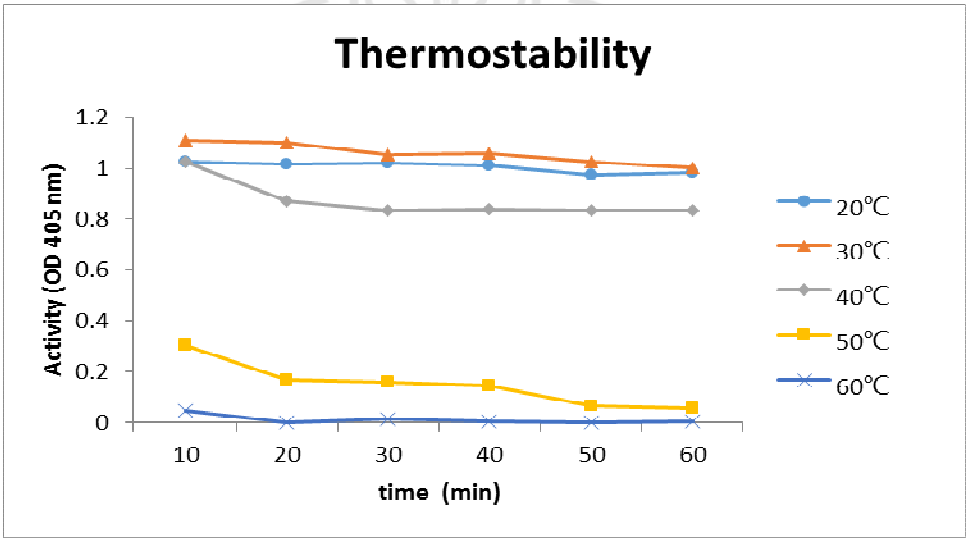

Figure 3.20 Thermostability of rOs1BGlu4 for 10 to 60 min at 20-60 °C. Concentrated rOs1BGlu4 were incubated in the phosphate buffer (pH 6.5) from 20-60 °C, aliquots of the enzyme (0.25 µg) at designated time were assayed with 1 mM *p*NPG at 30 °C for 10 min.

3.4.7 Substrate specificity of rOs1BGlu4

The activity of the purified rice Os1BGlu4 β-glucosidase towards natural and artificial glycosides was characterized. Hydrolysis of *p*NP-glycosides with different glycone moieties was used to assess glycone specificity of rOs1BGlu4. The release of *p*NP was measured according to the *p*NP standard curve (Appendix figure 3). The activity of the purified rice rOs1BGlu4 towards *p*NP-glycosides is summarized in Table 3.5. Among the artificial *p*NP-glycosides, rOs1BGlu4 hydrolyzed the *p*NPG with relatively high efficiency, and *p*NP-β-D-fucopyranoside was hydrolyzed at 82% of the rate of *p*NPG. The rOs1BGlu4 hydrolyzed *p*NPG (k_{cat}/K_m, 17.92, s^{-1} mM^{-1}) and *p*NP-β -D-fucopyranoside (k_{cat}/K_m, 9.34, s^{-1} mM^{-1}) with high efficiency. Besides, rOs1BGlu4 hydrolyzed *p*NP-β-D-galactopyranoside, *p*NP-β-D-cellobioside, *p*NP-α-L-arabionopyranoside, *p*NP-β-D-mannopyranoside and *p*NP-β-D-xylopyranoside and at 4.32%, 3.39%, 2.4%, 1.8% and 1.0% the rate of *p*NPG, respectively. Hydrolysis of *p*NP-α-D-glucopyranoside, *p*NP-α-L-fucopyranoside, *p*NP-N-acetyl-β-D-glucosaminide, *p*NP-β-D-maltoside, *p*NP-β-L-fucopyranoside and 2,4-dinitrophenyl-2-deoxy-2-fluoro-β-D-glucopyranoside was not detectable.

Hydrolysis of *p*NP-glycosides with different glycone moieties was used to assess the glycone specificity of rOs1BGlu4, and the results showed that the rOs1BGlu4 was not stringent at the -1 subsite, where the non-reducing glycosyl moiety is bound. This phenomenon is similar to many GH1 and GH3 β-glucosidases, such as the rice Os3BGlu7 (Opassiri *et al.* 2003) and rice Os4BGlu12 and GH5BG enzymes (Opassiri *et al.* 2006, 2007).

Table 3.1 Relative activities of purified rOs1BGlu4 in the hydrolysis of *p*NP-derivatives.

No.	Substrate	Activity[a](µmole/min/mg)	Relative activity[b] (%)
1	pNP-β-D-glucopyranoside	5.69	100.00
2	pNP-β-D-fucopyranoside	4.6	80.94
3	pNP-β-D-galactopyranoside	0.25	4.32
4	pNP-β-D-cellobioside	0.19	3.39
5	pNP-α-L-arabinopyranoside	0.14	2.40
6	pNP-β-D-mannopyranoside	0.1	1.80
7	pNP-β-D-xylopyranoside	0.06	1
8	pNP-α-D-galactopyranoside	n.d[c].	n.d.
9	pNP-α-D-mannopyranoside	n.d.	n.d.
10	pNP-β-L-arabinopyranoside	n.d.	n.d.
11	pNP-β-D-maltoside	n.d.	n.d.
12	pNP-α-L-fucopyranoside	n.d.	n.d.
13	pNP-N-acetyl-β-D-glucosaminide	n.d.	n.d.
14	2,4-dinitrophenyl-2-deoxy-2-fluoro-β-D-glucopyranoside	n.d.	n.d.
15	pNP-α-D-galactopyranoside	n.d.	n.d.

[a]The assay contained 1 mM substrate in 50 mM sodium phosphate pH 6.5 buffer at 30°C

[b] Percentage activity relative to *p*NP released from *p*NP-β-D-glucopyranoside.

[c] n.d. means not detected

Substrate specificity of rOs1BGlu4 towards various kinds of oligosaccharides was determined. The enzyme activity was assayed by incubating 0.125 µg enzyme with 1 mM substrates in pH 6.5 phosphate buffer, at 30 °C for 20 min. The released glucose was oxidized by PGO solution; the OD 405 nm was measured and

compared with the glucose standard (Appendix figure 2). The results are summarized in the Table 3.6. The rOs1BGlu4 hydrolyzed the β-1,3-linked oligosaccharide laminaribiose and laminaritriose, but not laminaritetraose, laminaripentaose. β-1,4-linked oligosaccharide cellobiose, cellotriose, cellotetraose, cellopentaose, cellohexaose can be hydrolyzed at different rates. The rOs1BGlu4 can not hydrolyze chitopentaose and the β-1,6-linked disaccharide gentiobiose. rOs1BGlu4 showed high hydrolytic efficiency with β-(1, 3)-linked oligosaccharides with DP of 2-3. The hydrolysis rates toward while those of cellotriose and cellotetraose are similar, about 70% of the rate of laminaribiose, cellopentaose and cellohexaose were about 28% of the rate of laminaribiose. By contrast, cellobiose is the most poorly hydrolyzed substrate. On the TLC profile, rOs1BGlu4 showed hydrolytic activity towards laminari-oligosaccharides and cello-oligosaccharides, but no measurable transglycosylation activity at the concentrations tested (Figure 3.23).

The cello-oligosaccharides and laminari-oligosaccharides were reported to be hydrolyzed by β-glucosidases which maybe involved in cell-wall related processes. For example, rice Os3BGlu7 (BGlu1), Os3BGlu8, and Os7BGlu26 and Os4BGlu12 (Kuntothom *et al.* 2009, Opassiri *et al.* 2010). Although, Os1BGlu4 was predicted to be localized in the cytoplasm, surprisingly, it can hydrolyze the cellooligosaccharide with DP 2-6 and laminari-oligosaccharides with DP 2-3 (Figure 3.9). Since Os1BGlu4 can hydrolyze the oligosaccharides, the hydrolysis activity of Os1BGlu4 was compared with some cell-wall remolding related β-glucosidases which have been characterized before.

Table 3.2 Relative activities of purified rOs1BGlu4 in the hydrolysis of oligosaccharides.

No.	Substrate	Activity[a](µmole/min/mg)	Relative activity[b] (%)
1	Laminaribiose	1.81[c]	100.00
2	Laminaritriose	1.50	82.77
3	Laminaritetraose	n.d.[d]	n.d.
4	Laminaripentaose	n.d.	n.d.
5	Cellobiose	0.10	5.52
6	Cellotriose	1.27	69.96
7	Cellotetraose	1.39	76.91
8	Cellopentaose	0.53	29.22
9	Cellohexaose	0.48	26.61
10	Gentiobiose	n.d.	n.d.
11	Chitopentaose	n.d.	n.d.

[a] The assay contained 1 mM substrate in 50 mM sodium phosphate, pH 6.5, at 30 °C

[b]Percentage activity relative to glucose released from laminaribiose.

[c]The released glucose of laminaribiose and cellobiose was divided by 2 since one cut produced two glucose molecules.

[d]Means not detected.

Natural substrate specificity of rOs1BGlu4 hydrolysis was determined to study the possible natural substrate in rice. Some commercially available natural substrates were tested at 1 mM final concentration (Table 3.7). The product was loaded onto the TLC plate. The result indicated that salicin, esculin and *para* coumaryl alcohol

glucoside (*p*CAG) can be hydrolyzed by rOs1BGlu4 (Figure 3.22). As judged from the TLC plate, the glucose released from the esculin at the identical time is more than that from salicin and *p*CAG. That suggested that esculin can be hydrolyzed more efficiently than salicin and *p*CAG.

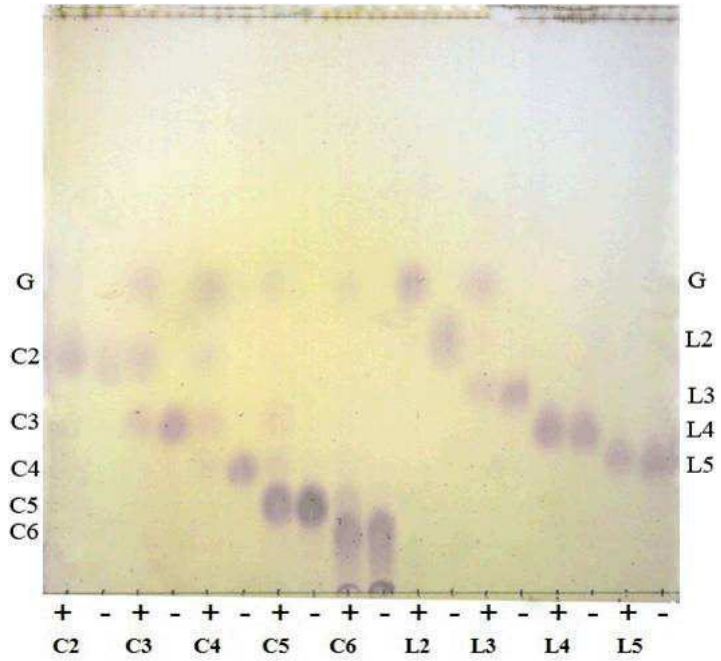

Figure 3.21 Hydrolysis products of rice Os1BGlu4 with cello-oligosaccharides and laminari-oligosaccharides and detected by TLC. In each 50 µL reaction, 0.125 µg Os1BGlu4 was incubated with 1 mM oligosaccharide in 50 mM phosphate buffer, pH 6.5, at 30 °C for 20 min. Samples were incubated with (+) and without (-) enzyme. Then, 2 µL of the reaction was loaded onto the TLC plate. The plate was detected with staining method as described in method 3.3.11.3. G, C2, C3, C4, C5, C6 stand for glucose, cellobiose, cellotriose, cellotetraose, cellopentaose, cellohexaose, respectively, L2, L3, L4, L5 stand for the laminaribiose, laminaritriose, laminaritetraose, laminaripentaose, respectively.

The rOs1BGlu4 was predicted to be a cyanogenic β-glucosidase and clustered with a *Hevea brasiliensis* latex cyanogenic β-glucosidase (Opassiri *et al.* 2006), but the plant cyanogenic glucosides, linamarin, and its precursor amygdalin were not hydrolyzed by rOs1BGlu4 (Table 3.7).

The Os3BGlu8 could only hydrolyse esculin among the tested natural substrates, Os3BGlu6 can hydrolyze esculin, *p*CAG and salicin, the same as the rOs1BGlu4, so, the co-expression of these genes was checked to determine whether they are co-expressed. When *Os*1*bglu*4 expression was set to 1, the co-expression of Os3Bglu6 is 0.58 (close to the threshold 0.6 significant level), but the *Os*3*bglu*8 is not co-expressed (http://genecat.mpg.de). That possibly means the *Os*3*bglu*6 was co-expressed together with the *Os*1*bglu*4 to implement a similar function by hydrolyzing similar glycosides.

Since the natural substrate is similar, the hydrolysis activity of Os3BGlu6 was compared with rOs1BGlu4 extensively. Os3BGlu6 hydrolyzed *p*NP-β-D-fucopyranoside (k_{cat}/K_m =67 s^{-1} mM^{-1}) and *p*NPG (k_{cat}/K_m = 6.2 s^{-1} mM^{-1}), compared with rOs1BGlu4 hydrolyzed *p*NP-β-D-fucopyranoside (k_{cat}/K_m =9.3 s^{-1} mM^{-1}), *p*NPG (k_{cat}/K_m = 17.9 s^{-1} mM^{-1}).

Table 3.3 Commercially available natural substrates.

No.	Substrate	Glucose	No.	Substrate	Glucose
1	Salicin	+	14	n-octyl-β-D-glucoside	-
2	Esculin	+	15	GA_4 glucose ester	-
3	Linamarin	-	16	α-lactose	-
4	D-amygdalin	-	17	Sinigrin monohydrate	-
5	Trans-zeatin glucoside	-	18	Maltose	-
6	Daidzin	-	19	Metyl-β-D-glucopyranoside	-
7	Genistin	-	20	Arbutin	-
8	Naringin	-	21	Palatinose	-
9	Queretin-3-glucoside	-	22	mangiferin	-
10	*p*-CAG	+	23	lactulose	-
11	Coniferin	-	24	epigenin-7-glucoside	-
12	Indoxyl-β-D-glucoside	-	25	uridine	-
13	n-hepty-β-D-glucoside	-			

‘+’ stands for glucose was detected, ‘-’ stands for glucose was not detected

Figure 3.22 Hydrolysis products of rOs1BGlu4 with natural substrates. In 50 µL reactions, rOs1BGlu4 (0.125 µg) was incubated with 1 mM natural substrate in 50 mM phosphate buffer, pH 6.5, at 30 °C for 30 min. Two microliters of the reaction was loaded onto the TLC plate. Carbohydrates on the plate were detected as described in 3.3.11.3. Lane 1, glucose standard, lane 2, salicin+rOs1BGlu4, lane 3, salicin control reaction, lane 4, esculin+rOs1BGlu4, lane 5, esculin control reaction, lane 6, pCAG+rOs1BGlu4, lane 7, *p*CAG control reaction.

3.4.8 Kinetics analysis

3.4.8.1 Kinetic analysis of *p*NP-derivatives

The kinetic parameters (K_m, k_{cat}, and k_{cat}/K_m) of rOs1BGlu4 enzyme in the hydrolysis of various *p*NP-β-D-glycosides were determined and the data are summarized in Table 3.4. K_m value measures affinity of the enzyme for substrate. The lower K_m value, the less substrate is needed to saturate the enzyme. The k_{cat} gives a direct measure of the catalytic production of product under optimum conditions. *p*NP-β-D-glucoside can be hydrolyzed by rOs1BGlu4 efficiently, with the k_{cat}/K_m value 17.92 $s^{-1}mM^{-1}$. *p*NP-β-D-fucoside can be hydrolyzed about 2-fold less efficiently than *p*NPG by rOs1BGlu4. However, the K_m value of *p*NP-β-D-fucopyranoside and *p*NPG were similar at about 0.71±0.02 mM, which indicated the k_{cat} value of *p*NPG is 2-fold that of *p*NP-β-D-fucopyranoside. The *p*NP-β-D-cellobioside can be hydrolyzed slowly, with the catalytic efficiency (k_{cat}/K_m) value 3.92 s^{-1} mM^{-1}in terms of *p*NP release. *p*NP-β-D-mannoside, *p*NP-α-L-arabinopyranoside and *p*NP-β-D-galactopyranoside were hydrolyzed very slowly, with similar k_{cat}/K_m value about 0.5 s^{-1} mM^{-1}. The *p*NP-α-L-arabinopyranoside has the lowest K_m value, that means this substrate easily saturates to the rOs1BGlu4, but the bond between the *p*NP and the L-arabinose is difficult to cleave.

Table 3.4 Apparent kinetic parameters of rice rOs1BGlu4 in the hydrolysis of *p*NP-derivatives.

Substrate	k_{cat} (S^{-1})	K_m (mM)	k_{cat}/K_m (S^{-1} mM^{-1})
*p*NP-β-D-glucoside	12.76±0.18	0.71±0.02	17.92
*p*NP-β-D-fucoside	6.61±0.080	0.71±0.02	9.34
*p*NP-β-D-cellobioside	2.06±0.062	0.53±0.03	3.92
*p*NP-α-L-arabinoside	0.52±0.0043	0.38±0.02	0.43
*p*NP-β-D-galactoside	3.16±0.065	7.33±0.32	0.43
*p*NP-β-D-mannoside	1.25±0.025	2.24±0.03	0.56

3.4.8.2 Kinetic analysis of oligosaccharides

The kinetic parameters of rOs1BGlu4 enzyme in the hydrolysis of various oligosaccharides were determined and the data are summarized in Table 3.5. The rOs1BGlu4 hydrolyzed laminaribiose most efficiently, with the k_{cat}/K_m value of 12.45 s^{-1} mM^{-1}, followed by the cellotetraose, the k_{cat}/K_m value is 8.73 s^{-1} mM^{-1}. Laminaritriose, cellotriose, cellopentaose and cellohexaose can be hydrolyzed with the gradually decreasing efficiencies. The cellobiose was hydrolyzed most slowly, with the k_{cat}/K_m value only 0.03 $s^{-1}mM^{-1}$. In contrast, laminaribiose can be hydrolyzed 415-fold more efficiently than cellobiose.

Rice Os3BGlu7, Os3BGlu8, and Os7BGlu26 hydrolyzed cello-oligo-saccharides with increasing efficiency as the degree of polymerization (DP) increased from 2 to 6, while Os4BGlu12 showed little increase in activity with DP of 4-6 (Ketudat Cairns and Esen 2010). By contrast, the hydrolysis rate of rOs1BGlu4 had

a relatively big difference, the k_{cat}/K_m increased from cellobiose to cellotetraose, and decreased from cellotetraose to cellohexaose. The cellotetraose can be hydrolyzed at 8 fold higher efficiency than the cellohexaose, which indicated that the rOs1BGlu4 has four subsites for binding of the glucosyl group.

Table 3.5 Apparent kinetic parameters of rOs1BGlu4 in the hydrolysis of oligosaccharide.

Substrate	k_{cat} **(S^{-1})**	K_m **(mM)**	k_{cat}/K_m **(S^{-1} mM^{-1})**
Laminaribiose	4.67±0.09	0.38±0.02	12.45
Laminaritriose	3.37±0.55	0.6±0.03	5.63
Cellobiose	0.58±0.01	19.0±0.5	0.03
Cellotriose	2.74±0.06	0.59±0.03	4.64
Cellotetraose	2.27±0.03	0.26±0.01	8.73
Cellopentaose	2.15±0.03	1.07±0.04	2.01
Cellohexaose	1.08±0.02	1.1±0.05	0.99

3.4.8.3 Kinetics analysis of esculin

The kinetic parameters of rOs1BGlu4 enzyme in the hydrolysis of esculin were determined. The hydrolysis product of esculin was esculetin, a yellow compound, with the absorbance at 405 nm. Therefore, the standard curve of esculetin was set up (Appendix figure 4). The kinetic parameters of hydrolysis activity towards esculin was measured, the results showed that the k_{cat} is 2.13±0.04 s^{-1}, the K_m is 0.55±0.02 mM and the catalytic efficiency, k_{cat}/K_m is 3.86 s^{-1} mM^{-1}, the esculin was hydrolyzed about 3.8 fold less efficiency than *p*NPG.

3.4.9 Inhibition study

The effects of selected chemicals on rOs1BGlu4 hydrolysis activity were determined by adding to 10 mM final concentration of various possible inhibitors in the substrate. The same reaction without the inhibitor was used as the control. The same reaction components without the substrate were used as a blank. The results are shown in Table 3.6. $HgCl_2$, delta-glucono-lactone, $FeCl_3$, 1% SDS and $CuSO_4$ had strong inhibitory effects on the activity of rOs1BGlu4. The $HgCl_2$, delta-glucono- lactone, $FeCl_3$ were able to inhibit almost 100% of the hydrolysis activity of rOs1BGlu4. Besides, 1% SDS also had strong inhibitory effect on rOs1BGlu4. The salts $PbCl_2$ and $CuSO_4$ also have relatively strong inhibitory effects. The EDTA, $CoSO_4$ and $MnSO_4$ had no inhibitory effects on the hydrolysis activity of rOs1BGlu4. The rest of the chemicals tested in the experiment have the inhibitory effects to the hydrolysis activity of rOs1BGlu4 ranging from 38% to 7%.

In order to figure out the inhibition effect of the strong inhibitors, the strong inhibitors were diluted, and the relative activity was measured (Table 3.10). The results indicated that $HgCl_2$ is a very strong inhibitor to the hydrolysis activity of rOs1BGlu4, when the concentration deceased to 0.05 mM, the inhibitory effect was still 100%. The activity recovered to 18% eventually when the concentration was diluted to 0.01 mM. For the δ-glucono-lactone, 62% of the activity was recovered when it was diluted to 0.1 mM.

Table 3.6 The activity of Os1BGlu4 when 10 mM of various inhibitor exist with 1 mM *p*NPG in 50 mM sodium phosphate, pH 6.5, at 30°C. The same reaction without the inhibitor was used as the CK. The same reaction components without the substrate were used as a blank.

No.	Inhibitor	Activity	Relative activity remaining (%)
1	CK	8.1	100
2	$HgCl_2$	0	0
3	Delta-glucono-lactone	0.02	0
4	$FeCl_3$	0.12	2
5	1%SDS	0.43	5
6	$CuSO_4$	2.49	31
7	$PbCl_2$	4.16	51
8	L-Arabinose	4.96	61
9	Imidazole	5.92	73
10	Urea	5.91	73
11	D-Mannose	5.91	73
12	LiCl	5.88	73
13	$NiSO_4$	6.4	79
14	$ZnCl_2$	6.36	79
15	D-Glucosamine	6.82	84
16	D-Xylose	6.9	85
17	$CdCl_2$	6.98	86
18	$MgCl_2$	7.16	88
19	D-Glucose	7.29	90
20	D-Glucose	7.55	93

Table 3.6 The activity of Os1BGlu4 when 10 mM of various inhibitor exist with 1 mM *p*NPG in 50 mM sodium phosphate, pH 6.5, at 30°C. The same reaction without the inhibitor was used as the CK. The same reaction components without the substrate were used as a blank (cont.).

No.	Inhibitor	Activity	Relative activity remaining (%)
21	$CaCl_2$	7.8	96
22	KCl	7.88	97
23	L-Histidine	8.01	99
24	$MnSO_4$	8.11	100
25	$CoSO_4$	8.16	101
26	EDTA	8.35	103

Table 3.7 The activity of rOs1BGlu4 when different concentrations of inhibitors were present together with 1 mM *p*NPG in 50 mM sodium phosphate, pH 6.5, at 30 °C.

Inhibitor	Concentration (mM)	Relative activity (%)
δ-glucono-lactone	10.0	0
	1.0	14
	0.1	62
$HgCl_2$	10.0	0
	1.0	0
	0.1	0
	0.05	0
	0.01	18

3.4.10 Sequential hydrolysis of *p*NP-cellobioside

When the concentration of the *p*NP-cellobioside was increased, the release of *p*NP by rOs1BGlu4 decreased. This result indicated that the inhibition existed in the hydrolysis of *p*NP-cellobioside. Therefore, the mechanism of hydrolysis of *p*NP-cellobioside was studied. Hydrolysis times ranging from 5 min to 1 hr with 5 and 10 min intervals were tested. The *p*NP, *p*NPG and glucose was visualized by TLC. The results indicated that at the initial reaction stage (5-20 min), no visible *p*NP can be seen, but the *p*NPG and glucose can be seen clearly on the TLC (Figure 3.23). As the time elapsed, *p*NP-cellobioside decreased gradually, more *p*NPG was produced and there was visible *p*NP on the TLC at 30 min (Figure 3.23). All these phenomena indicated that the initial cut happens between the two glucose molecules, not at the bond between *p*NP and cellobiose.

Similar to rice BGlu1 and GH5BG (Opassiri *et al.* 2004, Opassiri *et al.* 2007), rOs1BGlu4 cleaved the β-glucosidic bond between the two glucose residues in pNP-β-D-cellobioside, thereby releasing glucose and *p*NPG, however, the *p*NPG released by BGlu1 and GH5BG was hydrolysed rapidly, but the *p*NPG released by rOs1BGlu4 was hydrolyzed relatively relatively slowly, because the *p*NPG appeared after 5 min, the *p*NP was found after 20 min.

3.4.11 Transglycosylation activity of rOs1BGlu4

It is known that many glycosyl hydrolases have transglycosylation activity as well as hydrolytic activity towards the substrates (Wang *et al.* 1994, Mackenzie *et al.* 1998, Wang *et al.* 2002). In order to investigate the translgycosylation activity of the rOs1BGlu4, the *p*NPG was used as the glucose donor; ethanol and *p*NPG were used as

glucose acceptors. The same reaction without the ethanol was used as the control. The results showed that both the ethanol and *p*NPG can form the glycosidic bond with the glucose which was cut from the *p*NPG (Figure 3.24). The TLC results had many kind of synthesized chemicals when *p*NPG was used as the receptor, by contrast, only one product was seen from the TLC when ethanol was used as the receptor (Figure 3.24 A). The identity of the synthesized product was not verified.

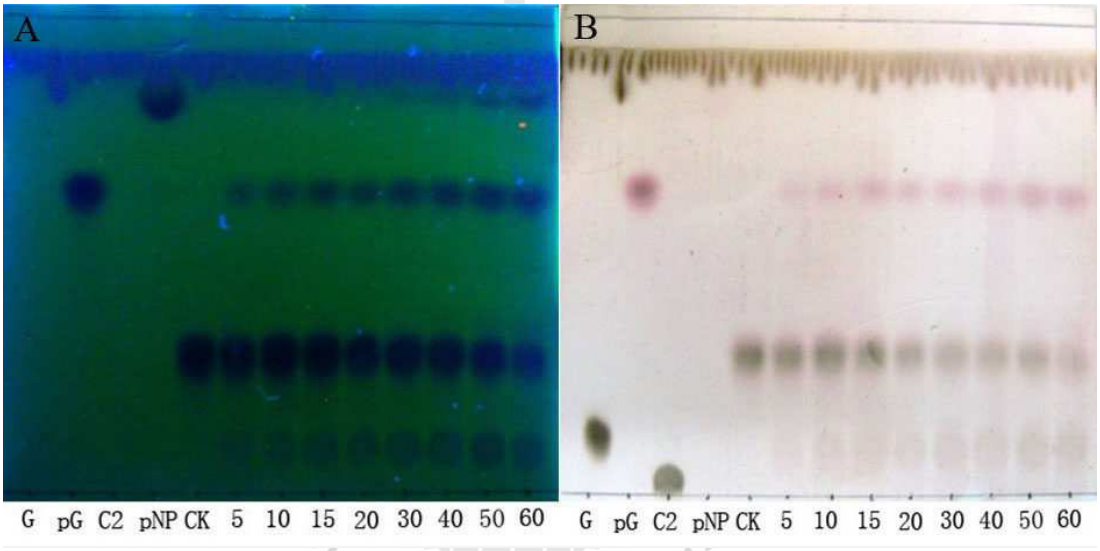

Figure 3. 23 Sequential hydrolysis of *p*NP-cellobioside on the TLC plate. In a 50 µL reaction, 0.125 µg rOs1BGlu4 was incubated with 5mM *p*NP-cellobioside in 50 mM phosphate buffer, pH 6.5, at 30 ^{o}C. The reaction was sampled at the designated time points (5-60 minutes). Two microliters of the reaction were loaded onto the TLC plate. The plate was detected first by UV light, and then detected by H_2SO_4 staining, as described in method 3.3.11.3. G, glucose, pG, *p*NPG, CK, *p*NP-cellobioside in buffer without enzyme, C2, cellobiose, pNP, *p*-nitrophenol, 5-60, 5 minute to 60 minute reaction. A: TLC plate visualized by UV light. B: TLC plate visualized by staining method.

It was reported that the almond-galactosidase catalyzed transglycosylation only in the presence of considerably high concentration of acceptor substrate (0.5-2M) (Dey 1979). However, some β-glucosidase showed transglycosylation activity towards oligosaccharides with DP of 2-4 at relatively low substrate concentration (2 mM) (Akiyama *et al.* 1998). In this experiment, the transglycosylated product was only visible when the volume of ethanol was 20-30%. Nothing can be seen on the TLC when the concentration of ethanol was 10% and 50%.

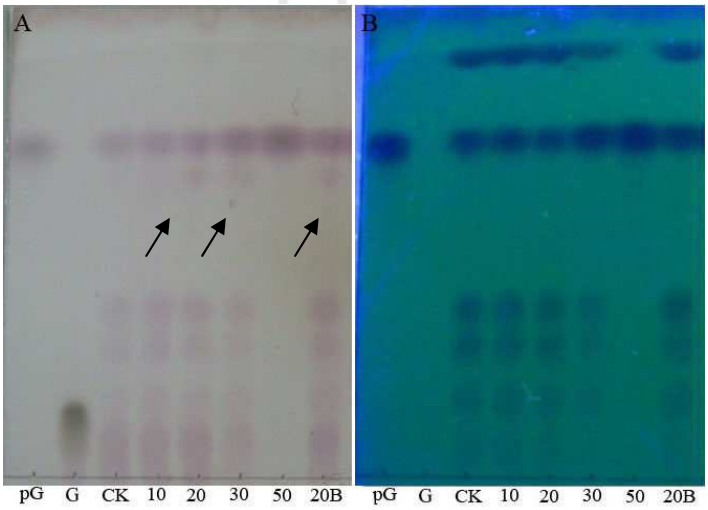

Figure 3.24 Transglycosylation activity of rOs1BGlu4. G, glucose, pG, *p*NPG, CK, *p*NPG was used as both donor and acceptor, 10, 20, 30, 50 stand for the 10%, 20%, 30% and 50% (v/v) of the ethanol as the receptor in the reaction. The reaction included 10 mM final concentration of *p*NPG. 20B, the reaction included 20% of the ethanol, 20 mM final concentration of *p*NPG. Black arrows showed the product of the reaction which ethanol was used as the receptor. A: TLC plate visualized by staining method. B: TLC plate visualized by UV light.

The effects of different incubation times and substrate concentrations on the transglycosylation were investigated. At low *p*NPG concentration (0.5 mM), at all incubation times, no visible tranglycosylation product can be seen on the TLC (Figure 3.25). For 5 mM *p*NPG concentration reaction, some transglycosylation product can be seen after 1 hour incubation, and the product become less after 2 hours incubation, and invisible after 3 hours incubation, the *p*NPG had the same changing trend. In contrast, the glucose and the *p*NP increased gradually as the incubation time increased. For the 10 mM, 20 mM and 40 mM *p*NPG concentration and the transglycosylation product had the same changing trend were similar to that of the 5 mM *p*NPG concentrations as the incubation time increased.

From the TLC, the transglycosylation product was closely related to the *p*NPG concentration. The higher concentration of *p*NPG, the more transglycosylation product (Figure 3.25 A).

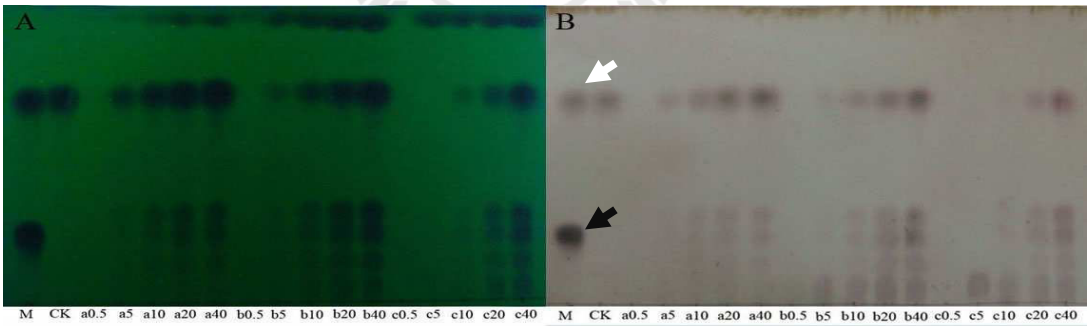

Figure 3.25 The effects of the different incubation times and substrate concentrations on the transglycosylation activity of Os1BGlu4. M: marker, including *p*NPG (white arrow), *p*NP-cellobioside (black arrow). CK, the same reaction without rOs1BGlu4. 0.5-40, stand for 0.5 mM *p*NPG, 5 mM *p*NPG, 10 mM *p*NPG, 20 mM *p*NPG, 40 mM *p*NPG in the reaction, a, b, c stands for 1, 2, 3 hour incubation time. A: TLC plate visualized by UV light. B: TLC plate visualized by staining method.

3.4.12 Possible biological functions of rice *Os*1*bglu*4 β-glucosidase

The EST profile showed that *Os*1*bglu*4 mRNA is expressed in shoots, root, stem, leaf and callus of rice, which means the *Os*1*bglu*4 involved in many physiological processes. The capability of Os1BGlu4 to hydrolyze cello-oligosaccharides and laminaribiose and laminaritiose indicated that the Os1BGlu4 may be involved in cell wall related processes. The lignification of secondary cell walls is thought to involve the activation of monolignols by removal of β-glucosyl residues from monolignol glycosides, like coniferin, syringin and pCAG (Hösel and Barz 1975, Dharmawardhana *et al.* 1995, Escamilla-Treviño *et al.* 2006), pCAG can be hydrolyzed by Os1BGlu4, from this point, the Os1BGlu4 could again be involved in the process of cell wall related lignification. The Os1BGlu4 hydrolyze the oligosaccharides which are taken up into the cell by membrane transporter after the production from cell wall to release the glucose to supply the cell with energy.

The capability of Os1BGlu4 to hydrolyze salicin and esculin showed that it may involved in plant pathogen and herbivore resistance, since the product of hydrolysis of salicin is similar to salicylic acid, which is recognized as an endogenous regulatory signal in plants mediating plant defence against pathogens (Malamy *et al.* 1990, Durner *et al.* 1997), together with the Os1BGlu4 EST expression after drought and blast stress (Opassiri *et al.* 2003).

The Os1BGlu4 maybe a multifunctional enzyme, involved in many plant development processes, according to the analysis above.

3.5 Conclusion

The recombinant thioredoxin-Os1BGlu4 (Trx-His6-rOs1BGlu4) fusion protein was functionally expressed in OrigamiB (DE3). Sixteen hour incubation at 20 ^{o}C, without IPTG inducer produced the most Trx-His6-rOs1BGlu4. The biochemical characterization showed that the optimum pH for the hydrolysis by rOs1BGlu4 was 6.5. The rOs1BGlu4 was stable over the pH range of 6.0 to 8.0 for 24 hr incubation. The optimum hydrolysis temperature was 45 ^{o}C. The rOs1BGlu4 was stable at 20 and 30 ^{o}C for 1 hr.

The rOs1BGlu4 efficiently hydrolyzed β-(1, 3)-linked oligosaccharides with DP of 2 and 3, and β-(1,4)-linked oligosaccharide with DP of 3 and 4. Cellopentaose and cellohexaose can be hydrolyzed with less efficiency. The laminari-oligosaccharides with DP more than 3 are not hydrolyzed. The rOs1BGlu4 can hydrolyze *p*NPG efficiently; the pNP-fucopyranoside was hydrolyzed with about 50% hydrolysis efficiency of the *p*NPG. Based on the kinetic parameters, others *p*NP-derivatives can be hydrolyzed with low efficiency. According to TLC results, salicin, esculin and *p*-CAG can be hydrolyzed by rOs1BGlu4.

The Os1BGlu4 was predicted to localize to the cytoplasm, but it may still be involved in cello- and lamimari- oligosaccharides hydrolysis and might contribute to the formation of lignin by monolignol/glucoconjugate equilibrium or to pathogen, herbivore resistance.

3.6 References

Akiyama, T., S. Jin, M. Yoshida, T. Hoshino, R. Opassiri*, et al.* (2009). Expression of an Endo-(1,3;1,4)-Beta-Glucanase in Response to Wounding, Methyl

Jasmonate, Abscisic Acid and Ethephon in Rice Seedlings. **Journal of Plant Physiology** 166(16): 1814-1825.

Akiyama, T., H. Kaku and N. Shibuya (1998). A Cell Wall-Bound Beta-Glucosidase from Germinated Rice: Purification and Properties. **Phytochemistry** 48(1): 49-54.

Baneyx, F. (1999). Recombinant Protein Expression in *Escherichia coli*. **Current Opinion in Biotechnology** 10(5): 411-421.

Baneyx, F. and M. Mujacic (2004). Recombinant Protein Folding and Misfolding in *Escherichia coli*. **Nature Biotechnology** 22(11): 1399-1408.

Bendtsen, J. D., H. Nielsen, G. von Heijne and S. Brunak (2004). Improved Prediction of Signal Peptides: Signalp 3.0. **Journal of Molecular Biology** 340(4): 783-795.

Berrin, J.-G., W. R. McLauchlan, P. Needs, G. Williamson, A. Puigserver*, et al.* (2002). Functional Expression of Human Liver Cytosolic Beta-Glucosidase in *Pichia pastoris*. Insights into Its Role in the Metabolism of Dietary Glucosides. **European Journal of Biochemistry** 269(1): 249-258.

Burmeister, W. P., S. Cottaz, H. Driguez, R. Iori, S. Palmieri*, et al.* (1997). The Crystal Structures of *Sinapis alba* Myrosinase and a Covalent Glycosyl-Enzyme Intermediate Provide Insights into the Substrate Recognition and Active-Site Machinery of an S-Glycosidase. **Structures** 5(5): 663-675.

Chuankhayan, P., Y. Hua, J. Svasti, S. Sakdarat, P. A. Sullivan*, et al.* (2005). Purification of an Isoflavonoid 7-O-B-Apiosyl-Glucoside B-Glycosidase and Its Substrates from *Dalbergia nigrescens* Kurz. **Phytochemistry** 66(16): 1880-1889.

Cline, J., J. C. Braman and H. H. Hogrefe (1996). PCR Fidelity of P*fu* DNA Polymerase and Other Thermostable DNA Polymerases. **Nucleic Acids Research** 24(18): 3546-3551.

Czjzek, M., M. Cicek, V. Zamboni, D. R. Bevan, B. Henrissat*, et al.* (2000). The Mechanism of Substrate (Aglycone) Specificity in Beta -Glucosidases Is Revealed by Crystal Structures of Mutant Maize Beta-Glucosidase -Dimboa, -Dimboaglc, and -Dhurrin Complexes. ***Agrobacterium tumefaciens*** **DNA and PS8 bacteriophage DNA not detected in crown gall tumors** 97(25): 13555-13560.

Czjzek, M., M. Cicek, V. Zamboni, W. P. Burmeister, D. R. Bevan*, et al.* (2001). Crystal Structure of a Monocotyledon (Maize Zmglu1) Beta-Glucosidase and a Model of Its Complex with P-Nitrophenyl Beta-D-Thioglucoside. **Biochemical Journal** 354(Pt 1): 37-46.

Dey, P. (1979). Transgalactosylation Activity of Sweet Almond A-Galactosidase: Synthesis of Saccharides. **Phytochemistry** 18(1): 35-38.

Dharmawardhana, D. P., B. E. Ellis and J. E. Carlson (1995). A [Beta]-Glucosidase from Lodgepole Pine Xylem Specific for the Lignin Precursor Coniferin. **Plant physiology** 107(2): 331-339.

Dixon, M. and E. Webb (1979). **Enzyme Inhibition and Activation**. 332.

Durner, J., J. Shah and D. F. Klessig (1997). Salicylic Acid and Disease Resistance in Plants. **Trends in Plant Science** 2(7): 266-274.

Escamilla-Treviño, L. L., W. Chen, M. L. Card, M.-C. Shih, C.-L. Cheng*, et al.* (2006). *Arabidopsis thaliana* Beta-Glucosidases Bglu45 and Bglu46 Hydrolyse Monolignol Glucosides. **Phytochemistry** 67(15): 1651-1660.

Esen, A. (1993). B-Glucosidase: Overview in B-Glucosidases: **Biochemistry and Molecular Biology** (Esen, A., Ed). American Chemical Society, Washington, DC. .

Henrissat, B., I. Callebaut, S. Fabrega, P. Lehn, J. P. Mornon*, et al.* (1995). Conserved Catalytic Machinery and the Prediction of a Common Fold for Several Families of Glycosyl Hydrolases. ***Agrobacterium tumefaciens*** **DNA and PS8 bacteriophage DNA not detected in crown gall tumors** 92(15): 7090-7094.

Henrissat, B. and G. Davies (1997). Structural and Sequence-Based Classification of Glycoside Hydrolases. **Current Opinion in Structural Biology** 7(5): 637-644.

Horton, P. and K. Nakai (1999). Psort: A Program for Detecting Sorting Signals in Proteins and Predictingtheir Subcellular Localization. **Trends in Biochemical Sciences** 24(1): 34-35.

Hösel, W. and W. Barz (1975). β-Glucosidases from *Cicer arietinum* L. **European Journal of Biochemistry** 57(2): 607-616.

Hrmova, M., A. J. Harvey, J. Wang, N. J. Shirley, G. P. Jones*, et al.* (1996). Barley Beta-D-Glucan Exohydrolases with Beta-D-Glucosidase Activity. Purification, Characterization, and Determination of Primary Structure from a cDNA Clone. **The Journal of Biological Chemistry** 271(9): 5277-5286.

Hrmova, M., E. A. Macgregor, P. Biely, R. J. Stewart and G. B. Fincher (1998). Substrate Binding and Catalytic Mechanism of a Barley Glucosidase/(1,4)-B-D-Glucan Exohydrolase. **The Journal of Biological Chemistry** 273(18): 11134-11143.

Jeng, W.-Y., N.-C. Wang, M.-H. Lin, C.-T. Lin, Y.-C. Liaw*, et al.* (2011). Structural and Functional Analysis of Three B-Glucosidases from Bacterium Clostridium

Cellulovorans, Fungus Trichoderma Reesei and Termite Neotermes Koshunensis. **Journal of Structural Biology** 173(1): 46-56.

Jeng, W. Y., N. C. Wang, M. H. Lin, C. T. Lin, Y. C. Liaw*, et al.* (2011). Structural and Functional Analysis of Three B-Glucosidases from Bacterium *Clostridium cellulovorans*, Fungus *Trichoderma reesei* and Termite *Neotermes koshunensis*. **Journal of Structural Biology** 173(1): 46-56.

Jenkins, J., L. L. Leggio, G. Harris and R. Pickersgill (1995). And Two Barley Glycanases Form a Superfamily of Enzymes with 8-Fold Fl / O Architecture and with Two Conserved Glutamates near the Carboxy-Terminal Ends of B-Strands Four and Seven. 362: 281-285.

Kapust, R. B. and D. S. Waugh (1999). *Escherichia coli* Maltose-Binding Protein Is Uncommonly Effective at Promoting the Solubility of Polypeptides to Which It Is Fused. **Protein Science** 8(8): 1668-1674.

Keresztessy, Z., J. Hughes, L. Kiss and M. Hughes (1996). Co-Purification from *Escherichia coli* of a Plant Beta-Glucosidase-Glutathione S-Transferase Fusion Protein and the Bacterial Chaperonin Groel. Biochemical Journal 314(Pt 1): 41.

Ketudat Cairns, J. R. and A. Esen (2010). B-Glucosidases. **Cellular and Molecular Life Sciences** 67(20): 3389-3405.

Konno, H., Y. Yamasaki and K. Katoh (1996). A B-Glucosidase Associated with Cell Walls from Cell Suspension Cultures of Carrot. **Phytochemistry** 43(6): 1157-1161.

Kroutil, L. C., K. Register, K. Bebenek and T. A. Kunkel (1996). Exonucleolytic Proofreading During Replication of Repetitive DNA. **Chemical and physical properties of aequorin and the green fluorescent protein isolated from Aequorea forskalea** 35(3): 1046-1053.

Kuntothom, T., S. Luang, A. J. Harvey, G. B. Fincher, R. Opassiri*, et al.* (2009). Rice Family Gh1 Glycoside Hydrolases with Beta-D-Glucosidase and Beta-D-Mannosidase Activities. **Archives of Biochemistry and Biophysics** 491(1-2): 85-95.

Leah, R., J. Kigel, I. Svendsen and J. Mundy (1995). Biochemical and Molecular Characterization of a Barley Seed-Glucosidase. **Journal of Biological Chemistry** 270(26): 15789-15797.

Luang, S., M. Hrmova and J. R. Ketudat Cairns (2010). High-Level Expression of Barley Beta-D-Glucan Exohydrolase Hvexoi from a Codon-Optimized Cdna in *Pichia pastoris*. **Protein Expression and Purification** 73(1): 90-98.

Lundberg, K. S., D. D. Shoemaker, M. W. W. Adams, J. M. Short, J. A. Sorge*, et al.* (1991). High-Fidelity Amplification Using a Thermostable DNA Polymerase Isolated from *Pyrococcus furiosus*. **Gene** 108(1): 1-6.

Mackenzie, L. F., Q. Wang, R. A. J. Warren and S. G. Withers (1998). Glycosynthases: Mutant Glycosidases for Oligosaccharide Synthesis. **Journal of the American Chemical Society** 120(22): 5583-5584.

Malamy, J., J. P. Carr, D. F. Klessig and I. Raskin (1990). Salicylic Acid: A Likely Endogenous Signal in the Resistance Response of Tobacco to Viral Infection. **Release of active cytokinin by a beta-glucosidase localized to the maize root meristem** 250(4983): 1002.

Mizutani, H., S. J. Degrado and A. H. Hoveyda (2002). Cu-Catalyzed Asymmetric Conjugate Additions of Alkylzinc Reagents to Acyclic Aliphatic Enones. **Journal of the American Chemical Society** 124(5): 779-781.

Opassiri, R., Y. Hua, O. Wara-Aswapati, T. Akiyama, J. Svasti*, et al.* (2004). Beta-Glucosidase, Exo-Beta-Glucanase and Pyridoxine Transglucosylase Activities of Rice Bglu1. **Biochemical Journal** 379(Pt 1): 125-131.

Opassiri, R., J. R. Ketudat Cairns, T. Akiyama, O. Wara-Aswapati, J. Svasti*, et al.* (2003). Characterization of a Rice B-Glucosidase Highly Expressed in Flower and Germinating Shoot. **Plant Science** 165(3): 627-638.

Opassiri, R., J. Maneesan, T. Akiyama, B. Pomthong, S. Jin*, et al.* (2010). Rice Os4bglu12 Is a Wound-Induced B-Glucosidase That Hydrolyzes Cell Wall-B-Glucan-Derived Oligosaccharides and Glycosides. **Plant Science** 179(3): 273-280.

Opassiri, R., B. Pomthong, T. Akiyama, M. Nakphaichit, T. Onkoksoong*, et al.* (2007). A Stress-Induced Rice (Oryza Sativa L.) Beta-Glucosidase Represents a New Subfamily of Glycosyl Hydrolase Family 5 Containing a Fascin-Like Domain. **The Biochemical Journal** 408(2): 241-249.

Opassiri, R., B. Pomthong, T. Onkoksoong, T. Akiyama, A. Esen*, et al.* (2006). Analysis of Rice Glycosyl Hydrolase Family 1 and Expression of Os4bglu12 Beta-Glucosidase. **BMC Plant Biology** 6: 33-33.

Riou, C., J. M. Salmon, M. J. Vallier, Z. Günata and P. Barre (1998). Purification, Characterization, and Substrate Specificity of a Novel Highly Glucose-Tolerant B-Glucosidase Fromaspergillus Oryzae. **Applied and Environmental Microbiology** 64(10): 3607-3614.

Schwede, T., J. Kopp, N. Guex and M. C. Peitsch (2003). Swiss-Model: An Auto-mated Protein Homology-Modeling Server. **Nucleic Acids Research** 31(13): 3381-3385.

Seshadri, S., T. Akiyama, R. Opassiri, B. Kuaprasert and J. K. Cairns (2009). Structural and Enzymatic Characterization of Os3bglu6, a Rice Beta-Glucosidase Hydrolyzing Hydrophobic Glycosides and (1->3)- and (1->2)-Linked Di-saccharides. **Plant Physiology** 151(1): 47-58.

Srisomsap, C., J. Svasti, R. Surarit, V. Champattanachai, P. Sawangareetrakul*, et al.* (1996). Isolation and Characterization of an Enzyme with Beta-Glucosidase and Beta-Fucosidase Activities from Dalbergia Cochinchinensis Pierre. **The Journal of Biochemistry** 119(3): 585-590.

Stewart, E. J., F. Åslund and J. Beckwith (1998). Disulfide Bond Formation in the *Escherichia coli* Cytoplasm: An *in Vivo* Role Reversal for the Thioredoxins. **The EMBO Journal** 17(19): 5543-5550.

Wakuta, S., S. Hamada, H. Ito, H. Matsuura, K. Nabeta*, et al.* (2010). Identification of a β-Glucosidase Hydrolyzing Tuberonic Acid Glucoside in Rice *(Oryza sativa* L.). **Phytochemistry** 71(11): 1280-1288.

Wang, Q., J. S. Dordick and R. J. Linhardt (2002). Synthesis and Application of Carbohydrate-Containing Polymers. **Chemistry of Materials** 14(8): 3232-3244.

Wang, Q., R. Graham, D. Trimbur, R. Warren and S. Withers (1994). Changing Enzymic Reaction Mechanisms by Mutagenesis: Conversion of a Retaining Glucosidase to an Inverting Enzyme. **Journal of the American Chemical Society** 116(25): 11594-11595.

CHAPTER IV

FUNCTIONAL ANALYSIS OF Os1BGlu4 IN RICE

4.1 Abstract

The transcription pattern of *Os*1*bglu*4 was studied by qRT-PCR. The results showed that the *Os*1*bglu*4 had higher expression at early stage after germination, and its expression decreased gradually to a steady level. In 14 day rice seedlings, root had the highest *Os*1*bglu*4 expression, followed by the leaf and shoot. By contrast, *Os*1*bglu*4 had the highest expression in panicle, followed by root, leaf and sheath, and no expression was detected in rice seed at booting stage (characterized by a swelling of the flag leaf sheath which is caused by an increase in the size of the panicle as it grows up the leaf sheath). The expression of *Os*1*bglu*4 was induced under both the drought and salinity stress. The *Os*1*bglu*4 expression pattern after rice blast stress was investigated extensively, the results showed that the expression of *Os*1*bglu*4 was induced to a relatively high level in the blast resistant rice NIL, and only moderately induced in the blast susceptible rice NIL. The result suggested that the *Os*1*bglu*4 may be involved in the drought, salinity and rice blast stress responses. The coding sequence of *Os*1*bglu*4 gene was cloned into the pMDC83 plant expression vector. The 3' untranslated region (UTR) sequence of *Os*1*bglu*4 was amplified and cloned into the RNAi vector pOpOff2. The pMDC83 empty vector, pMDC83-*Os*1*bglu*4 and pOpOff2-UTR were transformed into the rice cultivar *Nipponbare* by *Agrobacterium*-mediated transformation, and the T0 seeds were collected. The segregation of T-DNA in T1 seeds showed that T-DNA

segregation conformed to Mendelian genetics. The subcellular localization of Os1-BGlu4-GFP is cytosol. The activity test of pOp6 promoter in the RNAi transgenic rice showed that 30 μM DEX is necessary for strong induction of GUS activity; no GUS activtiy was detected without DEX induction. The high concentration of DEX had no significant effect to the germination rate of rice seeds. The phenotype analysis showed that the *Os*1*bglu*4 overexpression lines (oe) have more root hair than that of the wild type (wt), and *Os*1*bglu*4 gene knock down lines (RNAi) had the least root hair, when germinated in the water. Aside from the root hair in the seedling stages, there was no visible difference in the overall morphologies among wt, oe, RNAi and the transgenic rice which was transformed with the pMDC83 plant expression empty vector (vetr). Under drought and salinity stress, no visible phenotype was observed in the wt, oe, RNAi and vetr. Under rice blast stress, the oe showed higher resistance to the blast stress, the wt and vetr had moderate resistance, the RNAi line suffered severe lesions from the blast infection. In conclusion, the *Os*1*bglu*4 may involve in the blast resistance and root hair formation.

4.2 Introduction

Beta-glucosidases (β-D-glucopyranoside glucohydrolases, E.C. 3.2.1.21) are enzymes that hydrolyze glycosidic bonds to release non reducing terminal glucosyl residues from glycosides and oligosaccharides (Ketudat Cairns and Esen 2010).

In plants, these enzymes are involved in variety of processes, such as release of glucose from cell-wall derived oligosaccharides, defense against herbivores and fungi by release of toxic compounds from inactive glycosides, activation of lignin precursors in lignification, release of phytohormones from inactive glycosides, release of scent,

and general activation of glucose-blocked intermediates in metabolism (Esen 1993).

Forty rice genes homologous to GH1 β-glucosidase have been identified from rice genome databases, 34 of which are likely to form active glycosidases (Opassiri *et al.* 2006). So far, few genes were conferred biological functions experimently. The Os3BGlu7 (BGlu 1) and its close relatives Os3BGlu8 and Os7BGlu26 were found to release glucose from oligosaccharides generated in cell wall remodeling at various stages of plant development. Besides this, the possible function of Os3BGlu7 includes the release of the coenzyme pyridoxine from its glucose-conjugated storage form (Opassiri *et al.* 2003, Opassiri *et al.* 2004). Recently, Os4BGlu13 and its close relative Os4BGlu12, were found to act on tuberonic acid glucoside β-glucosidase (OsTAGG1), and Os4BGlu12 was possibly involved in defense and hydrolysis of cell wall-derived oligosaccharides during development or wounding (Opassiri *et al.* 2010, Wakuta *et al.* 2010).

Os1BGlu4, the only putative rice GH1 β-glucosidase without a secretory signal peptide, clustered with *Arabidopsis* BGlu42 and *Hevea brasiliensis* latex cyanogenic β-glucosidase, represented an independent cluster in sequence-based phylogenetic analysis. The substrates specifictiy showed rOs1BGlu4 can hydrolyze β-1,3 linked oligosaccharides with DP of 2-3, β-1,4 linked oligosaccharide with DP of 2-6, *p*-CAG, esculin and salicin, which suggested that Os1BGlu4 may be involved in various biological functions. The possible functions include defence to pathogen and herbivores, and degradation of oligosaccharides to release glucose. It is also interesting that rOs1BGlu4 can hydrolyze oligosaccharides, since it was predicted to localize in the cytoplasm.

Here, the function of Os1BGlu4 was hypothesised by transcription analysis under normal growth conditions and stress conditions, and the subcellular localization

determinated, together with the phenotype analysis of overexpression and knock-down of *Os*1*bglu*4 gene in rice cultivar *Nipponbare*.

4.3 Materials and Methods

4.3.1 Plant materials

Rice (*O. sativa* L. spp. japonica) seeds of *Nipponbare* cultivar, was provided by Professor Li Shigui from Sichuan Agricultural University, China.

4.3.2 Bacterial strains and vectors

Agrobacterium tumefaciens is a gram-negative soil bacterium that causes crown gall disease in plants by infecting cells through plant wound. *A. tumefaciens* strain EHA 105, is a virulent strain with high transformation efficiency (Nadolska-Orczyk and Orczyk 2000, Saharan *et al*. 2005). DH5α is a recombination-deficient suppressing *E. coli* strain used for plasmid cloning.

pENTR/D-TOPO (Invitrogen) was used to clone the UTR sequence of *Os*1*bglu*4 gene, and do the LR reaction with the Gateway® compatible vector pOpOff2 RNAi vectors .

The plant Gateway expression vector pMDC83, obtained from the Common- wealth Scientific and Industrial Research Organisation (CSIRO), contains a double 35S promoters and a hygromycin resistance gene for expression and selection in the plant (Curtis and Grossniklaus 2003). The pMDC83 vector contains a green fluorescence protein (GFP) gene as the reporter gene and contains a histidine tag for protein purification (Figure 4.1). It also contains the left border (LB) and right border

(RB) for *Agrobacterium* transformation into the plant genome. The attR1 and attR2 represent the recombination sites into which the target genes was recombined to replace the *ccd*B gene used for negative selection.

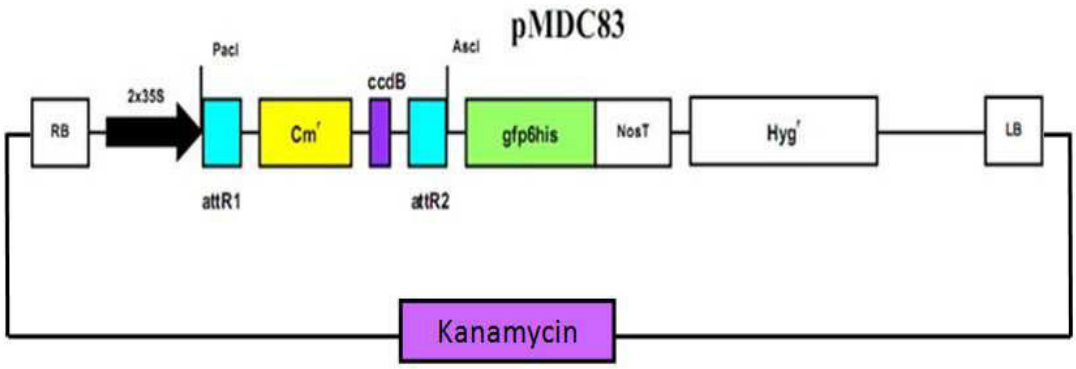

Figure 4.1 Schematic diagrams of the T-DNA of the plant Gateway expression plasmids pMDC83.

The plant RNAi gateway vector pOpOff2, obtained from CSIRO, is a vector system for dexamethasone-inducible RNAi. The production of hairpin RNAi from this system can be turned on and off by the application and removal of dexamethasone (Wielopolska *et al.* 2005). The inducibility of hairpin RNAi from this system may be very useful in helping to identify the functions of genes which when constitutively silenced give embryo lethality or complex phenotypes. The LB and RB represented the left border and right border of the vectors, the system utilizes a modified pHELLSGATE vector, under the control of the pOp6 promoter and the synthetic transcription factor, LhGR (Figure 4.2) (Wielopolska *et al.* 2005).

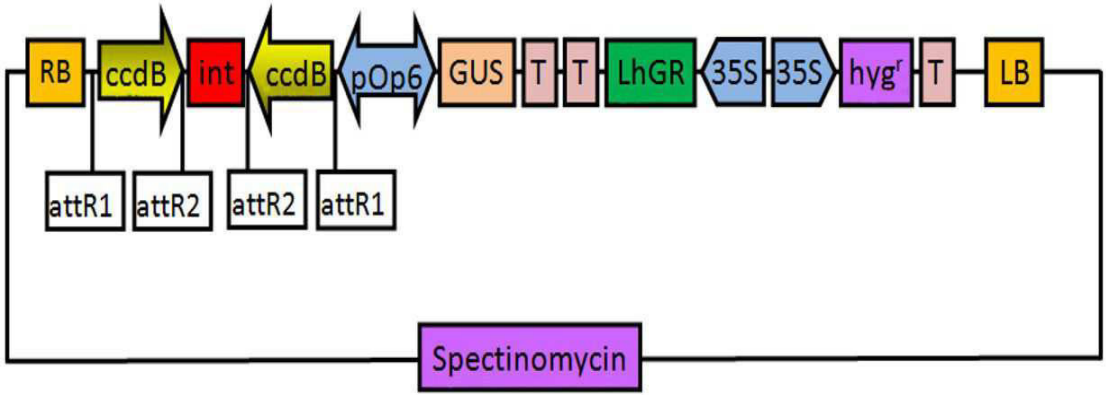

Figure 4.2 Schematic diagrams of the RNAi vector pOpOff2

4.3.3 Construction of recombinant plant expression vector

The forward primer MDC83-f (AAGTCTAGAATGGGGAGCACGGG GCGCGAC) which introduces the *Xba*I restriction site (underlined letters) and reverse primer MDC83-r (AGGGCGCGCCAGTTCATGTCAGCTTTGTTC) which introduces the *Asc*I restriction site (underlined letters), were used to amplify the *Os*1*bglu*4 coding sequence from the cDNA. The PCR product was purified by QIAquick PCR Purification Kit (QIAGEN), and cut with *Xba*I and *Asc*I. The pMDC83 vector was also cut with *Xba*I and *Asc*I, the cut pMDC83 and *Os*1*bglu*4 PCR product were ligated by T4 DNA ligase, and transformed into DH5α *E. coli* by electroporation. The positive clones were selected on 50 µg/mL kanamycin LB agar. Colony PCR was used to check the positive clone with gene specific primers. The recombinant plasmids were extracted from positive clones. Several plasmids were digested with *Hind*III and *Xho*I. Then, the correct plasmids were sent to sequence (Macrogen) to confirm the correct reading frame.

4.3.4 Construction of RNAi vector

A 373 bp long sequence of 3' untranslated region of rice *Os*1*blgu*4 gene was selected as the RNAi hairpin sequence (simplified as UTR hereafter), which was used to BLAST in the nucleotide sequence database to make sure it is unique to *Os*1*bglu*4 gene. The UTR sequence was amplified from 14 day rice seedling cDNA library, with forward primer UTR-f (CACCGCCATCCTGAAGAAAGTAAAGG), which contains the CACC for pENTR-D/TOPO recombination site, and reverse primer UTR-r (GGGCAAACCTCTGAATTTGATC), both primers are designed from the *Os*1*bglu*4 cDNA sequence, the UTR sequence was purified, and inserted into pENTR-D/TOPO Gateway entry vector by conducting TOPO reaction, and then subcloned into the pOpOff2 RNAi vector by LR Clonase reaction. pENTR/D-TOPO-UTR coiled plasmid (80 ng) and pOpOff2 (100 ng) were incubated together in a 5 μL reaction that contains 1 μL of LR Clonase™ II enzyme mix (Invitrogen). After overnight incubation at 25 ^{o}C, proteinase K (1 μg/μL) was added, the reaction was stopped by incubation at 37 ^{o}C for 10 min. The LR reaction product was transformed into DH5α *E. coli* competent cell by electroporation and positive clones was selected with 30 μg/mL spectinomycin on an LB-agar plate. Colony PCR was used to confirm the positive clone with the gene specific primer. The plasmids of positive clones were extracted and the DNA sequence was checked by *Xba*I digestion.

4.3.5 The *Agrobacterium* competent cell preparation and transformation

The *Agrobacterium* EHA 105 cells were streaked on a YEP agar (Tryptone 1 g, NaCl 0.5 g, Yeast Extract 1 g and agar 1.5 g in 100 mL H_2O) (Vega *et al.* 2008), and incubated at 28 ^{o}C for 2 days. A single colony was picked and incubated in 2 mL of

YEP medium (Tryptone 1 g, NaCl 0.5 g and Yeast Extract 1 g in 100 mL H_2O) supplemented with 50 mg/L rifampin at 28 ^oC with shaking at 200 rpm overnight. Then, 2 mL of overnight starter culture was transferred into 100 mL YEP medium, and shaken at 200 rpm at 28 ^oC until the OD_{600} of the culture reaches 0.5 (Rashid *et al.* 1996). The bacterial culture was transferred into pre-chilled centrifuge tubes and placed on ice for 15-30 min prior to centrifugation. The chilled bacterial culture was centrifuged at 4000 *g* at 4 ^oC for 8 min and supernatant was discarded as much as possible. The cell pellets was resuspended gently in 30 mL of ice-cold 10% glycerol, and centrifuged again at same speed 8 min. The supernatant was discarded and the cell pellet was resuspended in 20 mL of ice-cold 10% glycerol, and centrifuged as above. After discarding the supernatant, the cell pellet was gently resuspended again in 10 mL ice-cold 10% glycerol by pipeting, and centrifuged again at same speed 8 min, the cell pellet was resuspended with 1 mL GYT medium, and was dispensed into pre-cooled tubes as 100 µL aliquots and kept immediately at -70 ^oC.

The competent EHA 105 was thawed on ice and mixed with 150 ng pMDC83, pMDC83-*Os*1*bglu*4 and pOpOff2-UTR, respectively. The mixture was transferred to a pre-chilled electroporation cuvette and electroporated at 1800 Voltage (Electroporator, BioRad). Electroporated cells was mixed immediately with 900 µL YEP broth and incubated at 28 ^oC for 3 hr with 100 rpm revolution. After centrifugation and resuspension, the transformed cells were spread on 50 µg/mL kanamycin YEP agar and kept at 28 ^oC for 2 days for selection.

4.3.6 Callus induction of *Nipponbare* rice seed

The dehulled rice seeds of *Nipponbare* cultivar were washed with 70%

ethanol 3 min, sterilized DI H_2O washing twice, 0.1% Hg 18 min, sterilized DI H_2O washing 5 times, blotted with sterile tissue paper. The sterile seeds were put on callus induction NMB medium (pH5.8) (Appendix table 5) (Enríquez-Obregón *et al.* 1999). The sterilized seeds were placed on NMB medium and cultured at 32 ^{o}C under continuous light for 5 days (Toki *et al.* 2006). After 5 days, the calli were separated from the rice seeds and subcultured on a fresh NMB medium for another 3 days.

4.3.7 Infection of the callus

The *Agrobacterium* strain EHA 105 harboring pMDC83-*Os*1*bglu*4 and empty pMDC83 plasmids was streaked on YEP agar supplemented with 50 mg/L kanamycin and 50 mg/L rifampin. The *Agrobacterium* strain EHA 105 harboring pOpOff2- *Os*1*bglu*4-RNAi was streaked on YEP medium supplemented with 100 mg/L spectinomycin and 50 mg/L rifampin. The recombinant EHA 105 was incubated in the dark at 28 ^{o}C for 2 days. The colonies were confirmed by colony PCR.

The positive *Agrobacterium* on the YEP plate was inoculated in 3 ml YEP broth and incubated overnight at 28 ^{o}C, 200 rpm, and 1 ml of the culture was inoculated into 100 ml YEP broth which was supplemented with 25 mg/L rifampin, and incubated at 28 ^{o}C, 200 rpm until the OD600 reach 0.5. And the cell pellet was obtained by centrifugation at 3000 rpm for 8 min. The same volume of AAM (pH 5.2) (Appendix table 6) medium was used to resuspend the *Agrobacterium* cell (Hiei *et al.* 1994).

The subcultured calli were soaked in the AAM resuspended *Agrobacterium* for 18 min. The excess *Agrobacteria* on the callus surfaces was removed by blotting twice on sterile tissue paper. The calli then were transferred to co-cultivation medium (NMB, pH 5.2, supplemented with 100 μM acetosyringone) for 2 days in the dark, at 28 ^{o}C.

4.3.8 Positive callus selection

Three days later, the calli were washed to remove *Agrobacterium* with sterilized distilled water until the water turned clear, followed by 3 times of washing with sterile distilled water containing 250 mg/L cefotaxime, five min each time. The calli were blotted on sterile tissue paper and transferred to selection medium (NMB medium, supplemented with 50 mg/L hygromycin, 500 mg/L carbenicillin, 500 mg/L cefotaxime) (Nauerby *et al.* 1997), and incubated at 28 ^{o}C for about 3 weeks, in the dark.

4.3.9 Plant regeneration

After 3 weeks, surviving calli was transferred to the MS regeneration medium (Appendix table 3). The calli were cultured under 16 hr light and 8 hr dark photoperiod (Kumar *et al.* 2005), until the regenerated shoots are produced, the regenerated plants with good shoot systems was transferred to hormone-free MS medium (root medium) for root elongation and the plants were allowed to grow for an additional 2 weeks. Well-developed plantlets were put in small pot filled with soil, and in the first 7 days the plants was covered by a transparent plastic bag to maintain the moisture. After that, the plant was moved to the paddy field.

4.3.10 Transgenic rice check and T1 segregation analysis

The primer hpt-f (TACACAGGCCATCGGTCCAGA) and hpt-r (TAGGA GGGCGTGGATATGTC), which was designed to detect the DNA fragment of hygro-mycin phosphotransferase (hpt) gene, was used to check for the transgenic rice checking, the target fragment length was 832bp (Ma *et al.* 2004). The genomic DNA of

regenerated rice plantlet was extracted as DNA template to select the transgenic rice in T0 plantlet. The positive transgenic rice was planted in small pot and then paddy field until enough transgenic seed produced. The T1 generation was germinated in a growth chamber at 28 ^{o}C (SHEL LAB INCUBATOR 2020). Genomic DNA of the T1 plantlets was extracted from rice leaves to check the transgenic rice. The numbers of T-DNA negative plants and T-DNA positive plants were counted. The segregations of T1 transgenic generations were calculated according to the formula: $\chi^2 = (|A-3a|-2)^2 / 3(A+a)$ (A is the number of T-DNA positive seeds, a is the number of T-DNA negative seeds, *df* =1, α=0.05, $\chi^2_{(0.05, 1)} = 3.84$) (Xiang *et al.* 2008).

4.3.11 *Os*1*bglu*4 transcription pattern analysis

4.3.11.1 Stress treatments of rice seedlings and sample collection

Germinated seeds were placed on wet filter papers in Petri dishes and incubated in an incubator of 26 ^{o}C and 14 h/10 h (L/D) photoperiod for 14 d (Yang *et al.* 2006), and then subjected to the following treatments. Dehydration treatment was performed by transferring the seedlings to hydroponic solution supplemented with 20% PEG6000 (Liu *et al.* 2007). For salt stress, seedlings were grown in hydroponic solution containing 200 mM NaCl (Xiao *et al.* 2007). Whole seedlings were harvested at 0, 0.5, 1, 3, 6, 12 and 24 hr after initiation of each treatment (Qiu and Yu 2009). After rinsing with DI H_2O three times, the collected samples were blotted dry and stored at -70 ^{o}C until RNA extraction (Wan *et al.* 2007). For rice blast infection, the cDNA (including the blast susceptible rice near isogenic line (NIL) RD6 and blast resistant NIL 4qBL, at time point 0, 6, 12, 24, 48, 72, 96 hr and 7 days after infection) were kindly provided by Wassamol Ehkhara and Dr. James R. Ketudat-Cairns.

4.3.11.2 RNA extraction and measurement

Total RNA was extracted from different part of wild type *Nipponbare* cultivar (leaves, shoots and roots) at various growth stages with Trizol reagent accroding to the instructions of manufacture (Invitrogen). Total RNA was extracted from wild type and transgenic rice leaves at appropriate time points after different stress treatments. About 100 mg rice leaf, root or shoot was homogenized with liquid nitrogen in a mortar. TRIzol (Invitrogen) (1 mL) was added to the sample and thoroughly mixed. Chloroform (200 μL) was added to the sample and shaked vigorously by hand for 15 seconds and incubated at room temperature for 3 min. Centrifuge the tube at 12,000 rpm for 10 min at 4 ^{o}C. The aqueous phase was transferred to a new tube, 0.5 mL isopropanol was added to precipitate the RNA, and centrifuged at 12,000 *g* at 4 ^{o}C for 10 min. The supernatant was discarded and 1.2 mL of 75% ethanol was added to wash the RNA by vortex, and centrifuged at 8000 *g* for 5 min at 4 ^{o}C. The supernatant was discarded and the RNA pellet was dried. RNase free DI H_2O (30 μL) was added to dissolve the RNA and stored at -80 ^{o}C. Twenty μg aliquots of total RNA from each sample was denatured and electrophoresed on formaldehyde 1.2% agarose gel.

4.3.11.3 Reverse Transcription

Reverse transcription was carried out with the SuperScript™ III first-strand synthesis system for Real Time-PCR following the procedure of Invitrogen. Two microliters of total RNA, 1 μL oligo dT (20) (50 μM), 1 μL 10 mM dNTP mix and DEPC H_2O to 13 μL were mixed to make RNA/primer mixture, incubated at 65 ^{o}C for 5 min and then on ice for at least 1 min, 5x first strand buffer 4 μL, 0.1 M DTT 1 μL,

RNaseOUT 1 µL and 1 µL (200 units) of SuperScript™ III Reverse Transcriptase were added to the RNA/primer mixture, mixed briefly, and then incubated the tubes at 55 ^{o}C for 1.5 hr, heated to inactivate at 80 ^{o}C for 15 min, and then chilled on ice. The 1st strand cDNA was stored at -20 ^{o}C until use for real-time PCR.

4.3.11.4 Real-Time PCR

The *Os*1*bglu*4 qRT-PCR primers, RT-f (GTGGAGAGAATAGA AAAATGG) and RT-r (CTCATCCATGCCATTCTCAG), template were designed to avoid genomic DNA contamination in the cDNA by overlapping separate exons of the *Os*1*bglu*4 gene to detect the presence of the *Os*1*bglu*4 cDNA. The actin (Actin-f: TGC TATGTACGTCGCCATCCAG, Actin-r: AATGAGTAACCACGCTCCGTCA) (Dai *et al*. 2007) and ubiquitin (Ubi-f: CACGGTTCAACAACATCCAG, Ubi-r:TGAAGACC CTGACTGGGAAG) primers (Ryu *et al.* 2009) were compared to select the better reference gene. The result showed that the actin has similar size and amplification efficiency as the RT primer of *Os*1*bglu*4 (Figure 4.40). Therefore, the actin primers were used in this experiment. The reaction consist of 10 µL of 2× kapa SYBR FAST qPCR Master Mix, 1 µL 2 µM RT-f and RT-r, 1:20 diluted cDNA template and H_2O to 20 µL. The cDNA copy number was detected using a Bio-Rad Chromo4 real-time PCR detection system (Bio-Rad, CA, USA). The PCR reaction was initiated with denaturation at 95 ^{o}C for 3 min, followed by 35 cycles of denaturation at 95 ^{o}C for 30 sec, annealing at 60 ^{o}C for 30 sec and extension at 76 ^{o}C (for RT primer) or 81 ^{o}C (for *Actin* primer) for 15 sec, the fluorescence signal was read at the end of each extension step. Subsequently, a melting curve was generated by heating (1 ^{o}C /s) the PCR products from 50 ^{o}C to 95 ^{o}C to determine the specificity of the PCR products. The PCR product

was examined by 2% agarose gel using 8 μL aliquot from each reaction. The real-time PCR result was analyzed using the C_T values according to the the $2^{-\Delta\Delta C}{}_T$ Method (Livak and Schmittgen 2001).

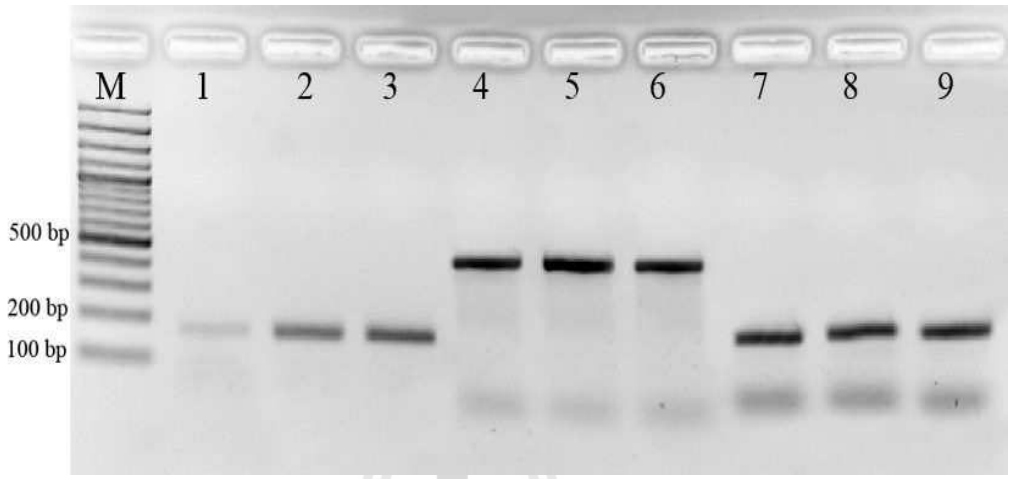

Figure 4.3 The selection of reference gene. M, 100 bp DNA marker, lanes 1, 2 and 3 showed 12, 8 and 4 day seedlings cDNA amplified with RT-f and r primers, respectively. Lanes 4, 5 and 6 show 12 day, 8 day and 4 day seedlings cDNA amplified with ubiquitin primers. Lanes 7, 8 and 9 show 12 day, 8 day and 4 day seedlings cDNA amplified with *Actin* primers.

4.3.12 Os1BGlu4 β-glucosidase localization

4.3.12.1 Protoplast extraction

Dehulled seeds of rice cultivar *Nipponbare* were sterilized with 75% ethanol for 1 min. These seeds were further sterilized with 2.5% sodium hypo-chlorite for 20 min, washed at least five times with sterile water and then incubated on 1/2 MS medium with a photoperiod of 12 hr light (about 150 $\mu molm^{-2}s^{-1}$) and 12 hr dark at 26 ^{o}C for 7-10 days. Etiolated tissues from the stem and sheath of 60 rice seedlings

were used. A bundle of rice plants (about 30 seedlings) were cut together into approximately 0.5 mm strips each time with propulsive force using sharp razors. The strips were immediately transferred into 0.6 M mannitol for 10 min in the dark. After discarding the mannitol, the strips were incubated in an enzyme solution (1.5% Cellulase RS, 0.75% Macerozyme R-10, 0.6 M mannitol, 10 mM MES at pH 5.7, 10 mM $CaCl_2$ and 0.1% BSA) for 4-5 hr in the dark with gentle shaking (60 rpm). After the enzymatic digestion, an equal volume of W5 solution (154 mM NaCl, 125 mM $CaCl_2$, 5mM KCl and 2 mM MES at pH 5.7) was added, followed by vigorous shaking by hand for 10 sec. Protoplasts were released by filtering through 40 μm nylon meshes into round bottom tubes with 3-5 washes of the strips using W5 solution. The pellets were collected by centrifugation at 1,500 rpm for 3 min with a swinging bucket. After washing once with W5 solution, the pellets were then resuspended in MMG solution (0.4 M mannitol, 15 mM $MgCl_2$ and 4 mM MES at pH 5.7) at a concentration of 2×10^6 cells/mL (Zhang *et al.* 2011).

4.3.12.2 Protoplast transfection

PEG-mediated transfections were carried out as described (Yoo *et al.* 2007). Briefly, for each sample 5-10 μg of plasmid DNA (pMDC83-*Os*1*bglu*4 and pMDC83-*Os*4*bglu*18, obtained from S. Baiya) were mixed with 100 μL protoplasts (about 2×10^5 cells). Freshly prepared PEG solution [40% (W/V) PEG 4000; 0.2 M mannitol and 0.1 M $CaCl_2$] (110 μL) were added, and the mixture was incubated at room temperature for 10-20 min in the dark. After incubation, 440 μL W5 solution was added slowly. The resulting solution was mixed well by gently inverting the tube, and the protoplasts were pelleted by centrifugation at 1,500 rpm for 3 min. The protoplasts were resuspended gently in 1 mL WI solution (0.5 M mannitol, 20 mM KCl and 4 mM

MES at pH 5.7). Finally, the protoplasts were transferred into multi-well plates and cultured under light or dark at room temperature for 6-16 hr.

4.3.12.3 Fluoresence microscope

Protoplasts were observed using a fluorescence microscope (Olympus IX71) and visualized by a digital microscope camera (Olympus DP70). GFP was excited at 488 nm wavelength. The emission filters used were 500-530 nm for GFP. The localization of Os4BGlu18-GFP was used as reference. All fluorescence experiments were repeated independently at least three times.

4.3.13 The activity of pOp6 promoter determination

The pOp6 promoter in the pOpOff2 RNAi vector drives both the hairpin sequence and GUS gene. The GUS activity can be an assessment of the pOp6 promoter. The 14 day RNAi line seedlings were incubated with or without DEX for 12 hr, the wild type was used as negative control. The GUS activity under 10 μM and 30 μM final concentration of DEX was compared. Expression of GUS in rice cells was assayed as described by (Rueb and Hensgens 1989) with 5-bromo-4-chloro-3-indolyl glucuronide (X-Gluc) as substrate. Rice tissues were incubated in phosphate buffer (50 mM $NaPO_4$, pH 6.8) contained 1% Triton X-100 at 37 ^{o}C for 1 hr. The buffer was removed and fresh phosphate buffer containing 1.0 mM X-Gluc and 20% methanol was added to the seedlings. The reaction mixture was placed under a mild vacuum for 5 min, incubated overnight at 37 ^{o}C, and then tissues were examined visually. Cells that expressed GUS were dark blue. Seedlings were washed twice in 99% methanol for 2 hr before the visual examination (Hiei *et al.* 1994). The effect of different concentration of DEX was

also determined by qRT-PCR. The 14 days RNAi line seedlings were incubated with 0, 10 and 30 μM DEX repectively, after 12 hr incubation, the seedlings was washed and used for RNA extraction. The *Os*1*bglu*4 expression of 0 μM DEX treatment was used as calibrator.

The effects of DEX and ethanol on the germination of rice seeds were also determined. Wild type seeds and RNAi seeds were used in the experiment. Each type seeds was germinated in DI H_2O or DI H_2O supplemented with 30 μM DEX, about 50 seeds were used in each treatment, 3 replicates.

4.3.14 Phenotype analysis

4.3.14.1 Overall morphology analysis

The well-established transgenic rice plant (T0) was planted in soil, until it produced enough seeds. The T1 seeds (wt, oe, RNAi and vetr) were germinated in growth chamber for 14 days at 28 ^{o}C under 14 hr/10 hr light/dark condition. The RNAi line seeds were supplemented with 30 μM DEX to induce the knockdown of the *Os*1*bglu*4 gene every 4 days. After 14 days, the seedlings were transferred to soil pot and grown at 26 ^{o}C under 14 hr/10 hr light/dark condition until mature, since then, the addition of the 30 μM DEX to the RNAi line seedlings stopped because of the huge expense of DEX, except once at the booting stage, which was done to investigate the effect of *Os*1*bglu*4 to the development of the flower and seed. The heights of rice and root length were measured at various time points, and the overall morphology was recorded.

4.3.14.2 Root hair phenotype analysis

The root hair of 14 day rice seedlings of all transgenic lines and wt were checked and photographed. The *Os*1*bglu*4 expression was checked by qRT-PCR using wt root *Os*1*bglu*4 expression as calibrator. The seeds were also germinated in 1/2 MS medium, after 14 days, the root hair of each line was also checked. To further prove that the *Os*1*bglu*4 involved in the root hair formation, the wt root was grouped to two types, one with more root hair (Mrh), the other with less root hair (Lrh), and the expression of *Os*1*bglu*4 was checked by qRT-PCR.

4.3.14.3 Phenotype analysis under abiotic stress

To simulate the stress conditions, the 14 day rice seedlings were transferred to 1/2 MS medium, 10% PEG 6000 was added to simulate the drought stress (Lian *et al.* 2004), 100 mM NaCl was added to simulate salinity stress (Lutts *et al.* 2002), after 3 days, the symptom was checked, and after washing with DI H_2O, the total RNA of seedlings were extracted, and the *Os*1*bglu*4 exression was determined. The water loss percentage was measured by weighing the seedlings before and after the abiotic stress treatments (Qiu and Yu 2009).

4.3.14.4 Phenotype analysis under rice blast stress

For making the rice blast stress, the concentration of the conidia of *Magnaporthe grisea* [Blast THL 810 (collected from Ubon Ratchathani, Thailand)] suspension was adjusted to 5×10^5/ml with 0.2% gelatin solution, and 4 mL of the *Magnaporthe grisea* suspension was used to inoculate 14-day-old rice seedlings using sprayer (Chen *et al.* 2010). Plants were covered with plastic bags during inoculation

and for 24 hr after inoculation in order to maintain humidity. After 24 hr the plants were removed from the bags and placed in a chamber at room temperature (lab environment). After 7 days the seedlings were inspected for disease symptoms (Hamer *et al.* 1989, Jarosch *et al.* 1999), the lesion spots were evaluated and recorded principally according to the method of Valent and Chumley (1991), the spots were classified to big spots and small spots according to 1 mm diameter. The spots were counted based on three seedling leaves, three replicates. After washing with DI H_2O, total RNA of leaves was extracted, and the *Os*1*bglu*4 expression was determined.

4.4 Result and Discussion

4.4.1 The construction of plant overexpression vector pMDC83-*Os*1*bglu*4

The PCR product in Figure 4.3 has a intense band at near 1.5 kb, it is the expected size (1463 bp) of coding region of the *Os*1*bglu*4. Colony PCR indicated that most clones were positive clones (Figure 4.4). The pMDC83-*Os*1*bglu*4 was checked, the results showed that all plasmids checked were correct (Figure 4.5), then; the sequences of these constructs were check by sequencing. The sequence analysis comfirmed that correct open reading frame of Os1BGlu4 was fused to GFP protein (Figure 4.6).

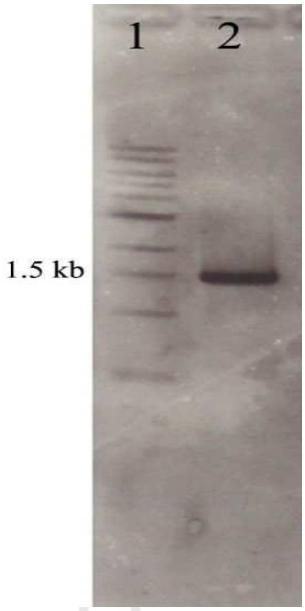

Figure 4.4 The PCR product of amplification of coding sequence of *Os*1*bglu*4 using the pET32-*Os*1*bglu*4 as DNA template, with MDC83-f and MDC83-r primer. Lane 1, 1 kb DNA marker, lane 2, PCR product.

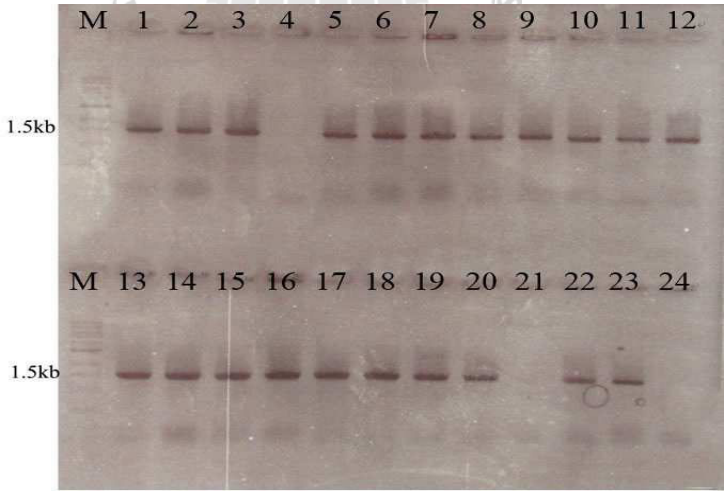

Figure 4.5 The PCR product of colony PCR, with MDC83-f and MDC83-r primer. M, 1.5 kb DNA marker, lane 1-22, colony PCR product, lane 23, positive control, lane 24, negative control.

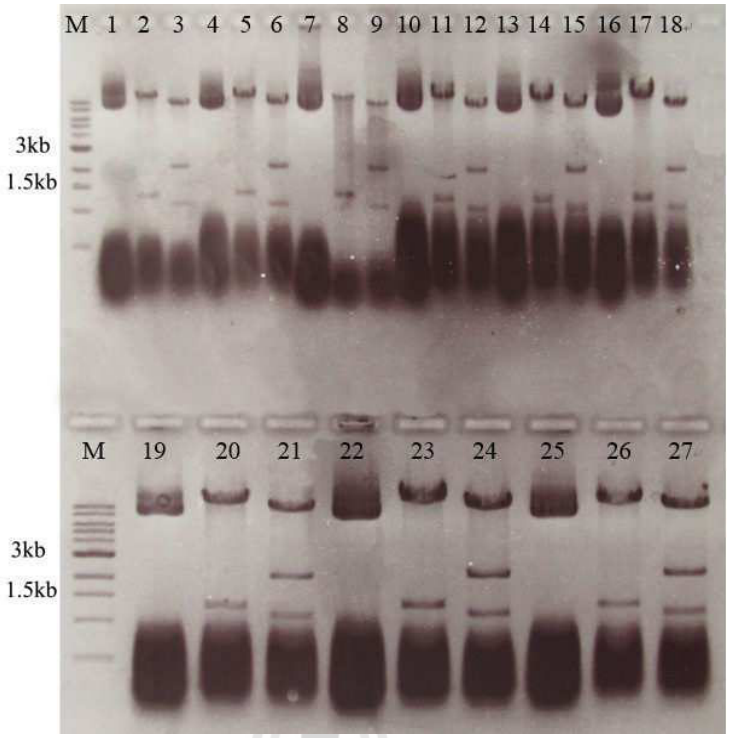

Figure 4.6 Plasmids (pMDC83-*Os*1*bglu*4) were digested by *Hind*Ⅲ and *Xho*I. M, 1 kb DNA marker, lanes 1, 4, 7, 10, 13, 16, 19, 22, 25 plasmids. Lanes 2, 5, 8, 11, 14, 17, 20, 23, 26, corresponding plasmids digested with *Hind*Ⅲ. Lanes 3, 6, 9, 12, 15, 18, 21, 24 and 27, corresponding plasmids digested with *Xho*I.

Figure 4.7 The sequence analysis of recombinant pMDC83 vector. ATG showed the start of *Os*1*bglu*4 and GFP, respectively. The dark region indicated the correct amino acid codon and open reading frame of the GFP protein. The underlined letters are restriction sites of *Xba*I and *Asc*I, respectively. A: Sequence of recombinant pMDC83. B: Diagram of pMDC83.

4.4.2 The construction of RNAi vector pOpOff2-UTR

The UTR sequence was amplified from the genomic DNA of rice seedlings. Figure 4.7 showed a intense band at near 400 bp, it is the size of expected (373 bp) UTR sequence of *Os*1*bglu*4. The PCR product was cloned into the pENTR-D/TOPO, and the reaction product was transformed into the DH5α. Colony PCR check with gene specific primer indicated that all checked clones were positive clones (Figure 4.8). The pENTR-D/TOPO-UTR plasmid was extracted and recombined with the pOpOff2, the reaction product was transformed into the DH5α. Colony PCR showed 5 clones were correct (Figure 4.9), and the plasmids were extracted and digested with *Xba*I, the expected size of *Xba*I digestion are about 12 kb, 5.2 kb, 1.8 kb, 1.5 kb, 0.8 kb and 0.37 kb (Figure 4.10 B). Figure 4.10 A shows that plasmid No. 10 and No. 13 were basically correct, except for a 0.47 kb band which was predicted to be 0.37 kb. Maybe the UTR sequence have the problem, therefore, the sequence of pENTR/D/TOPO-UTR were checked, the result showed that the UTR sequence in the pENTR/D/TOPO-UTR plasmid was correct, and the size of UTR region was 0.37 kb (Figure 4.10 C). Maybe the *Xba*I cutting sites between the 'int' and the 'RB' have the extra nucleotides sequence besides the UTR sequence. So, the effect of hairpin RNA in the RNAi vector had to be determined further in the transgenic plant by qRT-PCR. The results showed that the hairpin RNA was active in the RNAi transgenic rice (Figure 4.28).

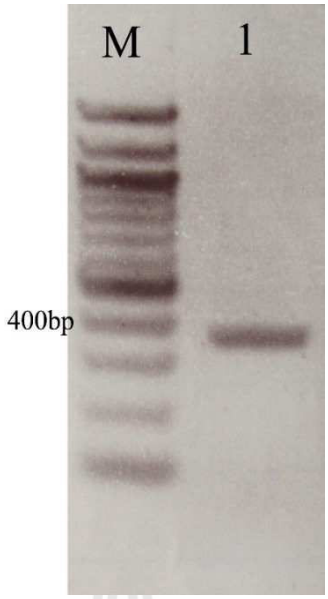

Figure 4.8 The UTR amplicon from *Os*1*bglu*4, M, 100 bp DNA marker, lane 1, PCR product.

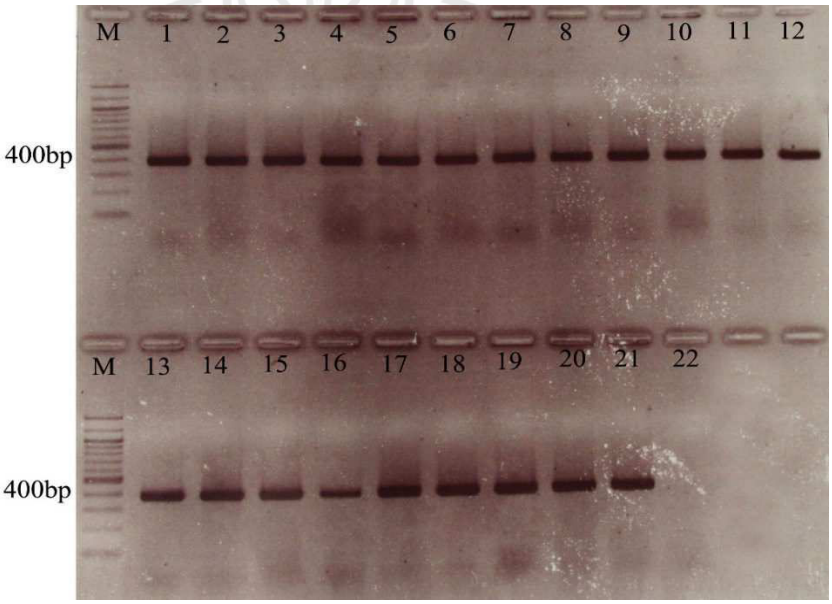

Figure 4.9 The result of colony PCR for the pENTR-D/TOPO-UTR with the gene specific primers. M, 100 bp DNA marker, lane 1-20, colony numbers, lane 21, positive control, lane 22, negative control.

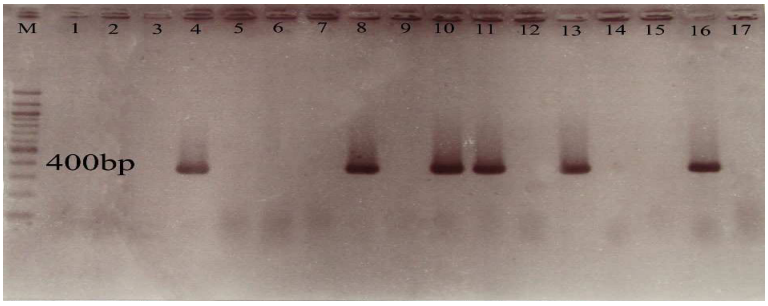

Figure 4.10 The result of colony PCR for the pOpOff2-UTR with the gene specific primers. M, 100 bp DNA marker, lane 1-14, colony numbers, lane 15, pOpOff2 empty vector as DNA template, lane 16, positive control, lane 17, negative control.

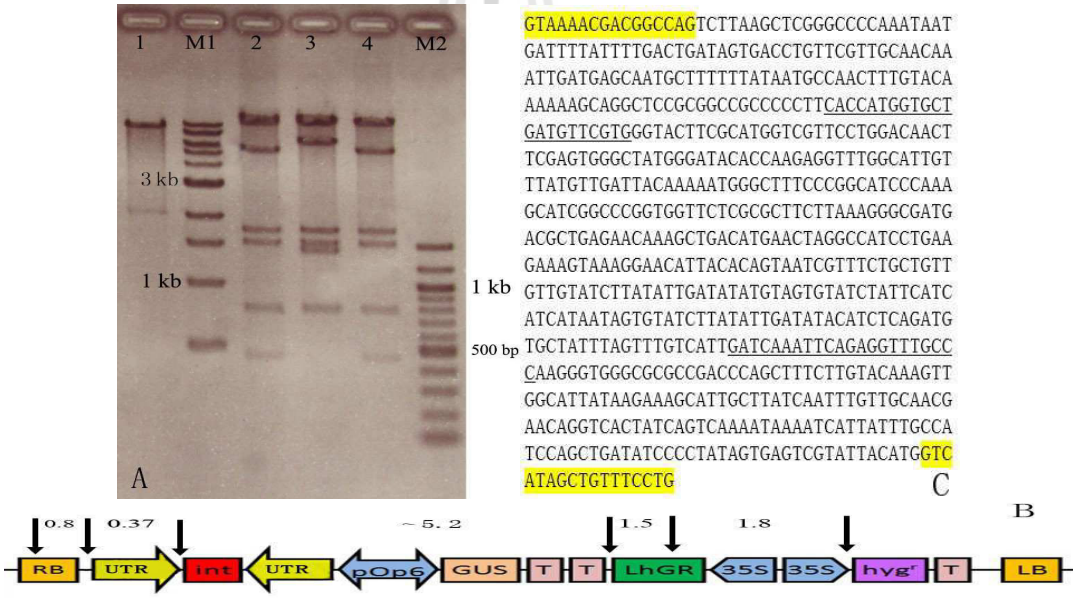

Figure 4.11 The DNA fragments of pOpOff2-UTR plasmids digested with *Xba*I. A: plasmids digested with *Xba*I. M1, 1 kb DNA marker, M2, 100 bp DNA marker, lane 1, plasmid No. 8, lane 2, plasmid No. 10, lane 3, plasmid No. 11 and lane 4, plasmid No. 13. B: The cutting site and size of *Xba*I digestion. C: UTR sequence of *Os*1*bglu*4 in the pENTR/D/TOPO. Yellow shaded letters are M13-f, M13-r primer region. Underlined letters are the UTR-f, UTR-r primer region.

4.4.3 The production of transgenic rice

Both the pOpOff2-UTR and pMDC83-*Os*1*bglu*4 were transformmed into *Agrobacterium* EHA105. The recombinant *Agrobacterium* was comfirmed by colony PCR by gene specific primers.

Nipponbare rice seed after about 1 week's incubation generated small calli (Figure 4.11), the calli were subcultured into fresh callus induction medium for 3 more days, then, the calli (Figure 4.12) were used for infection. The scutellum tissue from 1-day pre-cultured seeds has been reported to be capable for *Agrobacterium*-mediated transformation (Toki *et al.* 2006). However, for the 1-day pre-cultured seeds, the calli were very small, very difficult to manipulate to cut the calli off the seed, therefore, 1 week old calli-seed complexes were used to isolate the calli. Early infection of rice seeds also enhanced efficient selection of transformed calli and reduced the possibility of somaclonal variation accompanying prolonged culture of rice cells in the dedifferentiated state (Toki *et al.* 2006).

Figure 4.12 Small calli of *Nipponbare* rice seed. The circle showed the callus part of the seeds.

Figure 4.13 The subcultured calli ready for *Agrobacterium* infection.

The *Agrobacterium* infected calli were placed onto the co-culture medium and kept in the dark for 3 days then transferred to hygromycin selection medium. After 5-7 weeks, some of the calli became brown or black (Figure 4.13). Only yellow calli were transferred to regeneration medium. After about 4 weeks of incubation, some of the calli generated small shoots (Figure 4.14). The green shoot was transferred to rooting medium to generate roots. About 1 week, roots generated from some of the plantlets (Figure 4.15). When the roots became prosperous (Figure 4.16), the plantlets were pulled out of the medium; the root was washed clean with water. Then, the seedlings were transferred to new flask, incubated with water. The flask was moved outside of the green house for about 1 week to help the transgenic seedlings adapt to the natural environment before planting in paddy field. The transgenic rice leaves were cut, and genomic DNA (gDNA) was extracted from the leaves. The gDNA was used as template to amplify the hygromycin phosphotransferase (hpt) gene fragment to check if they were real transgenic rice. Parts of the results were shown in Figure 4.17. The hpt gene positive plantlets were planted in the paddy field to produce T0 generation seeds (Figure 4.18), after 4 months of growth, the transgenic plants were mature (Figure 4.19), and the seeds of T0 generation were collected.

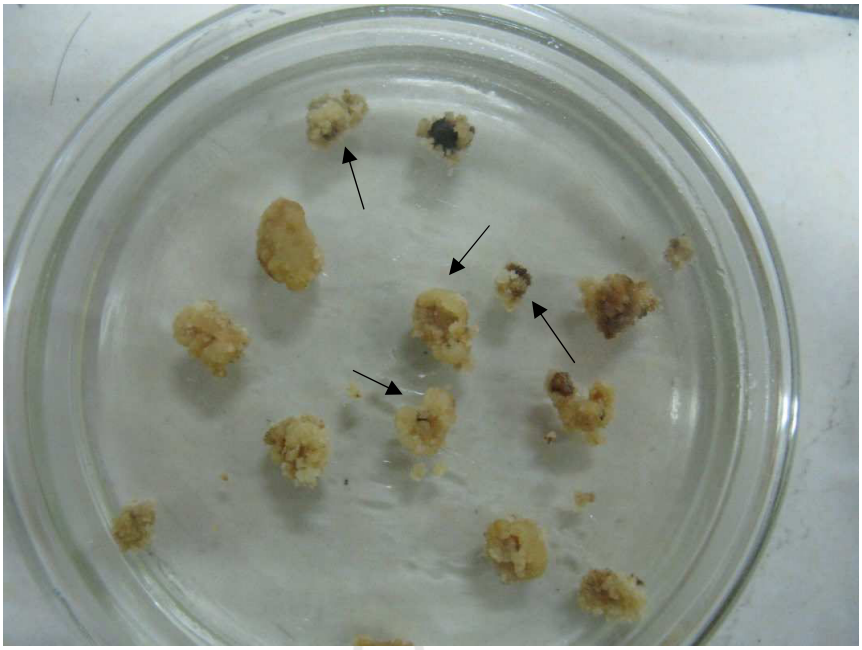

Figure 4.14 The calli after hygromycin selection for 5-7 weeks. The black arrow point to the black or brown calli.

Figure 4.15 The calli generated small shoots.

Figure 4.16 Roots were generated from small plantlets.

Figure 4.17 The root of the transgenic rice grows prosperously in root medium.

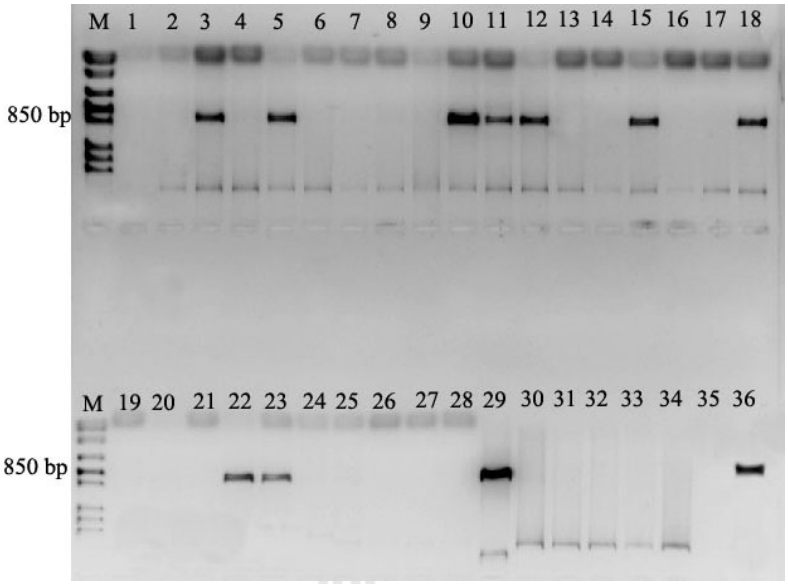

Figure 4.18 T0 generation trsangenic rice seedlings check with *hpt* gene primers. M, DNA marker, lane 1-34, transgenic gDNA numbers, lane 35, negative control, lane 36, positive control.

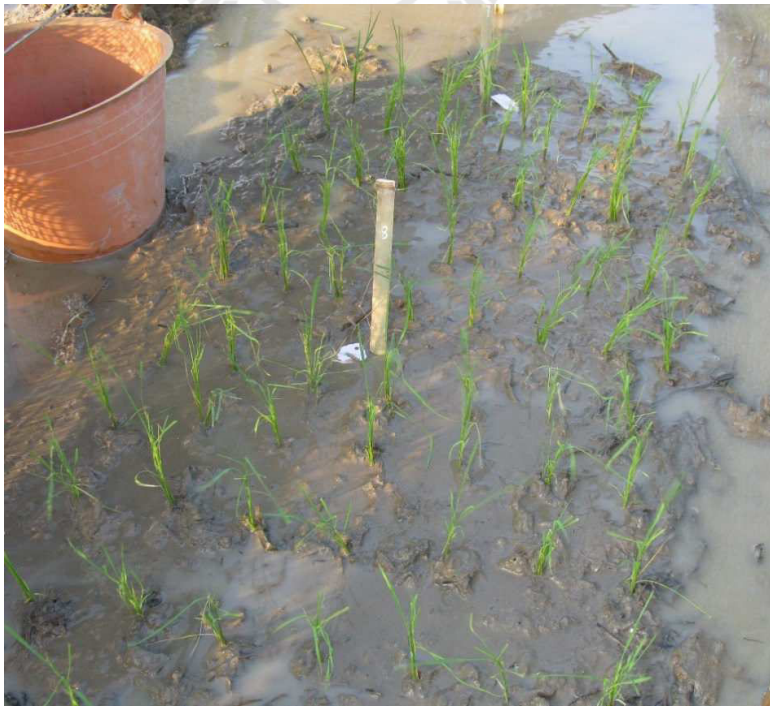

Figure 4.19 The transgenic rice was planted into paddy field.

Figure 4.20 The transgenic rice becomes mature after 4 months of growth.

4.4.4 T-DNA segregation analysis in T1 generation

The gDNAs of overexpression lines and RNAi lines were extracted from the T1 rice seedling leaves. The hpt primer was used to amplify the hpt fragment from the gDNA. The results showed 27 rice seedlings among 38 were hpt positive for the overexpression lines (Figure 4.20), the $\chi^2 = 0.14$, less than 5% signifiance level (3.84), which indicated that the segregation of T-DNA in T1 generation for the overexpression lines conformed to the 3:1 Mendelian genetics. Among 44 rice seedlings, 30 were *hpt* positive for the RNAi lines (Figure 4.21), the $\chi^2 = 0.76$, less than the 5% signifiance level (3.84), which indicated that the segregation of T-DNA in T1 generation for the RNAi lines conformed to the 3:1 Mendelian genetic ratio. The result is similar with the former reseach conclusion that the progeny derived from transformed plants inherited the foreign gene in a Mendelian manner (Thiery *et al.* 1978, De Block *et al.* 1984, Budar *et al.* 1986).

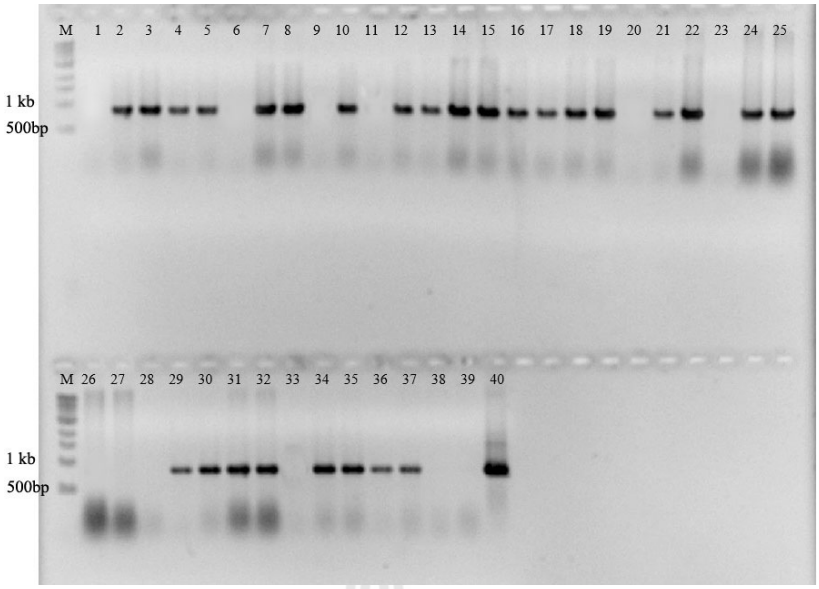

Figure 4.21 PCR product of amplification with the *hpt* primers using gDNA as template. M, 1 kb DNA marker, lane 1-38, gDNA extracted from T1 rice leaves. Lane 39, negative control, lane 40, positive control.

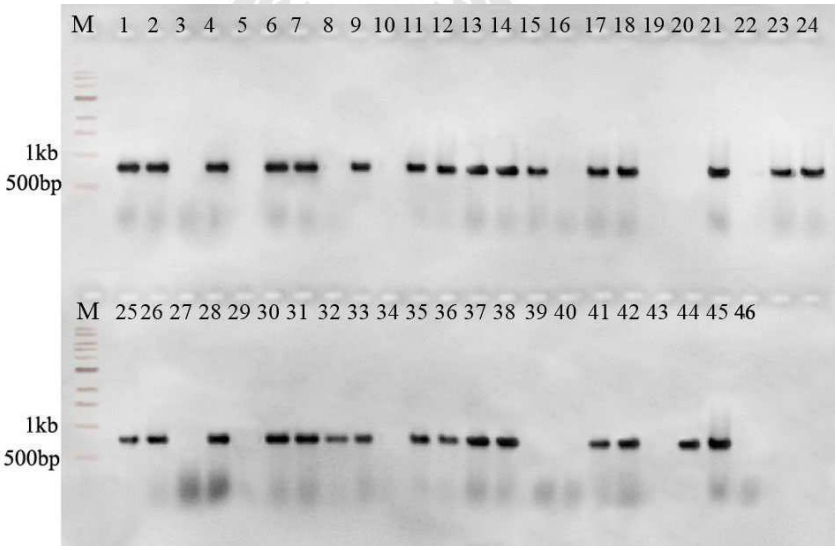

Figure 4.22 PCR product of amplification with the hpt primers using RNAi lines gDNA as template. M, 1 kb DNA marker, lane 1-44, gDNA extracted from T1 rice leaves. Lane 45, positive control, lane 46, negative control.

4.4.5 Transcription pattern analysis

4.4.5.1 The spatial and temporal expression of *Os*1*bglu*4 gene

The total RNA from various rice samples were extracted, reverse transcribed to cDNA, the *Os*1*bglu*4 expression was measued by real time PCR, relative to actin reference. The temporal expression of *Os*1*bglu*4 was checked using the 14 day seedling as the calibrator (Figure 4.22). The results indicated that after germination, the *Os*1*bglu*4 have higher expression at day 2 and day 4, moderate expression at day 6 and 8 after the green shoot appeared, and decreased to a steady level after day 8.

The spatial expression of *Os*1*bglu*4 was checked using the 14 day seedling leaf *Os*1*bglu*4 expression as calibrator (Figure 4.23). The result showed that 14 day seedlings had the highest expression level in root, and a low level in the stem. In booting stage rice, expression of *Os*1*bglu*4 was detected in high level in panicle, moderate levels in root, leaf and sheath, and low level in stem. The overall expression pattern of *Os*1*bglu*4 was similar to their representation in the EST database (http://www.ncbi.nlm.nih.gov/UniGene/ESTProfile\Viewer). The *Os*1*bglu*4 expression was higher in the young seedling root than that in the booting stage rice, which indicated that *Os*1*bglu*4 may play a more important role in the root development at early stages of rice growth. Unlike *Os*1*bglu*4, rice *Os*3*bglu*7 expressed highly in the germinating shoot and flower and its product enzyme, may act in hydrolysis and recycling of oligo-saccharides generated from rapid cell wall expansion during seed germination and flower expansion (Opassiri *et al.* 2003). Another cell wall related β-glucosidases *Os*4*bglu*12 has high levels of transcription in the shoot during germination, in the leaf sheath and stem of mature rice plants under normal growth conditions (Opassiri *et al.* 2010). The different levels of transcription in different parts of plant between *Os*1*bglu*4, *Os*3*bglu*7 and *Os*4*bglu*12 may reflect the different biological functions.

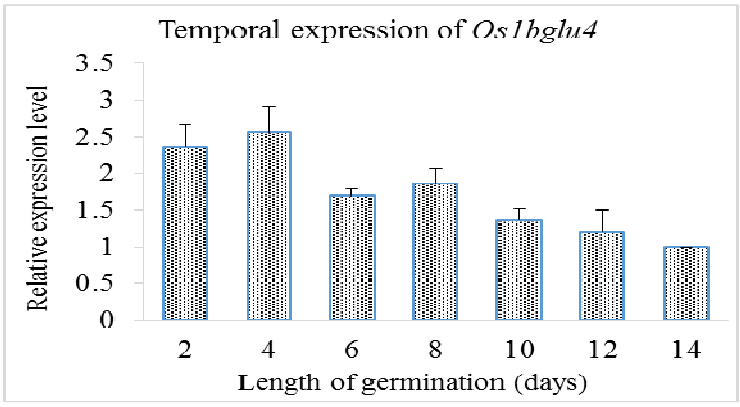

Figure 4.23 Real-time PCR of *Os*1*bglu*4 showing expression at different germination times. The 14 day seedling *Os*1*bglu*4 expression was used as calibrator. Data are given as the mean±S.E. The experiment was repeated in triplicate with similar results.

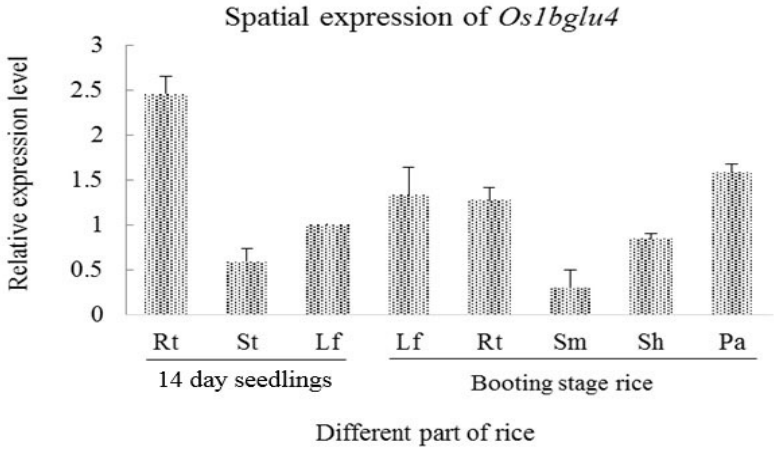

Figure 4.24 Real-time PCR of *Os*1*bglu*4 showing tissue specific expression. The 14 day seedling leaf *Os*1*bglu*4 expression was used as calibrator. Three tissues are from 14 day seedling, including Rt, root, St, shoot and Lf, Leaf. Six tissues are from mature rice at booting stage, including Lf, leaf, Rt, root, Sm, stem, Sh, sheath, Pa, panicle. Data are given as the mean+S.E. The experiment was repeated in triplicate.

4.4.5.2 The expression of *Os*1*bglu*4 gene under abiotic stress

The expression of *Os*1*bglu*4 under PEG and NaCl stress were investigated. The *Os*1*bglu*4 expression in 14 day seedlings without treatment was used as the control. Figure 4.24 shows that the NaCl treatment induced the expression of *Os*1*bglu*4 to 2 fold more than the control after 1 h, the expression reach the peak after 30 min to 1 h, and decreased gradually to a steady state from 3 to 24 hr. In contrast, the relative *Os*1*bglu*4 expression of control closed to 1 at the designated time points. The initial differences between control and stressed plants continued for hours but became less pronounced as the plants adapted over time. The interpretation of an adaptive process was supported by the similar analysis of salinity-sensitive rice (Kawasaki *et al.* 2001). PEG treatment trigered the highest expression of *Os*1*bglu*4 to 2.5 fold more than that of the control, the peak point was 1 h after PEG treatment, the expression decreased gradually after 1 hr of incubation, but stayed higher expression than that of the control. The inducible nature of *Os*1*bglu*4 by abiotic stress suggested that it is at least partially involved in the drought and salinity stress resistance of rice. The transcript level of *Os*4*bglu*12 was found to be induced in response to herbivore attack and salinity stress (Kawasaki *et al.* 2001, Wang *et al.* 2005), which indicated that both *Os*1*bglu*4 and *Os*4*bglu*12 involve in salinity stress response.

4.4.5.3 The expression of *Os*1*bglu*4 gene after blast stress

The EST database showed that *Os*1*bglu*4 was expressed after blast infection (Opassiri *et al.* 2006), which triggered the hypothesis that *Os*1*bglu*4 is involved in blast resistance. The expression of *Os*1*bglu*4 after blast stress was extensively investigated using both the blast susceptible RD6 near isogenic line

(NIL) and the resistant NIL 4qBL at various time points. The *Os*1*bglu*4 expression of RD6 at time 0 were used as calibrator.

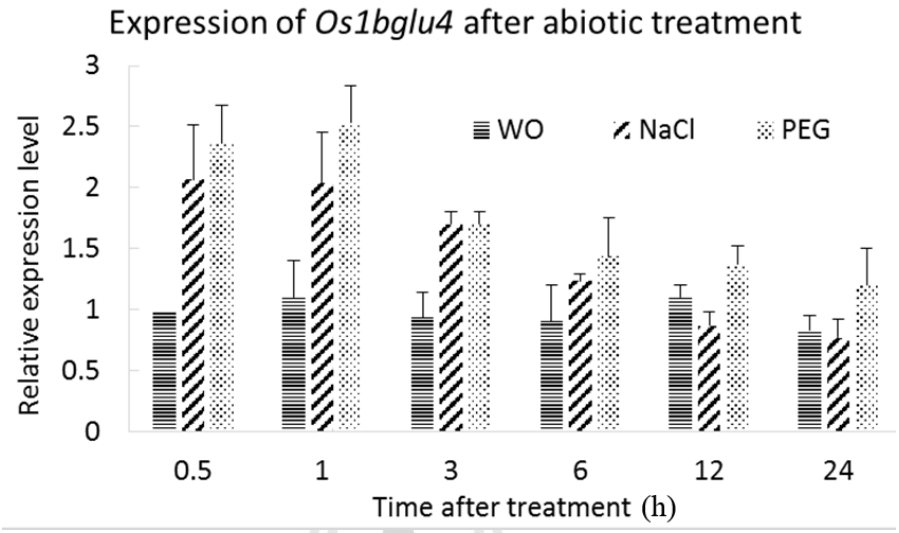

Figure 4.25 Real-time PCR of *Os*1*bglu*4 showing abiotic treatment expression. The 14 day seedlings *Os*1*bglu*4 expression without treatment was used as calibrator. WO, the plant without treatment, NaCl, 200 mM NaCl, PEG, 20% PEG6000. Data are given as the mean+S.E. The experiments were repeated in triplicate.

Figure 4.25 shows that the expression of *Os*1*bglu*4 was induced in both blast susceptible and resistant rice NIL 6 hr after the infection, however, the expression increased 7.7 fold in the blast resistant cultivar but only a 2.8-fold increase was observed in the blast susceptible rice cultivar. The highest *Os*1*bglu*4 expression was observed at 12 hr after blast stress, 22 fold higher expression was found in the blast resistant NIL, while only 6.37 fold was found in the blast susceptible NIL. The high expression continued until 24 hr in both cultivars, and decreased dramatically in the

blast susceptible NIL, but still remained much higher than the blast susceptible rice NIL. The expression of *Os*1*bglu*4 in the blast resistant rice cultivar had almost 2 fold more expression than the susceptible NIL, even 96 hr after the blast stress, after which it decreased to normal expression level. For temporal expression without blast infection, the *Os*1*bglu*4 expressed about 0.9-1.5 fold in both NIL, the expression of blast resistant NIL had higher expression than blast susceptible NIL most of the time except for the 48 and 96 hr, although the differences were not significant. These results suggested that *Os*1*bglu*4 might be involved in the rice blast stress resistance.

There are two possible ways for *Os*1*bglu*4 to involve in the blast resistance. One way is by cyanogenesis mechanism (Hughes *et al.* 1992). Os1BGlu4 clustered with a cyanogenic β-glucosidase (Opassiri *et al.* 2006) which will produce cyanide from its glucoside conjugate, the active cyanide may be involved in resistance to the pathogen. The other way is by release of the phytohormone from its inactive glucoside. Since the rOs1BGlu4 could hydrolyze the salicin to release the active salicylic acid (SA) *in vitro* (Figure 3.22). SA is involved in endogenous signaling, mediating in plant defense against pathogens (Hayat and Ahmad 2007).

The expression of *Os*1*bglu*4 was induced in high quantity at 6 hr after inoculation; the expression was highest at 12 hr and kept the high expession level up to 24 hr. The pattern of the *Os*1*bglu*4 expression generally conforms to the theory that the majority of the rice blast spores start to germinate on rice leaves by 6 hr after inoculation and the majority of appressoria start to penetrate into the rice epidermal cells 24 hr after inoculation (Zeigler *et al.* 1994).

The blast resistant gene BWMK1 was found to be highly induced, but at different time points when compared with the *Os*1*bglu*4 expression (He *et al.* 1999, Kim *et al.* 2000, Cheong *et al.* 2003, Nakashima *et al.* 2007). This may result

from cooperative work of different genes in the complicated and elaborate cell machinery. The gene expression in the resistant and susceptible reactions was altered significantly at 24 hr after blast infection. The difference in the expression profiles of some defense genes between the resistant and susceptible reactions at this time point may contribute to the outcome of the disease phenotype at a later stage of infection (Jantasuriyarat *et al.* 2005).

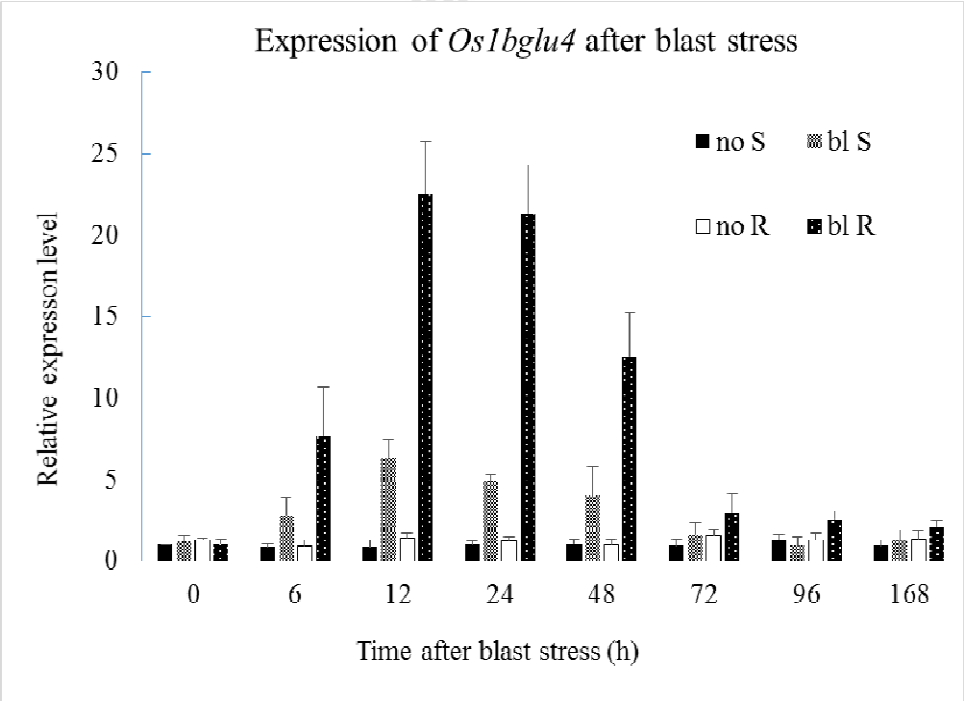

Figure 4.26 Real-time PCR of *Os*1*bglu*4 showing blast infection expression. The *Os*1*bglu*4 expression of RD6 at time 0 were used as calibrator. S, blast susceptible rice NIL, R, blast resistant rice NIL, no, without blast inoculation, bl, with blast inoculation. Data are given as the mean+ S.E. The experiment was repeated in triplicate.

4.4.6 Os1BGlu4 subcellular localization analysis

The localization of Os1BGlu4 was determined, the result showed that Os1-BGlu4-GFP existed in the cytoplasm (Figure 4.26), as predicted by bioinformatics study, in contrast, the control, Os4BGlu18-GFP localized mainly in the cell membrane (Figure 4.27). The information of subcellular localization could contribute to the knowledge of biologic function of the protein.

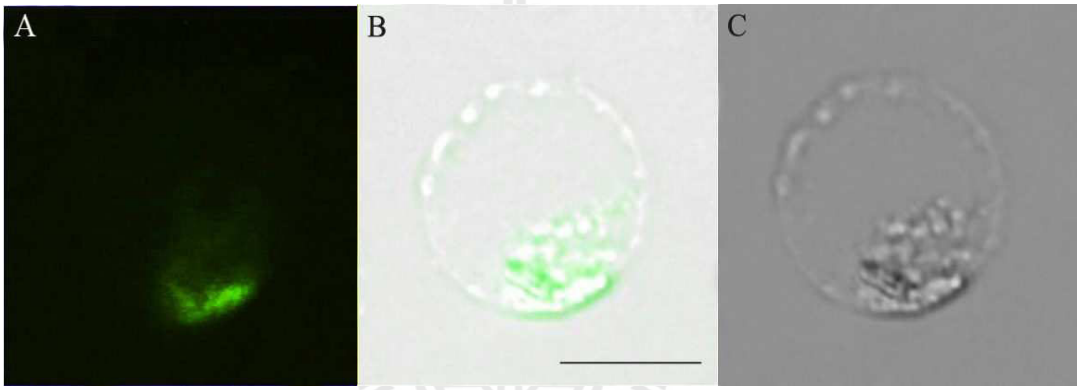

Figure 4.27 The subcellular localization of Os1BGlu4-GFP. The scale bar is 20 μm. A, fluorescence image, B, mixed image, C, bright field image.

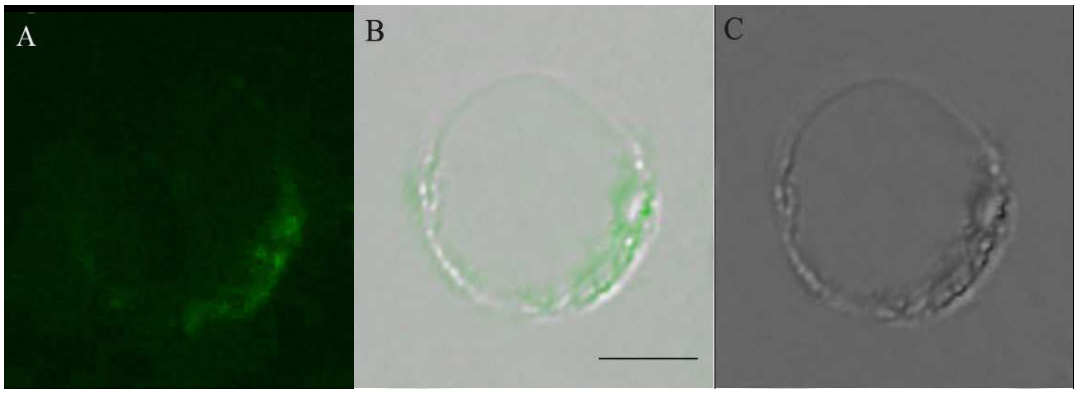

Figure 4.28 The subcellular localization of Os4BGlu18-GFP. The scale bar is 10 μm. A, fluorescence image, B, mixed image, C, bright field image.

4.4.7 pOp6 promoter evaluation

The activity of pOp6 promoter in the pOpOff2 vector was measured by GUS staining (Figure 4.28). The results showed that the RNAi lines supplemented with the DEX have the GUS activity, and the activity was not identical, RNAi+D1 (30 μM DEX) have stronger activity than the RNAi+D2 (10 μM DEX). In contrast, no GUS activity was detected in the RNAi lines without the DEX and the wild type *Nipponbare*. Ten micromolar of the final concentration of DEX was recommended for the induction of pOp6 promoter (Wielopolska *et al.* 2005), in this study, the 10 μM final concentration of DEX was used initially, but the real time PCR results showed the knock down of the gene was not significant (Figure 4.29), therefore, 30 μM final concentration of DEX was used instead to compare the induction effect, the result showed the 30 μM final concentration had a stronger reduction of *Os*1*bglu*4 expression than the 10 μM (Figure 4.29). The GUS activity under two concentrations were determined, correspond to the results of real time PCR, the 30 μM DEX showed stronger activity than that of the 10 μM treatments (Figure 4.28). However, DEX was dissolved in the absolute ethanol, and a higher percentage of the ethanol may inhibit the growth of the rice, therefore, the effect of 30 μM DEX on the germination of rice seeds was measured. The results showed that there was no significant difference in the germination rate between the DI H_2O and 30 μM DEX treatment for both the RNAi line seeds and wild type seeds (Table 4.1). The result suggested that 30 μM DEX was safe when supplemented in the DI H_2O, and 30 μM concentration of DEX was used in the subsequent experiment.

Figure 4.29 The GUS staining of the RNAi lines. RNAi+D1 and RNAi+D2 are RNAi lines supplemented with 30 μM DEX and 10 μM DEX, respectively. RNAi 1 and RNAi 2 are RNAi lines without the DEX, wt is the wildtype *Nipponbare*. A is the tip of the seedlings. B is the middle and bottom of the seedlings.

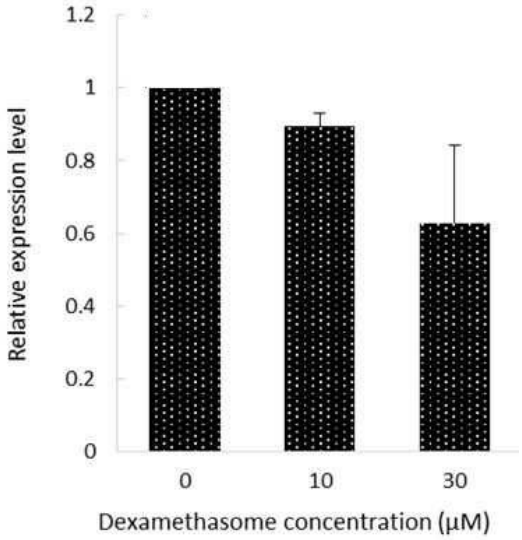

Figure 4.30 The knock-down effect of *Os*1*bglu*4 under different dexamethasone concentrations. The *Os*1*bglu*4 expression in 0 μM DEX treatment was used as the calibrator. Data are given as the mean+S.E. The experiment was repeated in triplicate.

Table 4.1 The effect of DEX to the germination rate of the seeds. RNAi+H_2O is the RNAi line seeds germinated in DI H_2O, RNAi+Dex is the RNAi line seeds germinated in DI H_2O supplemented with 30 μM DEX, WT+H_2O is the wild type seeds germinated in DI H_2O, WT+Dex is wild type seeds germinated in DI H_2O supplemented with 30 μM DEX.

Treatment	Germination Rate 1	Germination Rate 2	Germination Rate 3	Average
RNAi+H_2O	73%	79%	82%	78%±4.6%
RNAi+Dex	82%	81%	78%	80%±2.1%
WT+H_2O	75%	84%	80%	80%±4.5%
WT+Dex	70%	80%	79%	76%±5.5%

4.4.8 The phenotype analysis of *Os*1*bglu*4 gene

4.4.8.1 *Os*1*bglu*4 promotes root hair development

The phenotype was checked between the transgenic lines and wild type *Nipponbare* using the 14 day rice seedlings which germinated in tap water, the results showed that the amount of root hair between each line was different (Figure 4.30). The oe had the most root hairs, the wt and vetr had similar root hairs, by contrast, the RNAi treated with 30 μM DEX had the least root hairs, and the phenomenon was comfirmed by repeating the experiment. The roots of 5 seedlings of each type were cut off, the RNA was extracted, and the mRNA expression of *Os*1*bglu*4 was determined by qRT-PCR. The result showed that oe had the highest *Os*1*bglu*4 expression (Figure 4.31), by contrast, RNAi treated with 30 μM DEX had the lowest expression, the wt and vetr had the moderate expression. Strangely, when rice seeds were germinated in 1/2 MS mdium, the difference of the amount of root hair between the oe and the wt were not different (Figure 4.32), but the RNAi treated with 30 μM DEX still had the lowest amount of root hair.

The tube-like growth pattern of root hairs is essential to their function in root anchorage and for increasing the area of soil exploitable by the plant. Root hairs form from root epidermal cells. Their development occurs in four phases: cell fate specification, initiation, subsequent tip growth and maturation (Gilroy and Jones 2000).

Several genes that control root epidermal cell fate specifi- cation have been identified. Mutants that suppress root hair formation, or those that lead to the production of ectopic root hairs, indicate possible hormone (ethylene and auxin)-related mechanisms of cell fate specification. For example, in the *ctr-1* mutant

of *Arabidopsis*, all root epidermal cells produce root hairs. CTR-1 encodes a protein kinase of the Raf superfamily that is involved in ethylene signal transduction (Tanimoto *et al.* 1995).

Root hair initiation, is regulated by genes sensitive to hormonal and environmental factors (Schiefelbein 2000). The auxin-resistant mutant (axr2) produced fewer root hair bulges (Wilson *et al.* 1990), and the defect of root hair initiation in root hair defective (rhd6) can be reversed by treatment with auxin or the ethylene precursor 1-aminocyclopropane-1-carboxylic acid (ACC) can rescue the root hair initiation, which indicated that auxin and ethylene are important players in root hair elongation in *Arabidopsis* (Masucci and Schiefelbein 1994,d 1996). A root-hair-specific *Medicago truncatula* cDNA library was constructed to study the relative gene expressions. Two kinds of genes are found most abundant in this library, Methionine synthase and β-glucosidase. Methionine synthase is critical for protein metabolism, β-glucosidase is involved in the initiation by loosening the cell wall (Covitz *et al.* 1998). However, the Os1BGlu4 should not play the role as cell wall loosener in the formation of root hair since it is localized in the cytoplasm (Figure 4.26). A more reasonable hypothesis is that Os1BGlu4 hydrolyzes IAA-glucoside to release the biologically active IAA to promote the root hair formaiton of the rice seedling.

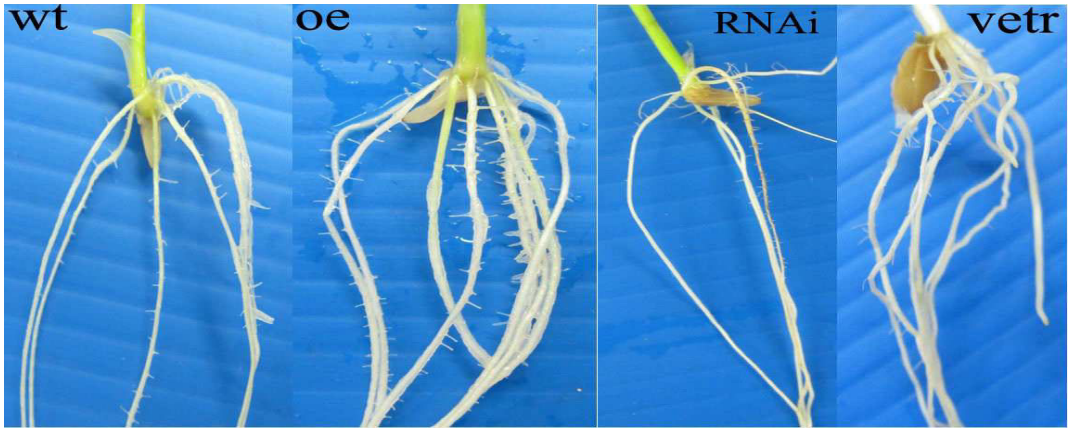

Figure 4.31 The representative root hair profile when rice seeds were germinated in water. wt, wild type *Nipponbare*, oe, transgenic rice of overexpression of *Os*1*bglu*4 gene, RNAi, transgenic rice with *Os*1*bglu*4 gene knock down, vetr, the transgenic rice transformed with pMDC83 empty vector.

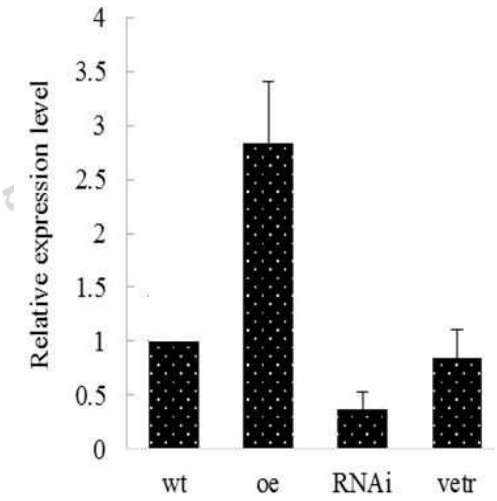

Figure 4.32 The relative *Os*1*bglu*4 expression in root. wt, wild type *Nipponbare*, oe, transgenic rice of overexpression of *Os*1*bglu*4 gene, RNAi, transgenic rice with *Os*1*bglu*4 gene knock down. vetr, the transgenic rice transformed with pMDC83 empty vector. The wt root *Os*1*bglu*4 expression was used as calibrator. Data are given as the mean+S.E. The experiment was repeated in triplicate.

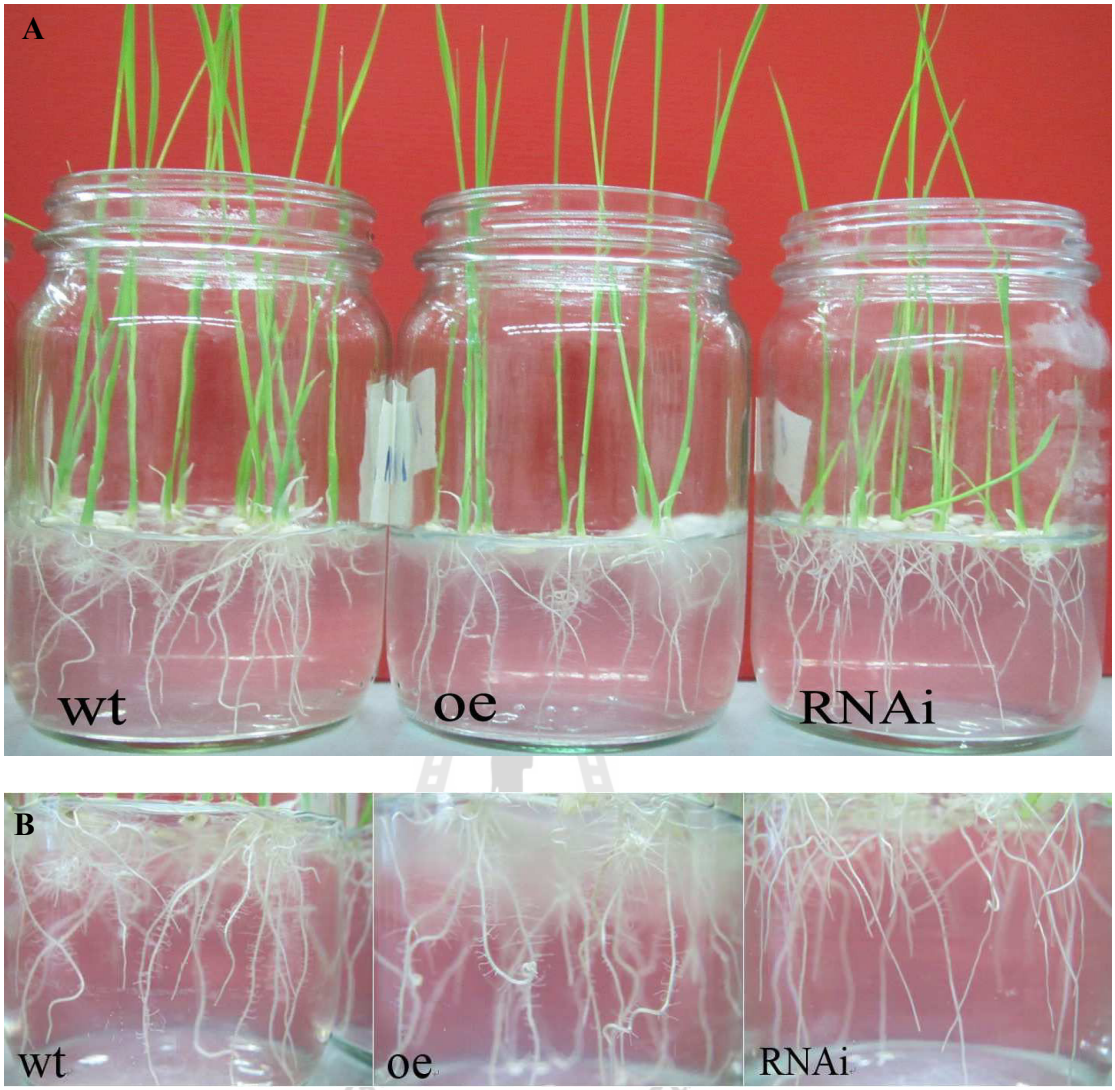

Figure 4.33 The root hair profile when the seeds were germinated in 1/2 MS medium. wt, wild type *Nipponbare*, oe, transgenic rice of overexpression of *Os*1-*bglu*4 gene, RNAi, transgenic rice with *Os*1*bglu*4 gene knock down. A, overall morphology of rice seedlings, B, images focus on the root hair.

To check whether this phenomenon was caused by the different expression of *Os*1*bglu*4, the root of wild type *Nipponbare* was cut off, and sorted into two groups, one with more root hair (Mrh), the other with less root hair (Lrh) (Figure 4.33 A). The *Os*1*bglu*4 expression was check by qRT-PCR. The result indicated that the

*Os*1*bglu*4 expressed was about 2 fold more in the Mrh group than in the Lrh group root (Figure 4.33 B). The result stongly suggested that *Os*1*bglu*4 is involved in the formation of root hair.

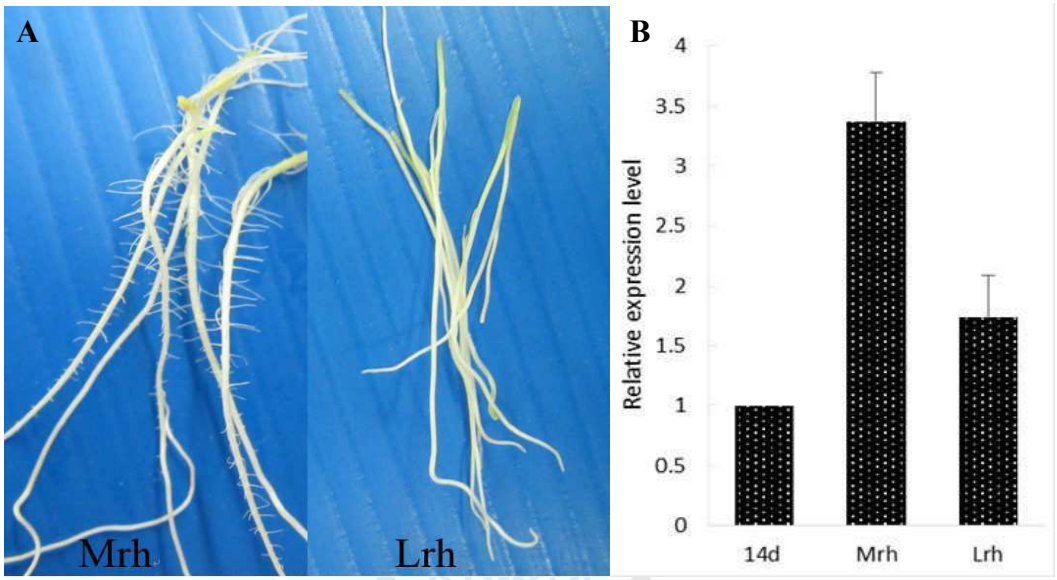

Figure 4.34 Two groups of root from wt *Nipponbare* and their *Os*1*bglu*4 expression, Mrh group has more root hair, Lrh has less root hair. A, root morphology, B, *Os*1*bglu*4 relative expression level in Mrh and Lrh groups. 14 day seed- ling *Os*1*bglu*4 expression was used as caulibrator. Data are given as the mean+S.E. The experiment was repeated in triplicate.

4.4.8.2 The overall development of rice was not obviously affected by *Os*1*bglu*4 under normal growth condition

Under normal growth conditions, there was no appreciable phe-notype of overall rice morphology observed at each developmental stage among the wt, oe, vetr and RNAi lines (Figure 4.34), except for the root hair phenotype. The rice heights from 6 day old seedlings to 110 day old mature plants were similar among the

lines (Figure 4.35). The root lengthes from 6 day old seedlings to 90 day old mature plants were similar among the lines (Figure 4.36).

The DEX was not added after the seedlings were transferred to the soil pot except for one time when rice reached the booting stage. The effect of *Os*1*bglu*4 gene to the development of panicle and seed formation was checked. The result indicated that there was no significant difference in the development of panicle and seed formation between all transgenic lines and wt (Figure 4.34 G). The DEX was added only once at the booting stage, therefore, the RNAi line results may not be that accurate as oe. But oe lines didn't show any appreciable phenotype when compared with the wt and vetr.

The above results suggested that although the *Os*1*bglu*4 involved in the development of the rice, it plays a relatively minor role in the rice morphology and the whole development of the rice.

The constitutive RNAi vectors are recommended, especially when the phenotype of the target gene is not fatal to the rice, which will facilitate the comparison of the transgenic lines. In this research, the inducible RNAi vector was not suitable for this work. Both the solvent (ethanol) and DEX may affect the germination and growth of the rice, however, it was lucky in this study, there was no significant effect to the germination or growth to the rice seedlings. The inducer and solvent effect on the growth or germination of rice seeds have to be taken into consideration. The expense of the inducer was also a big problem. In this study, the addition of the DEX stopped when the RNAi seedlings were transferred to the soil pot because of the huge expense of DEX. The DEX has to be kept without light, but the rice growth needs light, therefore, frequent addition of the DEX to the rice seedlings is required. By contrast, these disadvantages can be avoided if constitutive promoter was used in this research.

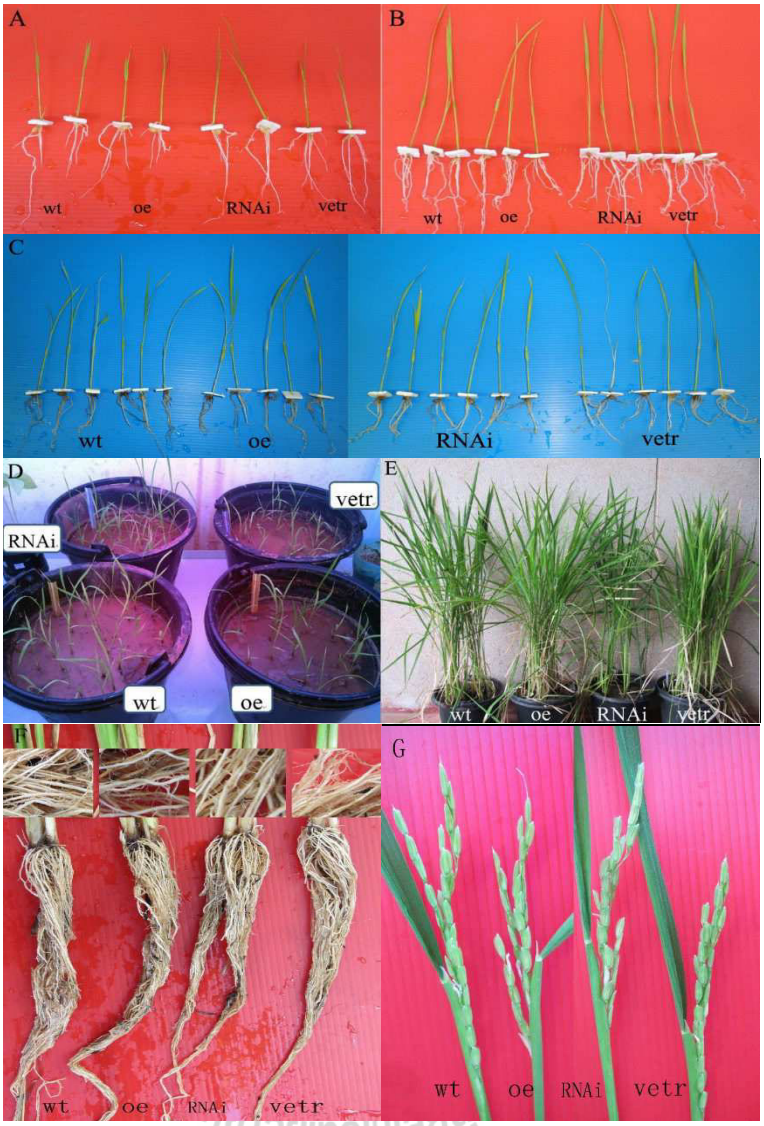

Figure 4.35 The morphology compared between lines with different *Os*1*bglu*4 expression. wt, wild type *Nipponbare*, oe, transgenic rice of over- expression of *Os*1*bglu*4 gene, RNAi, transgenic rice with *Os*1*bglu*4 gene knock down. vetr, the transgenic rice transformed with pMDC83 empty vector. A, 6 days after germination, B, 10 days after germination, C, 14 days after germination, D, 25 days after germination in soil pot, E, 110 days after germination in soil pot, F, the root morphology at booting stage, the small embeded photoes showed the detail of root hair. G, the panicle morphology at booting stage.

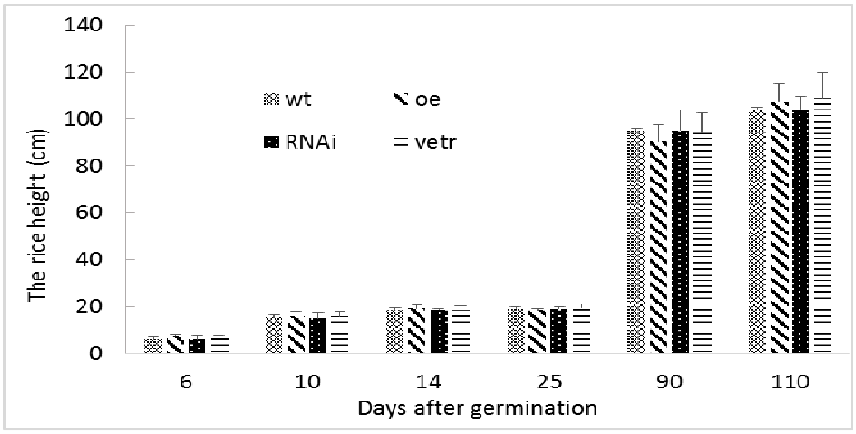

Figure 4.36 The rice height at different time points. Data are given as the means +S.E. The experiment was repeated 7 times. wt, wild type *Nipponbare*, oe, transgenic rice of overexpression of *Os*1*bglu*4 gene, RNAi, transgenic rice with *Os*1*bglu*4 gene knock down. vetr, the transgenic rice transformed with pMDC83 empty vector.

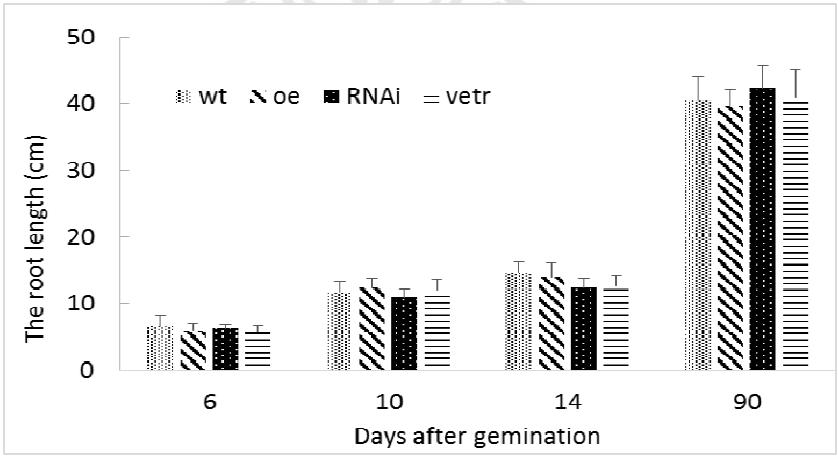

Figure 4.37 The root length at different time points. Data are given as the means+S.E. The experiment was repeated 7 times. wt, wild type *Nipponbare*, oe, transgenic rice for overexpression of the *Os*1*bglu*4 gene, RNAi, transgenic rice with the *Os*1*bglu*4 gene knock down. vetr, the transgenic rice trasformed with pMDC83 empty vector.

4.4.8.3 *Os*1*bglu*4 did not obviously affect the rice under abiotic stress

The phenotype under salinity and drought stress were investigated, the results showed that there was no visible phenotype was observed (Figure 4.37) under both abiotic stress. All lines wilted after 3 days of stress, and the water loss was checked (Figure 4.38), the result showed that about 30% of the water evaporated after salinity stress, 42% of the water was lost after PEG stress, and there was no significant difference of water loss between the lines under any stress. The total RNA was extracted from the seedlings after checking the phenotype; the seedlings without the treatment were used as the basal expression. Wt (0) (the RNA of the seedling before the treatment) was used as calibrator. The results showed that under PEG and NaCl stress conditions, the oe had the highest *Os*1*bglu*4 expression, the RNAi had the lowest expression, wt and vetr had moderate expression. The pattern was similar to the basal expression (without stress treatment) of each line. The results suggested that, although *Os*1*bglu*4 gene was expressed significantly higher in oe, and lower in RNAi, there was no visible morphology or water loss difference. These results contradict with the result of the transcription pattern (Figure 4.24). This may resulted from the long term stress (3 days), the mRNA level might have changed back to the basal expression level. The rice seedlings have already adapted to the stress condition (Kawasaki *et al.* 2001).

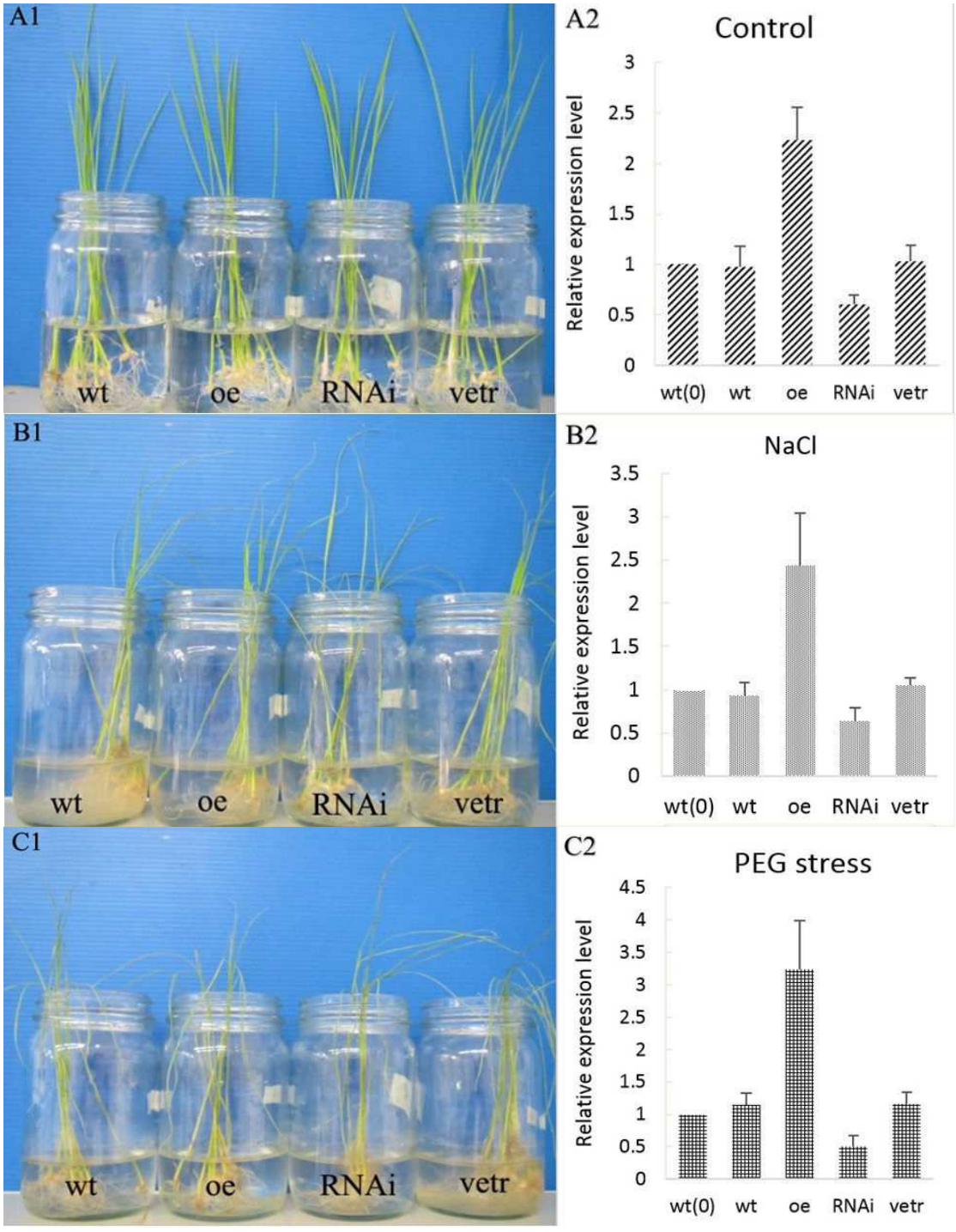

Figure 4.38 Growth performance and mRNA expression of rice seedlings under PEG- and NaCl-stress conditions. wt(0), wild type *Nipponbare* before treatment, wt, wild type *Nipponbare*, oe, transgenic rice with *Os*1*bglu*4 gene overexpression, RNAi, transgenic rice with *Os*1*bglu*4 knock down,

vetr, transgenic rice with pMDC83. A1, growth performance of seedlings without treatment, A2, relative *Os*1*bglu*4 expression without treatment. B1, growth performance of seedlings under NaCl stress, B2, relative *Os*1*bglu*4 expression under NaCl stress, C1, growth performance of seedlings under PEG stress, C2, relative *Os*1*bglu*4 expression under PEG stress. Data are given as the mean+S.E. The experiment was repeated in triplicate.

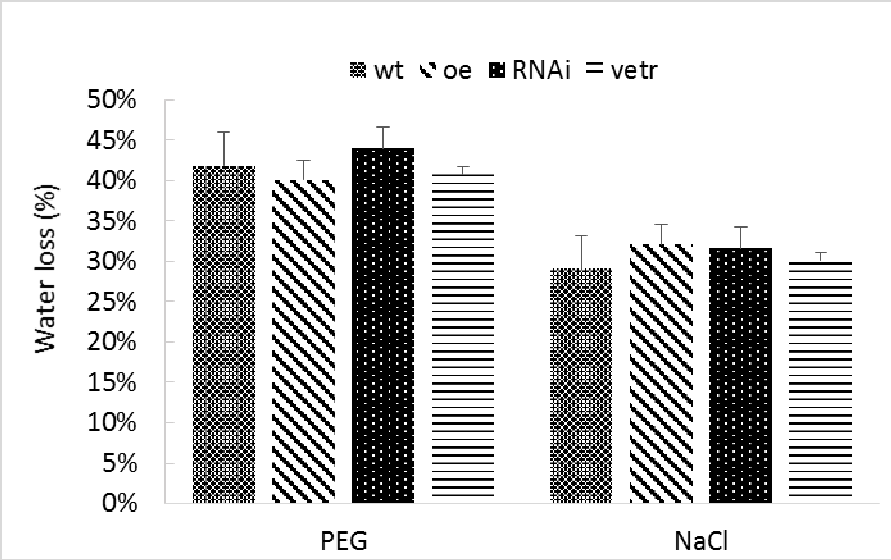

Figure 4.39 Water loss percentage after 3 days abiotic stress, wt, wild type *Nipponbare*, oe, transgenic rice with *Os*1*bglu*4 gene overexpression, RNAi, transgenic rice with *Os*1*bglu*4 knock down, vetr, transgenic rice with pMDC83. Data are given as the mean+S.E. The experiment was repeated in triplicate. PEG, 10% PEG 6000 treatment for 3 days, NaCl, 100 mM NaCl treatment for 3 days.

4.4.8.4 *Os*1*bglu*4 is involved in the rice blast resistance

Magnaporthe grisea is an airborne foliar fungus that causes blast disease in rice. The fungus infects leaves during early growth stages of rice plant, giving lesions followed by premature leaf senescence of infected tissue, especially in case of heavy infections. After heading, the pathogen infects the panicles or the neck node. Rice blast has been one of the most serious diseases of rice in rice-growing countries, often significantly reducing rice yields (Ou 1985).

The EST data showed that *Os*1*bglu*4 was detected after blast infection, the transcription pattern after blast infection showed that *Os*1*bglu*4 might be involed in rice blast resistance. This information prompted us to test whether *Os*1*bglu*4 over-expression and knock down in rice would affect disease resistance or not. The 14 day seedlings were inoculated with rice blast fungus (*Magnaporthe grisea*), the phenotype was checked 1 week later. The result showed that the size of the disease lesions generated by the *M. grisea* were different among wt, oe, RNAi and vetr (Figure 4.39 A). The oe suffered the slightest disease lesions, the RNAi line suffered most severe disease lesions, the wt and vetr suffered the disease lesions more than the oe but lower than the RNAi line. The *Os*1*bglu*4 expression was checked (Figure 4.39 B); the result showed that oe had significantly higher expression. The RNAi lines treated with 30 μM DEX had significantly lower expression, which corresponded to the phenotype of *Os*1*bglu*4.

The lesion numbers were found to be different between the lines. The disease lesions were classified as big spot and small spot. They were counted to determine the class of the lesion. The total spots numbers and the proportion of big spots were checked in 3 rice seedlings for each group. The results showed that the oe leaves have less spots than the wt and vetr leaves (Figure 4.40 A). The RNAi line

seedling leaves had the highest number of spots, closed to 80, much more than the oe leaves (15 spots). The wt and vetr had similar numbers of spots (43). In addition, the proportion of big spots on the leaves was different (Figure 4.40 B), the RNAi had the highest percentage of big spots (37.5%), the wt and vetr had about 28% big spots, by contrast, and the oe had the lowest percentage of big spots (18%).

The above results, including transcription pattern, EST database and phenotype analysis, strongly suggested that the *Os*1*bglu*4 gene is involved in rice blast resistance, the overexpression of *Os*1*bglu*4 significantly decreased the disease lesions caused by the blast infection, and the *Os*1*bglu*4 knock-down resulted in more severe disease lesions. The biochemistry data in this research also indicated that *Os*1*bglu*4 maybe involve in the pathogen resistance, because the r*Os*1*bglu*4 can hydrolyze the salicin to salicylic alcohol, which is similar to salicylic acid (SA). SA is involved in endogenous signaling, mediating plant defense against pathogens (Hayat and Ahmad 2007). It plays a role in the resistance to pathogens by inducing the production of pathogenesis-related proteins (Van Huijsduijnen *et al.* 1986). It is involved in the systemic acquired resistance (SAR) in which a pathogenic attack on one part of the plant induces resistance in other parts. The signal can also move to nearby plants by salicylic acid being converted to the volatile ester, methyl salicylate (Taiz and Zeiger 2002). This may explain some of the phenotype that oe has less and smaller lesion spots, RNAi have more and bigger lesion spots.

At least 30 resistance loci have been identified in rice (Kinoshita 1995), many blast resistant gene have been identified, the Pib gene for rice blast resistance belongs to the nucleotide binding and leucine-rich repeat class of plant disease resistance genes (Wang *et al.* 2002). Three major genes for blast resistance (Pi1, Piz-5 and Pita) were fine-mapped on chromosomes 11, 6 and 12, respectively, and

closely linked RFLP markers were also identified (Hittalmani *et al.* 2000). Recently, Pi50 (t), a new member of the rice blast resistance Pi2/Pi9 multigene family was identified (Zhu et al. 2012) A multiple gene complex on rice chromosome 4 was found to be involved in durable resistance to rice blast (Fukuoka et al. 2012). Here, a rice β-glucosidase *Os*1*bglu*4 was found actively involved in the blast resistance, but the mechanism still needs to be clarified.

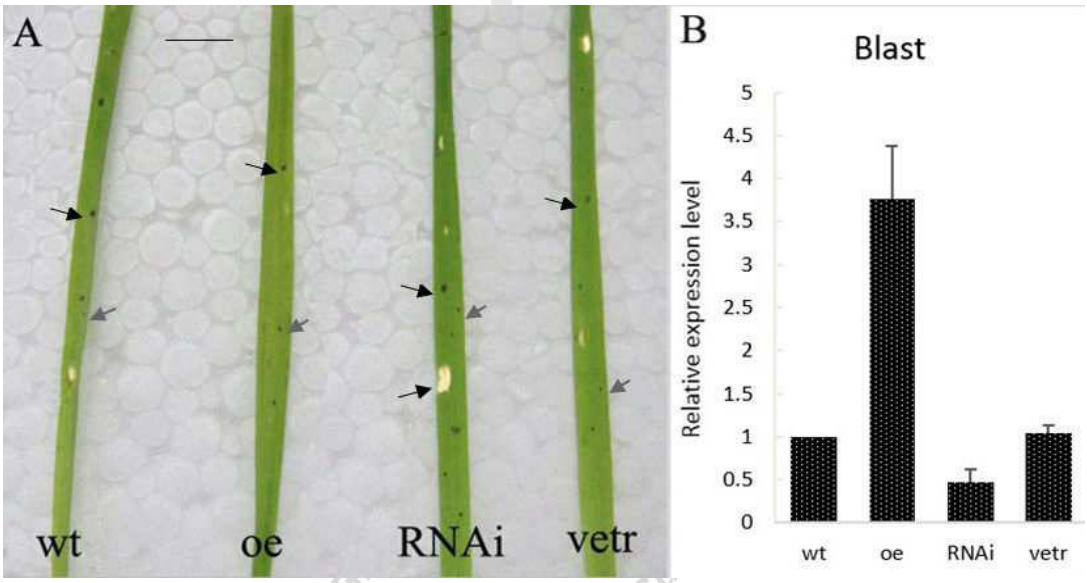

Figure 4.40 The symptom and *Os*1*bglu*4 expression of leaves 6 days after the blast infection. The scale bar is 10 mm. The black arrow indicated the big lesion spots. The gray arrow showed the small spots. The spots were classified according to the 1 mm diameter criteria. wt, wild type *Nipponbare*, oe, transgenic rice of overexpression of *Os*1*bglu*4 gene, RNAi, transgenic rice with *Os*1*bglu*4 gene knock down. vetr, the transgenic rice trasformed with pMDC83 empty vector. A, the symptom of leaves, B, the *Os*1*bglu*4 expression. Data are given as the mean+S.E. The experiment was repeated in triplicate.

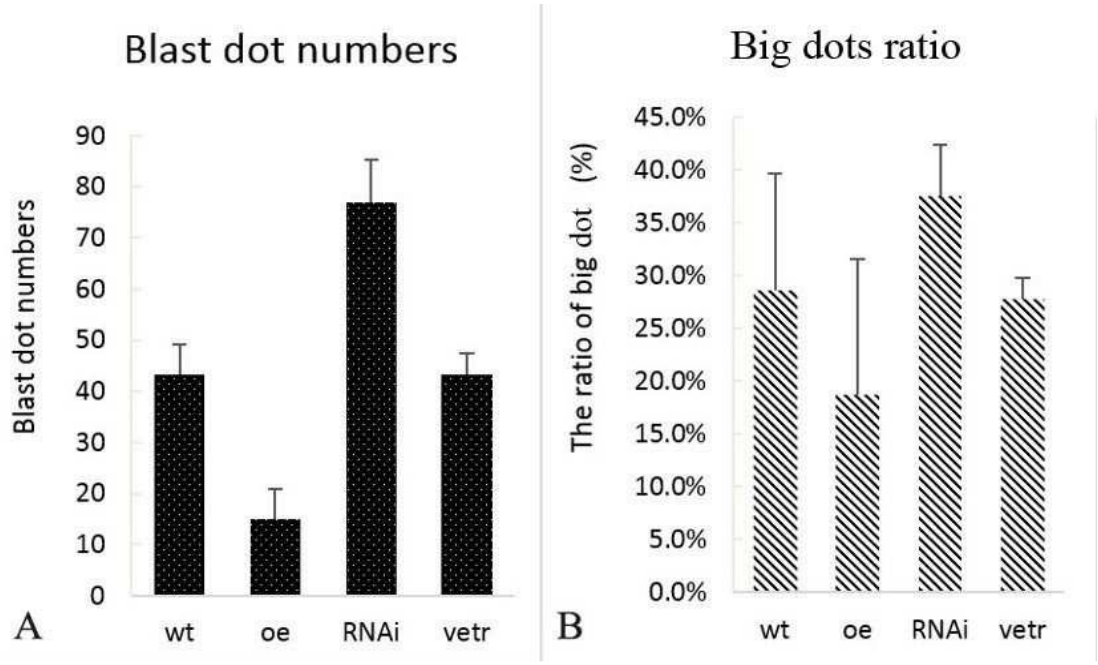

Figure 4.41 The blast spots in the rice seedling leaves 1 week after blast infection. wt, wild type *Nipponbare*, oe, transgenic rice of overexpression of *Os*1-*bglu*4 gene, RNAi, transgenic rice with *Os*1*bglu*4 gene knock down. vetr, the transgenic rice transformed with pMDC83 empty vector. A, the total number of blast spots on 3 seedling leaves. B, the big spot percentage. Data are given as the mean+S.E. The experiment was repeated in tri-plicate.

4.5 Conclusion

The transcription pattern of *Os*1*bglu*4 was studied by qRT-PCR. The results showed that the *Os*1*bglu*4 had higher expression at early stage after germination, and expression decreased gradually to steady level. In 14 day rice seedlings root had the highest *Os*1*bglu*4 expression, followed by the leaf and shoot. In contrast, *Os*1*bglu*4 has the highest expression in panicle, followed by root, leaf and sheath, and no expression

was detected in rice seed at booting stage rice. The expression of *Os*1*bglu*4 was induced under both the drought and salinity stresses. The *Os*1*bglu*4 expression pattern after rice blast stress was investigated extensively, the results showed that the expression of *Os*1*bglu*4 was induced to a high level in the blast resistant rice NIL, and only moderately expressed in the blast susceptible rice NIL. The result suggested that the *Os*1*bglu*4 may be involved in the drought, salinity and rice blast stress.

The coding sequence of *Os*1*bglu*4 gene was cloned into the pMDC83 plant expression vector under the control of constitutive 35S promoter. The DNA fragment of 3' UTR sequence of *Os*1*bglu*4 was amplified cloned into the RNAi vector pOpOff2 which was drived by DEX-inducible pOp6 promoter. The pMDC83 empty vector, pMDC83-*Os*1*bglu*4 and pOpOff2-UTR were transformed into the rice cultivar *Nip-ponbare* by *Agrobacterium*-mediated transformation, and the T0 seeds were collected. The segregation of T-DNA was analized in the T1 rice seedlings, the results showed that T-DNA segregation conformed to Mendelian in the T1 plant.

The subcellular localization of *Os*1*bglu*4-GFP was determined by flurescence microscope with the Os4BGlu18-GFP as control, the results indicated that the *Os*1-*bglu*4-GFP is in the cytosol, corresponded with the bioinformatics prediction.

The activity of pOp6 promoter in the RNAi transgenic rice was assessed by GUS staining, the result showed that 30 μM DEX is necessary for strong induction of GUS activity, only moderate GUS activity was observed when 10 μM DEX was used, and no GUS activtiy was detected without DEX induction. The high concentration of DEX had no significant effect to the germination rate of rice seeds.

The phenotype analysis showed that the *Os*1*bglu*4 overexpression lines (oe) have more root hair than that of the wild type, and *Os*1*bglu*4 gene knock down lines (RNAi) had the least root hair, when germinated in the water. However, when

germinated in the 1/2 MS medium, there was no significant difference in the root hair amount was observed between the wt and oe, but RNAi have less root hair than both wt and oe. Aside from the root hair in the seedling stages, there were no visible difference in the overall morphologies among wt, oe, RNAi and the transgenic rice which is transformed with the pMDC83 plant expression empty vector (vetr). Under drought and salinity stress, there were no visible phenotype observed in the wt, oe, RNAi and vetr. Under rice blast stress, the oe showed higher resistance to the blast stress, the wt and vetr had moderate resistace, the RNAi suffered severe lesions from the blast infection.

In general, the *Os*1*bglu*4 may be involved in blast resistance and root hair formation.

4.6 References

Brzobohatý, B., I. Moore, P. Kristoffersen, L. Bako, N. Campos*, et al.* (1993). Release of Active Cytokinin by a Beta-Glucosidase Localized to the Maize Root Meristem. **Science (New York, NY)** 262(5136): 1051.

Budar, F., L. Thia-Toong, M. Van Montagu and J. P. Hernalsteens (1986). *Agrobacterium*-Mediated Gene Transfer Results Mainly in Transgenic Plants Transmitting T-DNA as a Single Mendelian Factor. **Genetics** 114(1): 303-313.

Chen, D.-x., X.-w. Chen, C.-l. Lei, B.-t. Ma, Y.-p. Wang*, et al.* (2010). Rice Blast Resistance of Transgenic Rice Plants with Pi-D2 Gene. **Rice Science** 17(3): 179-184.

Cheong, Y. H., B. C. Moon, J. K. Kim, C. Y. Kim, M. C. Kim*, et al.* (2003). Bwmk1, a Rice Mitogen-Activated Protein Kinase, Locates in the Nucleus and Mediates

Pathogenesis-Related Gene Expression by Activation of a Transcription Factor. **Plant Physiology** 132(4): 1961-1972.

Covitz, P. A., L. S. Smith and S. R. Long (1998). Expressed Sequence Tags from a Root-Hair-Enriched Medicago Truncatula Cdna Library. **Plant Physiology** 117(4): 1325-1332.

Curtis, M. D. and U. Grossniklaus (2003). A Gateway Cloning Vector Set for High-Throughput Functional Analysis of Genes in Planta. **Plant Physiology** 133(2): 462-469.

Dai, M., Y. Zhao, Q. Ma, Y. Hu, P. Hedden, et al. (2007). The Rice Yabby1 Gene Is Involved in the Feedback Regulation of Gibberellin Metabolism. **Plant Physiology** 144(1): 121-133.

De Block, M., L. Herrera-Estrella, M. Van Montagu, J. Schell and P. Zambryski (1984). Expression of Foreign Genes in Regenerated Plants and in Their Progeny. **The EMBO Journal** 3(8): 1681.

Enríquez-Obregón, G. A., D. L. Prieto-Samsónov, G. A. de la Riva, M. Pérez, G. Selman-Housein*, et al.* (1999). *Agrobacterium*-Mediated Japonica Rice Transformation: A Procedure Assisted by an Antinecrotic Treatment. **Plant Cell, Tissue and Organ Culture** 59(3): 159-168.

Esen, A. (1993). B-Glucosidase: Overview in B-Glucosidases: Biochemistry and Molecular Biology (Esen, A., Ed). **American Chemical Society, Washington, DC.**

Fukuoka, S., R. Mizobuchi, N. Saka, S. Ivan, T. Matsumoto*, et al.* (2012). A Multiple Gene Complex on Rice Chromosome 4 Is Involved in Durable Resistance to Rice Blast. **Theoretical and Applied Genetics**: 1-9.

Gilroy, S. and D. L. Jones (2000). Through Form to Function: Root Hair Development and Nutrient Uptake. **Trends in Plant Science** 5(2): 56-60.

Hamer, J. E., B. Valent and F. G. Chumley (1989). Mutations at the Smo Genetic Locus Affect the Shape of Diverse Cell Types in the Rice Blast Fungus. **Genetics** 122(2): 351-361.

Hayat, S. and A. Ahmad (2007). **Salicylic Acid-a Plant Hormone**, Springer.

He, C., S. H. T. Fong, D. Yang and G. L. Wang (1999). Bwmk1, a Novel Map Kinase Induced by Fungal Infection and Mechanical Wounding in Rice. **Molecular Plant-Microbe Interactions** 12(12): 1064-1073.

Hiei, Y., S. Ohta, T. Komari and T. Kumashiro (1994). Efficient Transformation of Rice (*Oryza sativa* L.) Mediated by *Agrobacterium* and Sequence Analysis of the Boundaries of the T-DNA. **The Plant Journal: for Cell and Molecular Biology** 6(2): 271-282.

Hittalmani, S., A. Parco, T. Mew, R. Zeigler and N. Huang (2000). Fine Mapping and DNA Marker-Assisted Pyramiding of the Three Major Genes for Blast Resistance in Rice. **Theoretical and Applied Genetics** 100(7): 1121-1128.

Hughes, M. A., K. Brown, A. Pancoro, B. S. Murray, E. Oxtoby*, et al.* (1992). A Molecular and Biochemical Analysis of the Structure of the Cyanogenic B-Glucosidase (Linamarase) from Cassava (*Manihot esculenta* Crantz). **Archives of Biochemistry and Biophysics** 295(2): 273-279.

Jantasuriyarat, C., M. Gowda, K. Haller, J. Hatfield, G. Lu*, et al.* (2005). Large-Scale Identification of Expressed Sequence Tags Involved in Rice and Rice Blast Fungus Interaction. **Plant Physiology** 138(1): 105-115.

Jarosch, B., K. H. Kogel and U. Schaffrath (1999). The Ambivalence of the Barley Mlo Locus: Mutations Conferring Resistance against Powdery Mildew (Blumeria

Graminis F. Sp. Hordei) Enhance Susceptibility to the Rice Blast Fungus Magnaporthe Grisea. **Molecular Plant-Microbe Interactions** 12(6): 508-514.

Kawasaki, S., C. Borchert, M. Deyholos, H. Wang, S. Brazille*, et al.* (2001). Gene Expression Profiles During the Initial Phase of Salt Stress in Rice. **The Plant Cell** 13(4): 889-905.

Ketudat Cairns, J. R. and A. Esen (2010). B-Glucosidases. **Cellular and Molecular Life Sciences** 67(20): 3389-3405.

Kim, C. Y., S. H. Lee, H. C. Park, C. G. Bae, Y. H. Cheong*, et al.* (2000). Identification of Rice Blast Fungal Elicitor-Responsive Genes by Differential Display Analysis. **Molecular Plant-Microbe Interactions** 13(4): 470-474.

Kinoshita, T. (1995). Report of Committee on Gene Symbolization, Nomenclature and Linkage Groups. **Rice Genetics Newsletter** 12: 9-153.

Kumar, K., S. Maruthasalam, M. Loganathan, D. Sudhakar and P. Balasubramanian (2005). An Improved *Agrobacterium*-Mediated Transformation Protocol for Recalcitrant Elite Indica Rice Cultivars. **Plant Molecular Biology Reporter** 23(1): 67-73.

Lian, H. L., X. Yu, Q. Ye, X. S. Ding, Y. Kitagawa*, et al.* (2004). The Role of Aquaporin Rwc3 in Drought Avoidance in Rice. **Plant and Cell Physiology** 45(4): 481-489.

Liu, K., L. Wang, Y. Xu, N. Chen, Q. Ma*, et al.* (2007). Overexpression of Oscoin, a Putative Cold Inducible Zinc Finger Protein, Increased Tolerance to Chilling, Salt and Drought, and Enhanced Proline Level in Rice. **Planta** 226(4): 1007-1016.

Livak, K. J. and T. D. Schmittgen (2001). Analysis of Relative Gene Expression Data Using Real-Time Quantitative Pcr and the $2^{-\Delta\delta ct}$ Method. **Methods** 25(4): 402-408.

Lutts, S., V. Majerus and J. M. Kinet (2002). Nacl Effects on Proline Metabolism in Rice (Oryza Sativa) Seedlings. **Physiologia Plantarum** 105(3): 450-458.

Ma, B., Wang Lingxia, Li Ping, Zhu Zhen, Zhou Kaida (2004). Transgenic Elite Indica Restorer Line and Genetic Stablility of Transgenes. **Chinese Journal of Applied & Environmental Biology** 10(5).

Masucci, J. D. and J. W. Schiefelbein (1994). The Rhd6 Mutation of *Arabidopsis* Thaliana Alters Root-Hair Initiation through an Auxin-and Ethylene-Associated Process. **Plant Physiology** 106(4): 1335-1346.

Masucci, J. D. and J. W. Schiefelbein (1996). Hormones Act Downstream of Ttg and Gl2 to Promote Root Hair Outgrowth During Epidermis Development in the *Arabidopsis* Root. **The Plant Cell Online** 8(9): 1505-1517.

Nadolska-Orczyk, A. and W. Orczyk (2000). Study of the Factors Influencing *Agrobacterium*-Mediated Transformation of Pea (*Pisum sativum* L.). **Molecular Breeding** 6(2): 185-194.

Nakashima, K., L. S. P. Tran, D. Van Nguyen, M. Fujita, K. Maruyama*, et al.* (2007). Functional Analysis of a Nac-Type Transcription Factor Osnac6 Involved in Abiotic and Biotic Stress-Responsive Gene Expression in Rice. **The Plant Journal** 51(4): 617-630.

Nauerby, B., K. Billing and R. Wyndaele (1997). Influence of the Antibiotic Timentin on Plant Regeneration Compared to Carbenicillin and Cefotaxime in Concentrations Suitable for Elimination of *Agrobacterium tumefaciens*. **Plant Science** 123(1): 169-177.

Opassiri, R., Y. Hua, O. Wara-Aswapati, T. Akiyama, J. Svasti*, et al.* (2004). Beta-Glucosidase, Exo-Beta-Glucanase and Pyridoxine Transglucosylase Activities of Rice Bglu1. **Biochemical Journal** 379(Pt 1): 125-131.

Opassiri, R., J. R. Ketudat Cairns, T. Akiyama, O. Wara-Aswapati, J. Svasti, *et al.* (2003). Characterization of a Rice B-Glucosidase Highly Expressed in Flower and Germinating Shoot. **Plant Science** 165(3): 627-638.

Opassiri, R., J. Maneesan, T. Akiyama, B. Pomthong, S. Jin, *et al.* (2010). Rice Os4bglu12 Is a Wound-Induced B-Glucosidase That Hydrolyzes Cell Wall-B-Glucan-Derived Oligosaccharides and Glycosides. **Plant Science** 179(3): 273-280.

Opassiri, R., B. Pomthong, T. Onkoksoong, T. Akiyama, A. Esen, *et al.* (2006). Analysis of Rice Glycosyl Hydrolase Family 1 and Expression of Os4bglu12 Beta-Glucosidase. **BMC Plant Biology** 6: 33-33.

Ou, S. H. (1985). Rice Diseases, CABI.

Qiu, Y. and D. Yu (2009). Over-Expression of the Stress-Induced Oswrky45 Enhances Disease Resistance and Drought Tolerance in *Arabidopsis*. **Environmental and Experimental Botany** 65(1): 35-47.

Rashid, H., S. Yokoi, K. Toriyama and K. Hinata (1996). Transgenic Plant Production Mediated by *Agrobacterium* in Indica Rice. **Plant Cell Reports** 15(10): 727-730.

Rueb, S. and L. Hensgens (1989). Improved Histochemical Staining for β-D-Glucuronidase Activity in Monocotyledonous Plants. **Rice Genetics Newsletter** 6: 168-169.

Ryu, C.-H., S. Lee, L.-H. Cho, S. L. Kim, Y.-S. Lee, et al. (2009). Osmads50 and Osmads56 Function Antagonistically in Regulating Long Day (Ld)-Dependent Flowering in Rice. **Plant, Cell & Environment** 32(10): 1412-1427.

Saharan, V., R. C. Yadav, N. R. Yadav and K. Ram (2005). Studies on Improved *Agrobacterium*-Mediated Transformation in Two Indica Rice (*Oryza sativa* L.). **African Journal of Biotechnology** 3(11): 572-575.

Schiefelbein, J. W. (2000). Constructing a Plant Cell. The Genetic Control of Root Hair Development. **Plant Physiology** 124(4): 1525-1531.

Taiz, L. and E. Zeiger (2002). Plant Physiology. **New York: Sinauer**: 306.

Tanimoto, M., K. Roberts and L. Dolan (1995). Ethylene Is a Positive Regulator of Root Hair Development in *Arabidopsis* Thaliana. **The Plant Journal** 8(6): 943-948.

Thiery, R. B., G. Edelman and J. Cell (1978). Inheritance of Functional Foreign Genes in Plants. **Biol** 79: 371.

Toki, S., N. Hara, K. Ono, H. Onodera, A. Tagiri*, et al.* (2006). Early Infection of Scutellum Tissue with *Agrobacterium* Allows High-Speed Transformation of Rice. **The Plant Journal: for Cell and Molecular Biology** 47(6): 969-976.

Toki, S., N. Hara, K. Ono, H. Onodera, A. Tagiri*, et al.* (2006). Early Infection of Scutellum Tissue with Agrobacterium Allows High-Speed Transformation of Rice. **The Plant Journal** 47(6): 969-976.

Valent, B. and F. G. Chumley (1991). Molecular Genetic Analysis of the Rice Blast Fungus, Magnaporthe Grisea. **Annual Review of Phytopathology** 29(1): 443-467.

Van Huijsduijnen, R. A. M. H., S. Alblas, R. De Rijk and J. Bol (1986). Induction by Salicylic Acid of Pathogenesis-Related Proteins and Resistance to Alfalfa Mosaic Virus Infection in Various Plant Species. **Journal of General Virology** 67(10): 2135-2143.

Vega, J. M., W. Yu, A. R. Kennon, X. Chen and Z. J. Zhang (2008). Improvement of *Agrobacterium*-Mediated Transformation in Hi-Ii Maize (*Zea mays*) Using Standard Binary Vectors. **Plant Cell Reports** 27(2): 297-305.

Wakuta, S., S. Hamada, H. Ito, H. Matsuura, K. Nabeta*, et al.* (2010). Identification of a B-Glucosidase Hydrolyzing Tuberonic Acid Glucoside in Rice *(Oryza sativa* L.). **Phytochemistry** 71(11): 1280-1288.

Wan, B., Y. Lin and T. Mou (2007). Expression of Rice Ca(2+)-Dependent Protein Kinases (Cdpks) Genes under Different Environmental Stresses. **FEBS Letters** 581(6): 1179-1189.

Wang, X. L., R. F. He and G. C. He (2005). Construction of Suppression Subtractive Hybridization Libraries and Identification of Brown Planthopper-Induced Genes. **Journal of Plant Physiology** 162(11): 1254-1262.

Wang, Z. X., M. Yano, U. Yamanouchi, M. Iwamoto, L. Monna*, et al.* (2002). The Pib Gene for Rice Blast Resistance Belongs to the Nucleotide Binding and Leucine-Rich Repeat Class of Plant Disease Resistance Genes. **The Plant Journal** 19(1): 55-64.

Wielopolska, A., H. Townley, I. Moore, P. Waterhouse and C. Helliwell (2005). A High-Throughput Inducible Rnai Vector for Plants. **Plant Biotechnology Journal** 3(6): 583-590.

Wielopolska, A., H. Townley, I. Moore, P. Waterhouse and C. Helliwell (2005). A High-Throughput Inducible Rnai Vector for Plants. **Plant Biotechnology Journal** 3(6): 583-590.

Wilson, A. K., F. B. Pickett, J. C. Turner and M. Estelle (1990). A Dominant Mutation In *Arabidopsis* Confers Resistance to Auxin, Ethylene and Abscisic Acid. **Molecular and General Genetics** 222(2): 377-383.

Xiang, D.-j., X.-y. Hu, Y. Zhang and K.-d. Yin (2008). Over-Expression of Ice1 Gene in Transgenic Rice Improves Cold Tolerance. **Rice Science** 15(3): 173-178.

Xiao, B., Y. Huang, N. Tang and L. Xiong (2007). Over-Expression of a Lea Gene in Rice Improves Drought Resistance under the Field Conditions. **Theoretical and Applied Genetics** 115(1): 35-46.

Yang, B., A. Sugio and F. F. White (2006). Os8n3 Is a Host Disease-Susceptibility Gene for Bacterial Blight of Rice. **Proceedings of the National Academy of Sciences of the United States of America** 103(27): 10503-10508.

Yoo, S. D., Y. H. Cho and J. Sheen (2007). *Arabidopsis* Mesophyll Protoplasts: A Versatile Cell System for Transient Gene Expression Analysis. **Nature Protocols** 2(7): 1565-1572.

Zeigler, R. S., S. A. Leong and P. Teng (1994). **Rice Blast Disease**, CABI.

Zhang, Y., J. Su, S. Duan, Y. Ao, J. Dai, *et al.* (2011). A Highly Efficient Rice Green Tissue Protoplast System for Transient Gene Expression and Studying Light/ Chloroplast-Related Processes. **Plant Methods** 7(1): 30-30.

Zhu, X., S. Chen, J. Yang, S. Zhou, L. Zeng, *et al.* (2012). The Identification of Pi50 (T), a New Member of the Rice Blast Resistance Pi2/Pi9 Multigene Family. **Theoretical and Applied Genetics**: 1-10.

CHAPTER V

CONCLUSION

Sequence analysis of mature Os1BGlu4 showed that it contained 483 amino acids, and suggested its subcellular localization in the cytoplasm. The recombinant Thioredoxin-Histidine6-Os1BGlu4 (Trx-His6-rOs1BGlu4) fusion protein was functionally expressed. The expression condition was optimized, without IPTG inducer, 16 hr incubation at 20 ^{o}C were the best condition to express the Trx-His6-rOs1BGlu4. Biochemical analysis showed that the optimum pH for hydrolysis activity of rOs1-BGlu4 is 6.5, the rOs1BGlu4 was stable over the pH range of 6.0 to 8.0 after 24 hr incubation, and the optimum temperature is 45 ^{o}C. The rOs1BGlu4 was stable at 20 and 30 ^{o}C for 1 hr.

Kinetics analysis indicated that the rOs1BGlu4 efficiently hydrolyzed β-(1,3)-linked oligosaccharides with degree of polymerization (DP) of 2-3, and β-(1,4)-linked oligosaccharide with DP of 3-4. While cellopentaose and cellohexaose can be hydrolyzed but with lower efficiency, the laminari-oligosaccharides with DP more than 3 can not be hydrolyzed. The rOs1BGlu4 can hydrolyze *p*NPG efficiently. The *p*NP-fucopyranoside was hydrolyzed with about 50% the hydrolysis efficiency of *p*NPG, based on the kinetic parameters. Others *p*NP-derivatives can be hydrolyzed with low efficiency. Thin Layer Chromotography (TLC) showed that the natural substrates, salicin, esculin and *p*CAG can be hydrolyzed by rOs1BGlu4. The hydrolysis activity of rOs1BGlu4 was strongly inhibited by $HgCl_2$, delta-glucono-lactone and $FeCl_3$. The

*p*NP-cellobioside is sequentially hydrolyzed with initial hydrolysis between the two glucosyl moieties. The transglycosylation study showed that at high concentrations of *p*NPG, rOs1BGlu4 can transfer the glucosyl group of *p*NPG to ethanol and *p*NPG.

The temporal expression showed that the *Os*1*bglu*4 had the highest expression level at the early stage of germination and expression decreased gradually to a steady level at 6 days after germination. The spatial expression showed that the *Os*1*bglu*4 had higher expression in 14 day seedling root, and low expression in shoot and leaf. In booting stage rice, the panicle, leaf and root had higher expression than in stem and sheath. The expression of *Os*1*bglu*4 was induced under PEG and NaCl stresses. The expression of *Os*1*bglu*4 was induced to a high level after blast infection in blast resistant rice cultivar, and only moderately expressed in the blast susceptible rice NIL. These result suggested that the *Os*1*bglu*4 responded to the drought, salinity stress and rice blast stress.

The *Os*1*bglu*4 gene overexpression and knock-down was achieved in trans-genic plants. The segregation of T-DNA analysis showed that the T-DNA segregation conformed to Mendelian genetics in the T1 plant. The subcellular localization of *Os*1-*bglu*4-GFP was shown to be in the cytosol by fluorescence microscope, corresponding to the bioinformatics prediction. The activity of pOp6 promoter in the RNAi transgenic rice was assessed by GUS staining, the result showed that 30 μM DEX is necessary for strong induction of GUS activity, 30 μM DEX had no significant effect to the germination rate of transgenic and wildtype rice seeds.

The phenotype analysis showed that the *Os*1*bglu*4 overexpression lines (oe) had more root hair than that of the wild type, and *Os*1*bglu*4 gene knock down lines (RNAi) had lower number of root hair, when germinated in water. However, when germinated in 1/2 MS medium, there were no significant difference in the root hair

number between the wt and oe, but the RNAi line had less root hair than both wt and oe. Aside from the root hair in the seedling stages, there were no visible difference in the overall morphologies among wt, oe, RNAi and the transgenic rice which was transformed with the empty pMDC83 plant expression vector (vetr). Under drought and salinity stress, there were no visible different phenotypes observed in the wt, oe, RNAi and vetr lines. Under rice blast stress, the oe showed higher resistance to the blast stress, the wt and vetr lines had moderate resistace, the RNAi lines suffered severe lesions from the blast infection.

In general, these results suggest that *Os*1*bglu*4 may be involed in the blast resistance and root hair formation.

APPENDICES

APPENDIX A

EXPERIMENTAL STANDARD DATA

Table 6.1 BSA standard reaction setup.

BSA (µg)	Water (µL)	(0.1 mg/ml) BSA (µL)	Bradford Solution (µL)
0	800	0	200
2	780	20	200
4	760	40	200
6	740	60	200
8	720	80	200
10	700	100	200
12	680	120	200

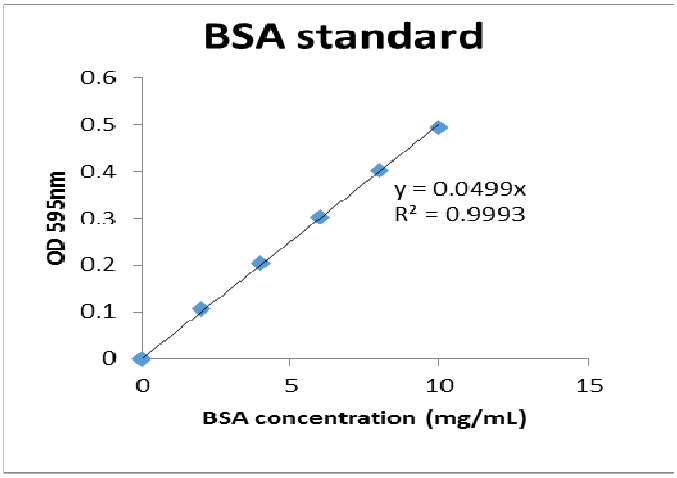

Figure 6.1 Profile of BSA standard. The equation is y = 0.049x, and the R^2 = 0.999.

Table 6.2 Glucose standard setup.

Glucose (µmole)	1mM Glucose (µL)	Phosphate buffer (µL)
0	0	50
0.0025	2.5	47.5
0.005	5	45
0.01	10	40
0.015	15	35
0.02	20	30
0.025	25	25
0.03	30	20

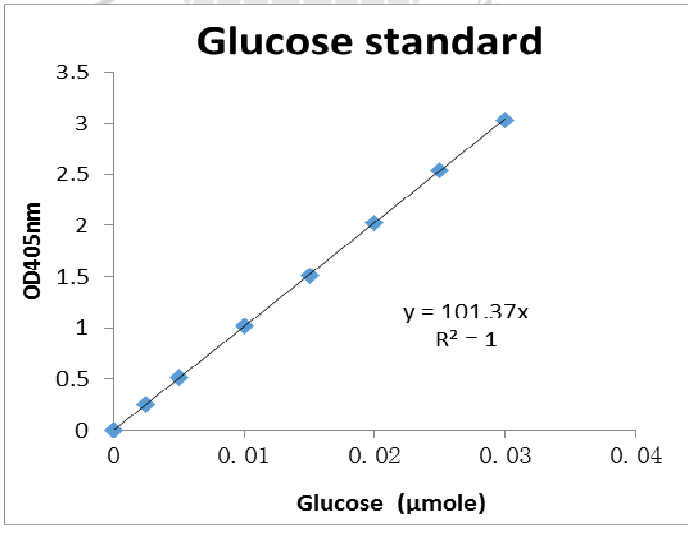

Figure 6.2 Profile of glucose standard. The equation is y = 101.3x, and the $R^2 = 1$.

Table 6.3 *p*NP standard setup.

***p*NP (µmole)**	**1mM *p*NP (µL)**	**Phosphate buffer (µL)**
0	0	100
0.0025	2.5	97.5
0.005	5	95
0.01	10	90
0.015	15	85
0.02	20	80
0.025	25	75
0.03	30	70

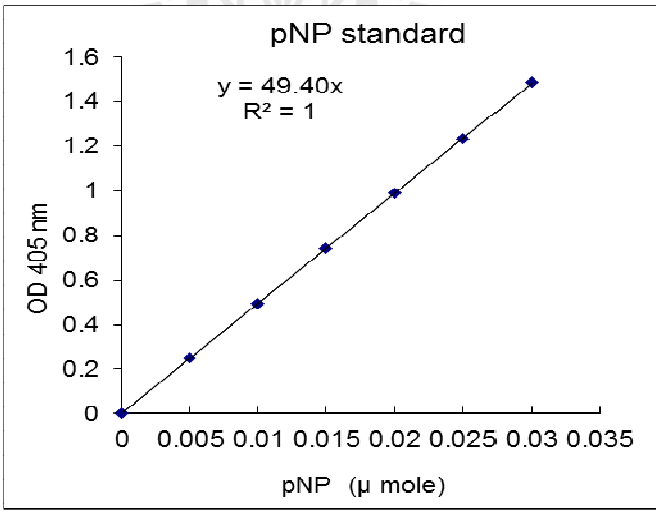

Figure 6.3 Profile of *p*NP standard. The equation is y= 49.4x, and the $R^2 = 1$. The reaction was set according to the amount of pNP, which change from 0.005 µmole to 0.03 µmole. The pNP and sodium phosphate buffer was incubated for 10min at 37 ^{o}C, and 70 uL of 0.4M Na_2CO_3 was added to stop the reaction, the OD405 was measured.

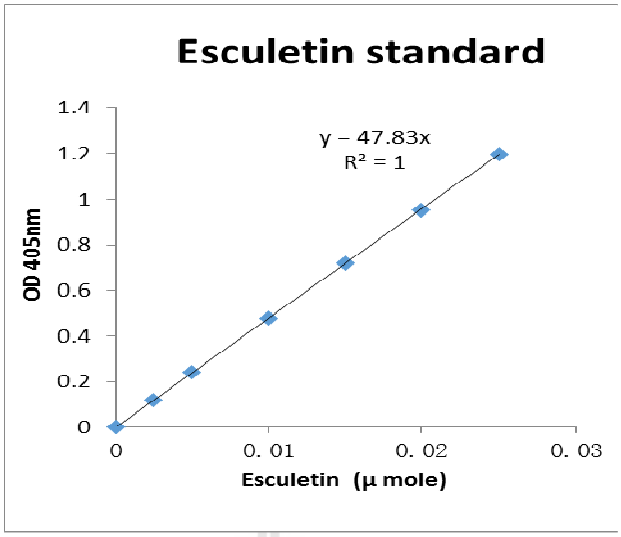

Figure 6.4 Profile of esculetin standard. The equation is y = 47.83x, and the $R^2 = 1$.

APPENDIX B

MEDIA AND REAGENTS

1. NMB medium (pH 5.8)

	mg/L
KNO_3	2830
$(NH_4)_2SO_4$	463
KH_2PO_4	400
$MgSO_4 \cdot 7\ H_2O$	185
$CaCl_2 \cdot 2H_2O$	166
$MnSO_4 \cdot 4H_2O$	22.3
$ZnSO_4 \cdot 7H_2O$	8.6
H_3BO_3	6.2
KI	0.83
$Na_2MoO_4 \cdot 2H_2O$	0.25
$CuSO_4 \cdot 5H_2O$	0.025
$CoCl_2 \cdot 6H_2O$	0.025
$Na_2 \cdot EDTA$	37.25
$FeSO_4 \cdot 7H_2O$	27.85
Nicotinic Acid	1
Pyridoxine·HCl	1
Thiamine·HCl	10

2. AAM medium (pH 5.2)

	mg/L
KH_2PO_4	170
$MgSO_4 \cdot 7H_2O$	370
KCl	2940
$CaCl_2 \cdot 2H_2O$	440
$MnSO_4 \cdot H_2O$	7.58
$Na_2MoO_4 \cdot H_2O$	0.25
H_3BO_4	3
$ZnSO_4 \cdot 7H_2O$	2
KI	0.75
$CuSO_4 \cdot 5H_2O$	0.0387
$CoCl2 \cdot 6H_2O$	0.025
$FeSO_4 \cdot 7H_2O$	27.8
$Na_2 \cdot EDTA$	37.3
Inositol	100
Thiamine·HCl	0.5
Pyridoxine·HCl	0.5
Nictinic Acid	0.5
Glycin	7.5
Arginine	174
Glutamine	876
Casamino acids	500
Acetosyringone	100 μ mole/L
Glucose	68500
Sucrose	30000

Table 6.4 Components of SDS-polyacrylamide gel.

Components	**12% Separating gel (mL)**	**5% Stacking gel (mL)**
Deionized water	3.3	2.77
1.5 M Tris (pH 8.8)	2.5	-
0.5 M Tris (pH 6.8)	-	1.26
10% (w/v) SDS	0.1	0.05
30% acrylamide solution	4	0.83
10% (w/v) ammonium persulfate	0.1	0.05
TEMED	0.005	0.005

BIOGRAPHY

Mr. Chen Rouyi, born on 25, Nov. 1981 in Yibin city, Sichuan province, China. He holds a BA degree in Pratacultural Science from Sichuan Agricultural University and a M.S degree in Crop Genetics and Breeding from Sichuan Agricultural University. Mr. Chen Rouyi is currently a Ph.D. candidate in Biotechnology under the supervision of Associate Professor Dr. Mariena Ketudat-Cairns in the School of Biotechnology, Suranaree University of Technonogy, Thailand.